VANDERMOLEN, KAREN M., Ph.D. Quantitative Analysis of Grapefruit Constituents Involved in Diet-Drug Interactions and Modification of the Microbial Metabolome. (2014)
Directed by Dr. Nicholas H. Oberlies. 114 pp.

The term “natural product” refers to secondary metabolites produced by living organisms, and therefore encompasses a number of research concentrations ranging from traditional medicines to microbial lead compounds to the impacts of diet on human health. The projects described here involve several diverse investigations that cover some of the great breadth of natural products research. One project examined the drug-diet interaction between grapefruit constituents and first-pass metabolism enzymes, including cytochrome P450s and organic anion transporter proteins. The bioactive components of grapefruit juices and dietary supplements, including several furanocoumarins and flavonoids, were quantified. A contrasting project, related to drug discovery through the screening of fungi, explores a different facet of natural products research. The impact of media modification on the production of fungal secondary metabolites was examined, using known metabolites to track production potential of various culture media. In addition, a chemical epigenetics approach was used to induce new secondary metabolites by causing the transcription of normally silent fungal genes. Finally, a review article explored the history of a microbial metabolite that made it through the drug development process to become an anti-cancer treatment.

QUANTITATIVE ANALYSIS OF GRAPEFRUIT CONSTITUENTS INVOLVED IN DIET-DRUG INTERACTIONS AND MODIFICATION OF THE MICROBIAL METABOLOME

by

Karen M. VanderMolen

A Dissertation Submitted to
the Faculty of the Graduate School at
The University of North Carolina at Greensboro
in Partial Fulfillment
of the Requirements for the Degree
Doctor of Philosophy

Greensboro
2014

Approved by

Nicholas H. Oberlies

Committee Chair

To my family and friends; thank you for your support and love.

APPROVAL PAGE

This dissertation, written by Karen M. VanderMolen, has been approved by the following committee of the Faculty of The Graduate School at The University of North Carolina at Greensboro.

Committee Chair Nicholas H. Oberlies

Committee Members Nadja B. Cech

Ethan W. Taylor

Stanley H. Faeth

December 16, 2013
Date of Acceptance by Committee

December 16, 2013
Date of Final Oral Examination

ACKNOWLEDGEMENTS

Nicholas Oberlies

Tyler Graf

Ray Carney

Nadja Cech

Mary Paine

Christina Won

Garrett Ainslie

Huzefa Raja

Tamam El-Elimat

Brandie Ehrmann

Amninder Kaur

David Brown

TABLE OF CONTENTS

Page

CHAPTER

CHAPTER I

COMPOUNDS LEADING TO DIET-DRUG INTERACTION

History of the "Grapefruit Juice Effect"

There is a common misconception that because something is natural, it is safe. While the fallacy of this notion is easily disproved (pathogens, for example, are both natural and quite harmful), consumer products are increasingly labeled "all-natural." This trend could potentially lead to consequences, as most people do not expect or even suspect the food or supplements they ingest to interfere with their medication.

In the last several decades, grapefruit has made such interactions more widely known. Its effect was first discovered serendipitously, during a 1989 clinical trial examining potential interactions between alcohol and felodipine, an antihypertensive drug.[1] Grapefruit juice was used as a matrix to mask the flavor of the ethanol. Unexpectedly, plasma concentrations of the felodipine were three and five times what was expected in all patients, not just those consuming alcohol. The authors of the paper postulated that the grapefruit juice matrix was the cause, and confirmed this in a subsequent paper two years later.[2]

The primary mechanism for this interaction was shown in 1998 to be the irreversible inhibition of cytochrome P450s (CYPs).[3] The CYP enzymes are major mediators of first-pass metabolism, and their inhibition can result in various side effects,

ranging from headaches to kidney toxicity.[4-7] The class of compounds in grapefruit responsible for this inhibition was identified as furanocoumarins, most notably bergamottin and 6´,7´-dihydroxybergamottin (DHB; Fig. 1).[4]

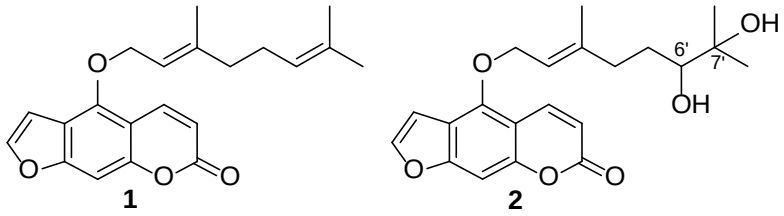

Figure 1. Bergamottin (**1**) and 6′, 7′-dihydroxybergamottin (DHB; **2**)

Interactions with Cytochrome P450 Enzymes

The CYP enzymes have been reported to account for almost half of the overall elimination of commonly prescribed drugs,[8] though its isoforms are involved in the metabolism of many more. The CYP3A isoforms alone, including both CYP3A4 and CYP3A5, are involved in the metabolism of over half of common medications, making the CYP3As arguably the most important family.[6]

Furanocoumarins have been shown to inhibit multiple isoforms *in vitro*, including subfamilies from the CYP1, CYP2, and CYP3 families. The *in vitro* inhibition of the CYP3A4s by furanocoumarins varies by compound; the potency of DHB, for example, is greater than that of bergamottin and bergaptol but less than the paradisins (dimers of DHB).[9, 10] A study using paradisin C, DHB, bergamottin, and bergaptol determined IC_{50} values of 0.09, 0.42, 10, and 69 μM, respectively.[6] In addition to differing IC_{50} and K_i values,[11] DHB and bergamottin differ in their time courses for CYP3A4 inhibition; while

maximal inhibition by DHB was achieved within 30 min, up to 3 h was required for bergamottin to significantly reduce CYP3A4 activity.[12] Such *in vitro* studies suggest that the importance of DHB in potential drug-diet interactions far outweighs that of bergamottin. This is corroborated by studies demonstrating no clinically significant inhibition by two beverages known to contain high levels of bergamottin, but no DHB.[13, 14] Pure bergamottin in doses up to 12 mg also failed to increase mean felodipine AUC.[15] Similar studies for the paradisins are not available.

CYP3A inhibition by the furanocoumarins is primarily mechanism-based; *i.e.*, the compounds bind irreversibly to the enzyme, precipitating a loss of the enteric CYP3A proteins without affecting CYP3A mRNA.[16] The consequence of this fact is that prior exposure to grapefruit juice is sufficient to produce a reaction; grapefruit, or its active components, do not need to be consumed concurrently with medication to induce a reaction.[17] Recovery of CYP3A activity requires the production of new enzymes, a process with a half-life of approximately 24 h.[18]

Interactions with P-glycoprotein

P-glycoprotein (P-gp) is a transmembrane protein localized to the apical membrane of hepatocytes and enterocytes. It acts to decrease absorption of medications by transporting drugs into the bile and intestinal lumen. Its substrate specificity overlaps widely with CYP3A,[19] and its potential role in augmenting the increase in drug exposure by CYP3A inhibitors has been investigated. Grapefruit juice, as well as the furanocoumarins Paradisin A, bergamottin, DHB, bergapten, and bergaptol have

demonstrated P-gp inhibition *in vitro*.[9, 20] Despite these *in vitro* studies, there is little evidence grapefruit juice has more than a minimal effect on P-gp activity.[6, 21-23]

Interactions with Organic Anion Transporter Proteins

Complicating the drug metabolism story are the organic anion transporter proteins (OATPs), found throughout the body, including enterocytes. The OATPs are involved in drug uptake, and their inhibition can decrease AUC. Furanocoumarins are OATP inhibitors, but *in vitro* and *in vivo* data indicate that flavonoids are primarily responsible for OATP inhibition by grapefruit juice.[24-27] This effect varies depending on which probe substrate is used. Unlike CYP3A inhibition, OATP inhibition by grapefruit components is brief, lasting less than 4 h.[28]

Similar to P-gp, many drugs are substrates for both CYP3A and OATP, and OATPs may therefore play a minimal role in drug exposure in the context of grapefruit inhibition.[29] However, the overlapping substrate specificity of these enzymes also suggests that the most accurate way to analyze the impact of grapefruit juice and its components on a drug's metabolism is to perform clinical pharmacokinetic studies.[6]

Aims of this project

Furanocoumarins and flavonoids, while natural compounds, have the potential to cause severe side effects when consumed with medications that undergo metabolism by cytochrome P450s. Grapefruit juice, as well as botanical supplements that contain grapefruit or its active components, pose a risk to uninformed consumers. To assess this

risk, several grapefruit juices and nutritional supplements were analyzed. In concert with clinical studies that examined the biological impact of the juices and supplements, a quantitative chemical analysis was performed to gain an understanding of the expected concentrations of potentially harmful natural products.

CHAPTER II

RAPID QUANTITATION OF FURANOCOUMARINS AND FLAVONOIDS IN GRAPEFRUIT JUICE USING ULTRA PERFORMANCE LIQUID CHROMATOGRAPHY

This chapter has been published in the journal *Phytochemical Analysis* and is presented in that style. VanderMolen, K.M., Cech, N.B., Paine, M.F., Oberlies, N.H. *Phytochem. Anal*. **2013**. 24, 654-660.

Introduction

Grapefruit juice has been shown to increase the systemic exposure of a diverse array of oral medications that undergo extensive pre-systemic metabolism by cytochrome P450 3A (CYP3A) in the intestine, including felodipine, lovastatin, and cyclosporine.[4-7] The increase in systemic drug exposure can be sufficient to cause untoward effects, ranging from relatively mild (*e.g*., hypotension and dizziness with some calcium channel blockers) to potentially severe (*e.g*., nephrotoxicity with some immunosuppressants). The mechanism underlying these interactions is irreversible inhibition of intestinal CYP3A activity by grapefruit juice.[3, 4, 6, 21] Furanocoumarins, a class of compounds present in grapefruit juice, have been established as major CYP3A inhibitors in human volunteers.[4] This effect may be augmented if the "victim" drug also is a substrate for P-glycoprotein(P-gp), a transmembrane efflux transport protein located on the apical membranes of numerous cell types, including enterocytes.[6, 21] P-gp demonstrates

substrate specificity that overlaps with that of CYP3A substrates,[19] and several *in-vivo* and *in-vitro* studies have shown an inhibitory effect by grapefruit juice and/or furanocoumarins towards P-gp activity.[30-35] A more recently discovered mechanism underlying grapefruit juice-drug interactions is inhibition of intestinal organic anion transporting polypeptides (OATPs), which are uptake transporters located on the apical membranes of enterocytes and other cell types.[7, 36] Opposite to P-gp, OATPs in the intestine act to facilitate drug absorption. Thus, inhibition of these transport proteins leads to a decrease in systemic exposure of drug substrates, including the antihistamine fexofenadine[36, 37] and the antihypertensive agent aliskiren,[38, 39] with the consequent potential for therapeutic failure. Candidate OATP inhibitors in grapefruit juice include the flavonoids naringin and hesperidin.[40] The potential for drug interactions with a widely available food product necessitates an understanding of the expected concentrations of a suite of structurally diverse and potentially bioactive compounds.

Reported analytical methods for measuring furanocoumarins in fruit juices typically require separation times of one hour or more.[38, 39, 41-44] For example, in 2005, a study of the distribution of furanocoumarins in grapefruit juice fractions utilized a 65-min high performance liquid chromatography (HPLC) method.[44] The same year, an exhaustive analysis of several furanocoumarins and furanocoumarin dimers in 58 juices employed a similar 65-min method.[45] The following year, a 45-min HPLC method was utilized to determine the concentrations of bergamottin and 6′,7′-dihydroxybergamottin in grapefruit juice.[43] In 2009, a shorter HPLC method was developed for the determination of five furanocoumarins (bergaptol, psoralen, bergapten, bergamottin, and 6′,7′-

dihydroxybergamottin) in citrus juices that required a run time of 23 min, which appears to be the most rapid method published to date.[46] As with the furanocoumarins, analytical procedures for measuring flavonoids often employ methods of one hour or more. A survey of 9 commercial grapefruit juices and associated flavonoid concentrations published in 2000 utilized a 60 min method.[41] Six years later, a 65 min method in a similar survey of orange and grapefruit juices was published,[39] followed the next year by another 60 min method for the simultaneous analysis of adrenergic amines and flavonoids in fruit jams and juices.[38] De Castro *et al.* utilized a 70 min separation to determine the concentrations of naringin and naringenin.[43] The most rapid HPLC analyses of flavonoids reported in the literature was a 45 min method published in 2008.[47] A handful of UPLC analyses of flavonoids in food, supplements and traditional Chinese medicines have appeared in the literature in the last few years as well. The majority of these studies[48-51] utilize a C18 column and UV detection, though one expansive study quantifying 39 phenolic compounds in apples[52] additionally used electrospray ionization mass spectrometry (ESI-MS) to confirm the identity of the analytes. The most rapid of these UPLC studies quantified 11 flavonoids (including those listed in this paper) in three citrus fruit extracts, and had a run time of 5.5 min.[50]

Ultra performance liquid chromatography (UPLC) offers significant advantages in sensitivity and speed compared to conventional high performance liquid chromatography (HPLC). After overcoming the difficulties presented by working with very high pressures,[53-55] early studies demonstrated enhanced resolution and sensitivity, reduced solvent consumption, and rapid analyses[56-58] with UPLC compared to that which can be

achieved with HPLC. With greater integration in diverse research areas, UPLC offers the opportunity to streamline quantitative determinations, such as those described herein, reducing cost and expediting research.

The goal of this study was to develop rapid (< 5.0 min) methods for the quantitation of two furanocoumarins (bergamottin and 6′,7′-dihydroxybergamottin) and four flavonoids (naringin, naringenin, narirutin, and hesperidin) in grapefruit juice using UPLC (Fig. 2). An additional goal was to apply these methods to determine the concentrations of the aforementioned analytes in five grapefruit juices used in previous clinical interaction studies.

Experimental

Instrumentation

UPLC analyses were performed using a Waters Acquity UPLC system (Milford, MA) equipped with an autosampler, photodiode array detector (PDA), column manager, and binary solvent manager. Data were collected and analyzed using Empower software. An HSS C18 column (50 mm × 2.1 mm i.d., 1.8 µm, Waters, Milford, MA) was used for all chromatographic analyses.

Materials

Bergamottin (purity ≥ 96.9%) was purchased from ChromaDex (Irvine, CA, USA); narirutin (purity ≥ 99.0%) was purchased from Indofine (Hillsborough, NJ, USA); naringin (purity ≥ 96.8%), naringenin (purity ≥ 99.9%), hesperidin (purity ≥ 97.0%), and

6′,7′-dihydroxybegamottin (purity ≥ 97.2%) were purchased from Sigma-Aldrich (St. Louis, MO, USA). Purity of standards are reported as determined by HPLC by the manufacturers. Methanol, ethyl acetate, and acetonitrile were purchased from Pharmco-Aaper (Shelbyville, KY, USA).

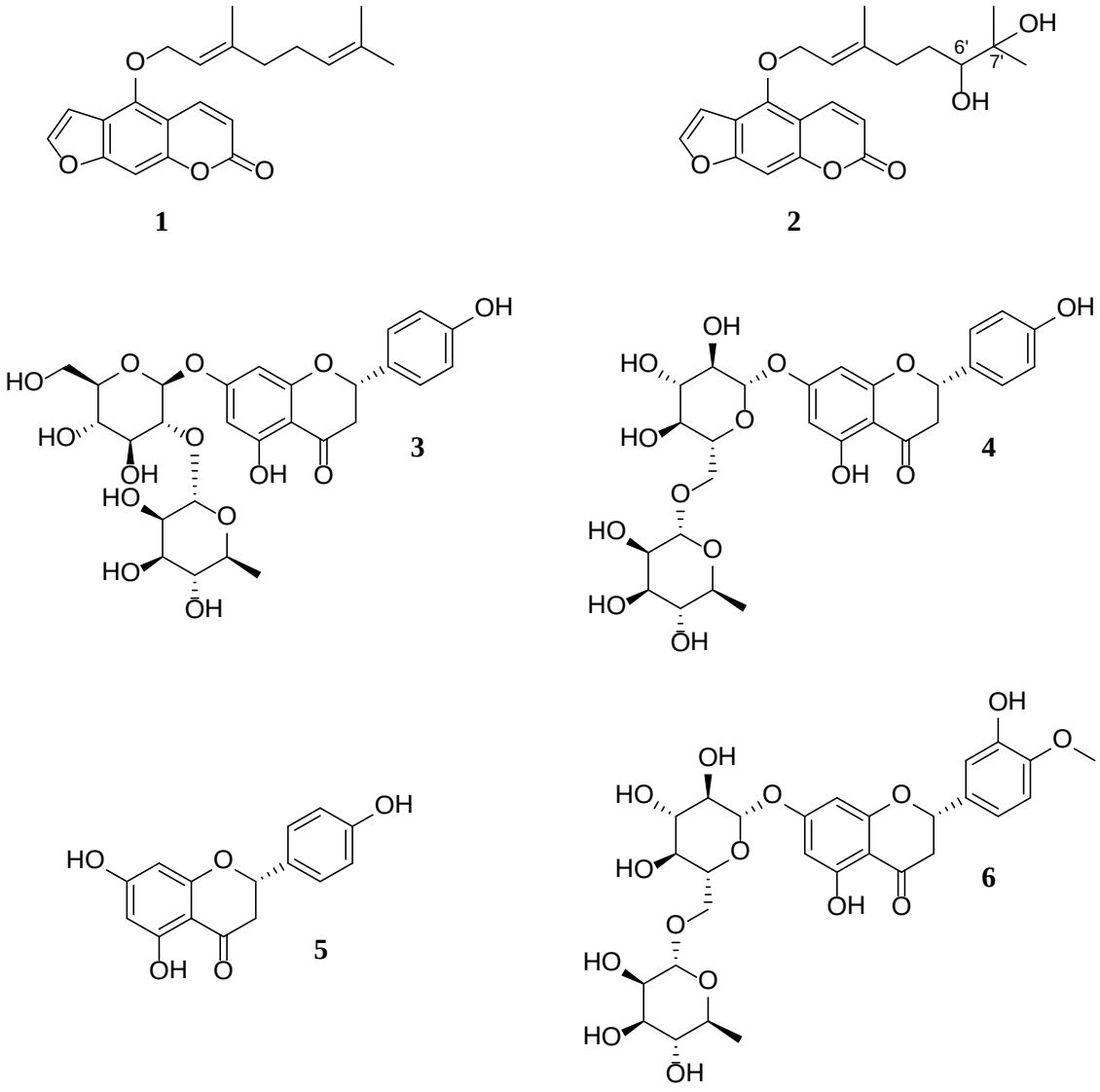

Figure 2. Structures of the furanocoumarins bergamottin (**1**) and 6′,7′-dihydroxybergamottin (**2**) and the flavonoids naringin (**3**), narirutin (**4**), naringenin (**5**), and hesperidin (**6**).

Juices A and B were used in clinical studies with felodipine,[4] cyclosporine,[35] and fexofenadine.[59] Juice A was a commercially available product. Juice B was the same juice, but the furanocoumarin fractions were removed using a series of food-grade solvents and absorption resins and column chromatography.[4] Juice C was a commercially available concentrated grapefruit juice (Minute Maid Premium 100% Pure Frozen Concentrated Grapefruit Juice with added calcium). A dilution of Juice C was used in a clinical study examining the effect of grapefruit juice on the systemic exposure of loperamide and the CYP3A-mediated metabolite, desmethylloperamide.[60] Juice D (Florida's Natural Original Ruby Red 100% Pure Florida Grapefruit Juice) and Juice E (Simply Orange Juice Co. Simply Grapefruit 100% Pure Squeezed Grapefruit Juice) were commercially available not-from-concentrate juices and were purchased from a local grocery store.

Standards preparation

Bergamottin and 6′,7′-dihydroxybergamottin were dissolved in methanol to produce a 1.03 mM (bergamottin) and 1.00 mM (6′,7′-dihydroxybergamottin) multi-standard stock solution. This solution was used to prepare seven standard solutions at concentrations ranging from 10.3 to 659 μM (bergamottin) and from 10.0 to 640 μM (6′,7′-dihydroxybergamottin). Naringin, narirutin, naringenin, and hesperidin were dissolved separately in methanol to produce stock solutions of 10.0 mM, 7.92 mM, 10.2 mM, and 9.97 mM, respectively. These stock solutions were used to prepare standard solutions for each compound (six for naringin, five for each of the other flavonoids) at

concentrations ranging from 0.649 to 5.00 mM (naringin), 0.198 to 3.17 mM (narirutin), 3.18 to 814 µM (naringenin), and 3.12 to 798 µM (hesperidin).

Sample preparation

Juice extracts were prepared by transferring 25.0 mL of each juice to a 50-mL conical polypropylene tube. After adding 20.0 mL of ethyl acetate, the contents were shaken vigorously and centrifuged (2500 × *g* for 30 min at 25 °C). The resulting organic layer was transferred by Pasteur pipette to a 250 mL round-bottom flask. An additional 20.0 mL of ethyl acetate were added to the remaining contents of the tube, shaken and centrifuged, and the resultant organic layer was combined with the first organic layer. This extraction procedure was repeated a third time, and the combined organic layers were evaporated *in vacuo*. The residue in the round-bottom flask was transferred quantitatively to a 2 mL vial, using methanol as a rinse, and evaporated to dryness under air. This material was resuspended with 5.00 mL of methanol, yielding a 5-fold concentrated extract of each juice.

Chromatographic conditions

Quantitative analysis of furanocoumarins (bergamottin and 6',7'-dihydroxybergamottin). A 6 µL volume of each 5-fold concentrated juice extract was injected and analyzed at a wavelength of 250 nm. Chromatographic separations were carried out with a mobile phase consisting of HPLC-grade acetonitrile (solvent A) and nanopure water (solvent B) at a flow rate of 0.6 mL/min. The following linear gradient

was used: 0.0 min, 30% A; 4.0 min, 100% A; 4.5 min, 100% A. The column temperature was 30 °C.

Quantitative analysis of flavonoids (naringin, narirutin, naringenin, and hesperidin). A 6 µL volume of each 5-fold concentrated juice extract was injected and analyzed at a wavelength of 310 nm. The following linear gradient was used: 0.0 min, 10% A; 1.0 min, 20% A; 2.0 min, 20% A; 2.5 min, 40% A; 3.5 min, 100% A; 4.0 min, 100% A. Solvents A and B, the flow rate, and column temperature were the same as described in the previous section.

Method Validation

The identities of analyte peaks in the juice extracts were confirmed by comparing the UV spectra of the peaks and their standards, as well as, in the case of the flavonoids, by co-injection of the standards with the juices (Appendix, Figures S1 and S2).

Linearity of the calibration curves was assessed by least-squares analysis. Precision and accuracy were determined by calculating the relative standard deviation (RSD) and relative error (RE), defined as the percent difference between the mean observed concentration and the nominal concentration, of three replicate analyses of the standards. All analyses were performed in triplicate in a single day. Interday RSD and RE were determined by analyzing the standard solutions in triplicate on three separate days. The limit of detection (LOD) was defined as the concentration corresponding to the signal detection limit, which was defined as $b + 3s_y$, where b is the y-intercept of the

calibration curve, and s_y is the standard deviation of the vertical deviations.[61] The limit of quantitation (LOQ) was defined as $b + 10s_y$.

Results and Discussion

Method Validation

All standard curves exhibited coefficients of determination (r^2) greater than 0.999 (Table 1). Baseline resolution of all analytes (Fig. 3), both as standards and in the juice extracts, was achieved (Figs. 3 and 4). Precision and accuracy data are summarized in Table 2. RSD of the furanocoumarin standards (**1** and **2**) was below 0.33% (intraday) and 3.1 % (interday) for all standard concentrations. The intraday RSD values of analytes **3**, **4**, and **5** were below 1.5%, 2.6%, and 2.9%, respectively, while the interday RSD averages for each analyte remained below 1.0%. For analyte **6**, the largest RSD value was 4.7% at the lowest concentration of that standard, while the interday RSD was 3.1%. For the furanocoumarins (**1** and **2**), intraday RE remained below 5.7% (**1**) and 2.8% (**2**). Interday RE values predominantly remained under 3.0%, except for the lowest concentrations of **1** and **2**, the highest variation being 21% for the lowest concentration of **1**. The RE values (both intraday and interday) of the flavonoids (**3**-**6**) were predominantly below 5%, and all below 15%. The only exception was the lowest of the standard concentrations of **5** (3.18 µM), which had much higher RE values (32%); thus, this concentration was below the LOQ as defined above. For each analyte measured, all standard concentrations above the LOQ resulted in an RE value of ≤ 15%. LOD values

for analytes **1**, **2**, **5**, and **6** were all below 5 µM. LOD values for analytes **3** and **4** were higher (18 and 69 µM, respectively).

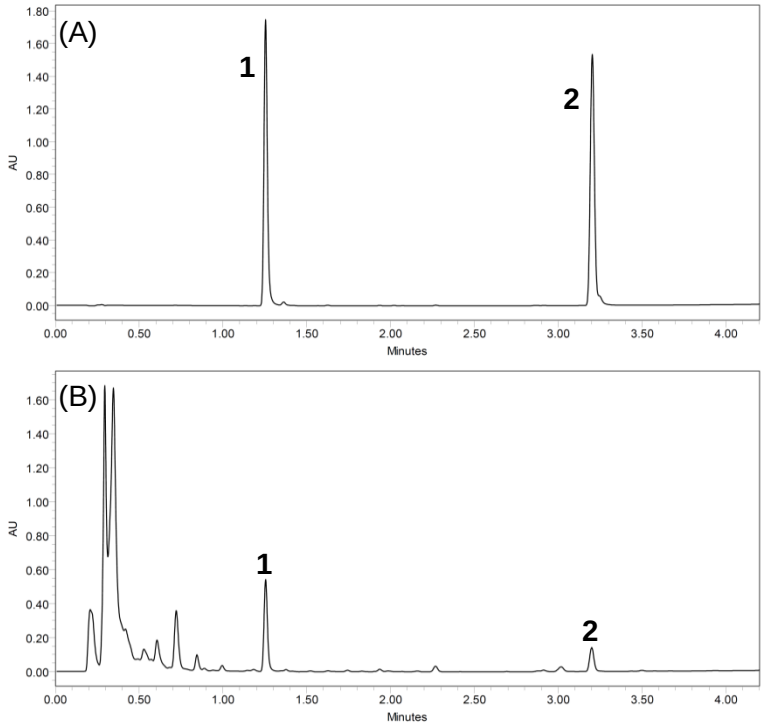

Figure 3. UPLC separation of furanocoumarins. Numbered peaks correspond to the compounds in Fig. 2. (A) Furanocoumarin standards (659 and 640 µM, respectively) and (B) Juice A.

Rapidity of Method

Compared to HPLC analyses of furanocoumarins and flavonoids in the literature, the UPLC method described above markedly reduces the time required for the analyses of these compounds in grapefruit juice. A run time of 4.5 min represents an 80% reduction in the time required to analyze furanocoumarin content when compared with the most rapid published method,[46] whereas a run time of 4.0 min represents an order of magnitude less time required for the analysis of flavonoids.[47] Such methods facilitate the

determination of furanocoumarin and flavonoid concentrations in several grapefruit juices in a single day, reducing costs associated with both labor and materials. Moreover, the time saved expedites the characterization of juices used in *in vitro* or *in vivo* studies, thus accelerating the evaluation and determination of active constituents.

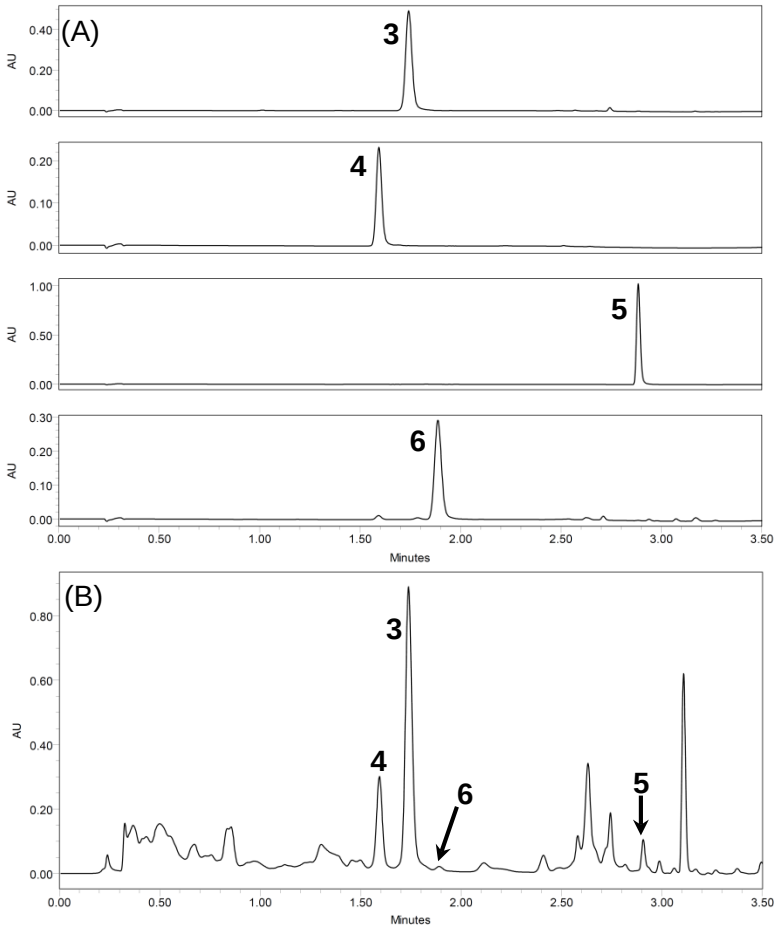

Figure 4. UPLC separation of flavonoids. Numbered peaks correspond to the compounds in Fig. 2. (A) Flavonoid standards (1080, 500, 800, and 800 μM, respectively) and (B) Juice A.

Table 1. Calibration curve data for analytes **1**-**6**.

Analyte	Slope (± SD)	r^2	LOD [a] (μM)	LOQ [b] (μM)
1	4.338×10^3 (± 9)	1.000	0.78	2.6
2	3.784×10^3 (± 5)	1.000	1.1	3.8
3	9.04×10^2 (± 7)	0.999	69	230
4	9.98×10^2 (± 7)	0.999	18	58
5	1.626×10^3 (± 6)	1.000	2.5	8.4
6	8.95×10^2 (± 5)	1.000	3.9	13

[a] Limit of detection
[b] Limit of quantitation

Concentrations of Analytes in Grapefruit Juices

Five different grapefruit juices, four of which were commercially available products, were analyzed to measure the concentrations of selected furanocoumarins and flavonoids (Fig. 2). Samples were analyzed in the same run with the standards to eliminate concerns of systematic error introduced by day-to-day variability in instrument response. Each juice was analyzed using a 5-fold concentrated extract, and the reported values (Table 3) have been adjusted to reflect the concentration in the original juices. Considerable variation in the concentration of each compound was observed. Regarding the furanocoumarins, the concentrations of **1** and **2** in four of the juices ranged from 7.48 (± 0.17) to 24.73 (± 0.16) μM and 7.65 (± 0.17) to 89.03 (± 0.17) μM, respectively. These values were consistent with those reported in the literature using HPLC.[43, 45] The highest concentration of **2** (Juice C) was slightly higher than the ranges reported by De Castro *et al.*,[43] though this was to be expected, as Juice C was a juice concentrate. Regarding the flavonoids, the concentrations of **3** and **4** ranged from 309 (± 15) to 1182 (± 16) μM and 73.4 (± 4.8) to 286.5 (± 3.8) μM, respectively, which again were consistent with literature values using HPLC.[41, 43]

Table 2. Precision (RSD) and accuracy (RE) for analysis of analytes **1**-**6**.

Analytes	Concentration of Standard Solution Injected (μM)	Intraday		Interday	
		RSD (%)	RE (%)	RSD (%)	RE (%)
1	10.3	0.33	5.7	3.1	21.
	20.6	0.27	4.4	0.48	8.5
	41.2	0.091	1.6	0.31	2.4
	82.4	0.19	0.21	0.53	1.1
	165	0.16	0.03	0.26	2.1
	330	0.29	1.2	0.16	0.83
	659	0.32	0.29	0.32	0.33
2	10	0.15	2.8	1.2	9.2
	20	0.11	1.1	0.67	2.7
	40	0.017	0.94	0.62	0.69
	80	0.21	0.10	0.56	2.1
	160	0.16	0.64	0.59	2.5
	320	0.26	0.70	0.61	2.1
	640	0.31	0.13	0.53	1.4
3	649	1.5	15.	0.84	17.
	1081	1.3	4.6	0.14	5.7
	1802	1.1	0.81	0.38	0.79
	3003	0.36	3.3	0.45	3.0
	5005	0.72	3.6	0.29	2.1
	10010	0.99	1.0	0.28	1.9
4	198	1.6	13.	0.67	7.7
	396	2.6	1.4	0.72	2.1
	792	1.5	1.6	0.43	1.3
	1584	1.3	2.5	0.26	2.0
	3168	0.72	0.66	0.78	0.55
5	3.18	1.4	32.	0.03	32.
	12.7	2.9	9.7	0.32	5.3
	50.9	1.4	0.4	0.23	1.4
	203	0.23	1.6	0.35	0.66
	814	1.2	0.094	0.18	0.39
6	3.12	4.7	2.4	3.1	3.7
	12.5	0.64	2.8	0.96	8.3
	49.9	0.93	3.5	0.69	9.0
	199	0.71	4.1	0.47	8.1
	798	1.6	3.0	0.72	1.4

Table 3. Concentrations of analytes **1**-**6** in grapefruit juices.

Juice	Concentration[a] (μM) ± SD					
	Bergamottin (**1**)	DHB[b] (**2**)	Naringin (**3**)	Narirutin (**4**)	Naringenin (**5**)	Hesperidin (**6**)
A	11.76 ± 0.16	41.31 ± 0.16	412 ± 15	100.5 ± 4.5	18.89 ± 0.66	NQ
B	ND[c]	ND	309 ± 15	73.4 ± 4.8	ND	NQ
C	24.73 ± 0.16	89.03 ± 0.17	1182 ± 16	286.5 ± 3.8	34.72 ± 0.55	39.48 ± 0.83
D	7.48 ± 0.17	7.65 ± 0.17	371 ± 15	85.2 ± 4.7	NQ[d]	NQ
E	12.26 ± 0.16	11.58 ± 0.16	381 ± 15	103.5 ± 4.5	5.60 ± 0.79	NQ

Each juice was analyzed in triplicate using a 5-fold concentrated extract, and the values reported have been adjusted to reflect the concentration in the juices, not in the extract.
[b] 6′,7′-dihydroxybergamottin
[c] Not detected
[d] Indicates that the analyte was detected but was below the limit of quantitation

The concentration of **6** ranged from below LOQ (although detected in all juices) to 39.48 (± 0.83) μM. The concentration of **5** ranged from below LOQ to 34.72 (± 0.55) μM, which agrees with literature values.[62, 63] As with the furanocoumarins, the highest concentrations of the flavonoids were in Juice C. The concentrations of **1**-**4** in Juices A and B were measured previously using an HPLC method.[4, 59] The concentration of the furanocoumarins (**1** and **2**) were consistent between methods (within 30 and 7%, respectively), whereas the concentrations of the flavonoids (**3** and **4**) by HPLC were approximately 2-fold higher than those by UPLC. Reasons for this difference remains unexplored, as a between-laboratory validated study was beyond the scope of this work. The extracts used in this study were analyzed at a 5-fold concentration. In the future, the accuracy of the measurements for analytes present in very low concentrations could be improved by using a more concentrated extract.

Wide between-juice variation in the concentrations of each grapefruit juice constituent was observed, as would be expected for natural products, and the concentrations agreed well with values reported in the literature using HPLC. This marked variation between commercially available brands undoubtedly contributes to the large between-study differences in effect size (*i.e.*, change in drug area under the curve [AUC]) associated with clinical grapefruit juice-drug interaction studies.[7] Quantitation of one or more constituents in a given juice would provide a means for between-study comparisons of clinical, as well as *in vitro*, data. The UPLC methods developed in the current work offer a rapid means for the quantitation of representative constituents. While the methods were applied to grapefruit juices, they should be applicable to other foods, including other fruit juices.

Acknowledgments

This research was supported by the National Institutes of Health/National Institute of General Medical Sciences via grant R01 GM077482.

CHAPTER III

LABELED CONTENT OF TWO FURANOCOUMARINS IN DIETARY SUPPLEMENTS CORRELATES WITH NEITHER ACTUAL CONTENT NOR CYP3A INHIBITORY ACTIVITY

This chapter is intended for submission to the journal *Pharmaceutical and Biomedical Analysis* and is presented in that style. Coauthors include Garrett R. Ainslie, Mary F. Paine, and Nicholas H. Oberlies.

Introduction

Dietary supplements are a thriving industry in the United States, surpassing $30 billion in sales in 2011[64] and encompassing various facets of the market. They can include single- or multi-vitamins, minerals, herbs and botanicals,[65] weight-loss aids, and sports nutrition products. Of these, sports nutrition supplements made up 12% of the total sales.[64, 66] Some of these supplements are labeled to contain 6′,7′-dihydroxybergamottin (DHB) and/or bergamottin (Fig. 1), two furanocoumarins normally found in grapefruit juice, that have been shown to interfere with cytochrome P450 3A (CYP3A) in the intestine through irreversible inhibition of the enzyme.[3, 4, 6, 21]

Intestinal CYP3A contributes significantly to the pre-systemic (‘first-pass’) metabolism of numerous orally-administered drugs, including felodipine, lovastatin, and cyclosporine.[4-7] Inhibition of intestinal CYP3A by furanocoumarins can increase the systemic exposure of these ‘victim’ drugs to an extent that leads to side effects ranging

from relatively mild (*e.g.*, hypotension and dizziness with some calcium channel blockers) to potentially severe (*e.g.*, nephrotoxicity with some immunosuppressants). CYP3A also is involved in the oxidative metabolism of both endogenous and exogenous androgens, including testosterone[11] and synthetic steroids marketed as legal body building supplements. For example, two synthetic steroids in the supplements Finaflex 1-Andro and Finaflex 1-Alpha included 3-hydroxy-5α-androst-1-ene-17-one and 3-enanthoxy-5α-androst-1-ene-17-one, respectively. These additives can be sold as mixtures labeled to contain DHB and/or bergamottin, allegedly enhancing the effect of the steroids by "mak[ing] the active ingredient more bio-available" (Finaflex 1-Andro). At least one supplement, SciFit DHB 300, was labeled to contain 300 mg of pure DHB in each capsule, and was presumably intended to be taken concomitantly with other products of the consumer's choice. Grapefruit juice contains between 0.2 and 89.0 μM DHB and 2.5 and 36.3 μM bergamottin,[43, 45, 67] equating to between 0.02 to 7.4 mg DHB and 0.2 to 2.9 mg bergamottin per 8-oz (240-mL) serving. Grapefruit juice containing 2.7 mg DHB and 2.2 mg bergamottin per 240-mL serving doubled median area under the curve of felodipine relative to control.[4] Supplements containing DHB or bergamottin at similar amounts may pose a risk for consumers taking concomitant medications that undergo extensive CYP3A-mediated intestinal metabolism.[4-7]

Other dietary supplements have been shown to modulate drug metabolism with subsequent unwanted effects, most notably *Hypericum perforatum* L. (St. John's wort). Opposite to grapefruit juice, St. John's wort induces the expression[68] of intestinal (and hepatic) CYP3A, as well as P-glycoprotein (P-gp), an apically-located transmembrane

efflux protein that transports susceptible substrates back into the intestinal lumen or into bile.[19] Induction of CYP3A and P-gp can decrease significantly the systemic exposure and efficacy of diverse drugs, including oral contraceptives, cyclosporine, and methadone.[69-72] The risk of supplement-drug interactions is exacerbated by both the lack of pre- and post-launch scrutiny of supplements,[65, 73] as well as chronic underreporting of supplement use by patients.[74-77]

To address the possibility of dietary substance-drug interactions perpetrated by supplements containing DHB or bergamottin, both quantitative analysis and a CYP3A inhibitory activity bioassay were employed. The quantification method utilized ultra-performance liquid chromatography (UPLC) for rapid (3.0 min) separation of the supplement extracts, coupled to both a photodiode array detector (PDA) and a triple quadrupole mass spectrometer (MS) for quantification. Based on a previously published study,[67] this method was refined for faster analysis and made use of the MS to identify more easily the analyte peaks in the complex extracts. The quantification was used to evaluate the labeled vs. actual content of DHB and bergamottin in selected supplements, while the bioassay was used to assess whether the actual content of the furanocoumarins correlated with CYP3A inhibitory activity.

Materials and Methods

Chemicals and Materials

6′,7′-Dihydroxybegamottin was purchased from Sigma-Aldrich (purity ≥ 97.2%) and Cayman Chemical (Ann Arbor, MI; purity ≥ 98.0%); bergamottin was purchased

from ChromaDex (Irvine, CA; purity ≥ 96.9%) and Sigma-Aldrich (St. Louis, MO; purity ≥ 98.0). Midazolam (purity ≥ 99.9%), 1-hydroxymidazolam (purity ≥ 98.0%), ketoconazole (purity ≥ 98.0%), alprazolam (purity ≥ 99.0%), and NADPH were purchased from Sigma-Aldrich. Purity of standards is reported as determined by HPLC (TLC in the case of alprazolam) by the manufacturers. Methanol (MeOH) was purchased from Pharmco-Aaper (Shelbyville, KY) and Fischer Scientific (Waltham, MA). UPLC-grade water (H_2O) and acetonitrile (CH_3CN) were purchased from Fisher Scientific. Pooled human intestinal microsomes (HIM) (n = 18 donors) were purchased from Xenotech (Lenexa, KS).

Supplements Analyzed

Six supplements labeled to contain DHB or bergamottin were selected: SciFit DHB 300 (SciFit, Oakmont PA; lot 57454), Trisorbagen (Anabolic Xtreme, Tempe AZ; lot 202609), Xceler8 DHB (VitaSport, Chino Hills CA; lot US 37700), AttentionLink (Hi-Tech Pharmaceuticals, Inc., Norcross GA; lot 08132039), Finaflex 1-Alpha (Redefine Nutrition, Alpharetta GA; lot 824912013), and Finaflex 1-Andro (Redefine Nutrition, Alpharetta GA; lot 0500313). Five capsules from each product were analyzed quantitatively; an additional five capsules from each product were tested in CYP3A inhibition assays (Section 2.7). With the exception of AttentionLink, all capsules were opened and their contents weighed. Because the AttentionLink capsules contained a viscous material encased in a microcrystalline cellulose outer layer, they were weighed in their entirety (Appendix, Table S1).

Extraction of Supplements

The contents of the capsules (and in the case of AttentionLink, the entire capsule) were shaken for 5 h at 100 rpm in 3.0 mL of MeOH. Aliquots (600 mL) of the extract were filtered using 1.7 mL polypropylene Spin-X centrifuge tube filters (0.22 µm) and centrifuged for 10 min at 14×10^3 rpm. This method was modified from a study measuring furanocoumarins in teas, fruits and vegetables that found MeOH to be the most efficient solvent.[78]

Preparation of Standards

Bergamottin and DHB were dissolved in MeOH to create stock solutions of 1.6 mM each. Two calibration curves containing both standards were prepared form these stocks solutions. One standard curve (PDA curve) used six concentrations ranging from 5.00 µM to 160.0 µM for both bergamottin and DHB; the second standard curve (MS curve) used five concentrations ranging from 0.313 µM to 5.00 µM for both bergamottin and DHB.

UPLC-PDA-MS Analysis

UPLC separations of the stock solutions and supplement extracts were performed using a Waters Acquity UPLC system (Milford, MA) equipped with an autosampler, photodiode array detector (PDA), column manager, and binary solvent manager. An HSS C18 column (50 mm × 2.1 mm i.d., 1.8 µm, Waters, Milford, MA) was used for all chromatographic separations, held at a constant temperature of 40 °C. The gradient

system consisted of A, 0.1% formic acid in CH_3CN and B, 0.1% formic acid in H_2O, at a flow rate of 0.6 mL/min: 0-1.2 min, 30-60% A; 1.2-2.0 min, 60-100% A; 2.0-3.0 min, 100% A. Both standards and samples were injected in triplicate, at a volume of 2.0 µL.

The UPLC system was coupled to a Thermo Scientific TSQ Quantum Access triple quadrupole mass spectrometer (Waltham MA) with a heated electrospray ionization (HESI) source. Analyses were conducted in positive mode, with spray voltage 3800 V, vaporizer and capillary temperatures 300 °C and 350 °C, respectively, sheath gas and auxiliary gas 45 and 35 (arbitrary units), respectively. Tube lens offset and skimmer offset were 89 and 0, respectively. The mass spectrometer was calibrated externally using polytyrosine. Data were collected on the mass spectrometer using full scan mode, using a scan time of 0.3 s, and mass range of 150-500 *m/z*; data were collected at 250 nm on the PDA. All data were analyzed using Xcalibur V2.2 software.

Method Validation

Linearity of the calibration curves was assessed by least-squares analysis. Precision and accuracy were determined by calculating the relative standard deviation (RSD) and relative error (RE), defined as the percent difference between the mean observed concentration and the nominal concentration, of three replicate analyses of the standards. All analyses of the extracts were performed in triplicate on a single day. Interday RSD and RE were determined by analyzing the standard solutions in triplicate on three separate days. The limit of detection (LOD) and limit of quantification (LOQ) were defined as 3.3*s*/*m* and 10*s*/*m*, respectively (where *s* is the standard deviation of the

response and *m* is the slope of the calibration curve), as per the guidelines set forth by the International Conference on Harmonisation (ICH).[79]

Matrix effect was evaluated by comparing the relative responses of analyte spiked into a MeOH blank and the supplement extracts.[80] A 2.5 µL aliquot of a 20 mM bergamottin and DHB solution was added to 497.5 µL of MeOH and supplement extract; a 2.5 µL aliquot of MeOH was added to 497.5 µL of the same supplement extracts to provide a comparison to the unspiked supplements. The analyte peak areas of the spiked supplements (*S*) minus the peak areas of the unspiked supplements (*U*) were compared to the average peak area of the spiked MeOH (*M*) and expressed as a percent recovery: (*S-U)*/*M*×100. Extraction efficiency was evaluated by adding 30 µg of bergamottin and DHB to four capsules of each supplement. The supplements were extracted as described in Section 2.3 and quantification was performed as described in Section 2.5. The average amount measured in unspiked capsules was subtracted from the amount measured in spiked capsules, and the remainder was used to calculate percent recovery.

CYP3A Inhibition Assays

A dilution scheme was devised using the product with the highest measured amount of DHB (SciFit DHB 300). The corresponding extract was reconstituted with 130 µL MeOH, which was diluted 1:10 in MeOH. Each of these methanolic solutions was diluted further into incubation mixtures (see below) to yield final DHB concentrations of 1 and 0.1 µM; the higher concentration approximates the K_i of DHB towards CYP3A using human intestinal microsomes (HIM) and midazolam as the probe substrate.[11] All

other supplements were reconstituted and diluted in the same manner as SciFit DHB 300.The final concentration of MeOH (1.0%) was the same in all incubations.

Midazolam (4 μM) was incubated with (0.05 mg/mL protein) for 4 min at 37°C in the presence of diluted extracts, DHB, bergamottin, ketoconazole, or vehicle control; the final concentrations of DHB, bergamottin, and ketoconazole were 1 and 0.1 μM. Reactions were initiated with nicotinamide adenine dinucleotide phosphate (1 mM final concentration) and were terminated by removing a 100-μL aliquot and adding to 300 μL of ice-cold CH_3CN containing an internal standard (300 μg/mL alprazolam). Samples were vortexed (~30 s) and centrifuged (3000 *g* × 10 min at 4 °C), after which 100 μL of supernatant were removed and analyzed for 1′-hydroxymidazolam by LC-MS-MS on an API 6500 QTrap operated in MRM mode and equipped with an electrospray ionization source. Calibration standards were matrix-matched and were linear from 3.9 to 2000 nM. The QTrap was coupled to a Shimadzu Nextera UHPLC system (Kyoto, Japan). Chromatographic separation of midazolam, 1′-hydroxymidazolam, and alprazolam was achieved on a Thermo Scientific Aquasil C_{18} (2.1 × 50 mm, 3 μm) HPLC column (Waltham, MA) using a gradient method following a 7-μL injection of each supernatant. The gradient system consisted of A, 0.1% formic acid in CH_3CN and B, 0.1% formic acid in H_2O, at a flow rate of 0.75 mL/min: 0-0.4 min, 5% A; 0.4-1.5 min, 5-95% A; 1.5-2.1 min, 95% A; 2.1-2.11, 95-5% A; 2.11-3.0, 5% A. Sample and column temperatures were 4°C and 40°C, respectively. Quality controls (QC) of 10, 100, and 1500 nM were used to assess accuracy. All standards and (QC) were accurate to within 20% of the nominal value; QC precision was <15% RE.

Results and Discussion

Method Validation

The PDA calibration curve (5.00 µM to 160.0 µM) showed excellent linearity in UV response (DHB R^2 = 0.9996, bergamottin R^2 = 0.9995); however, the MS response exhibited a limited linear dynamic range (0.156 µM to 5.00 µM). Because of the latter, the UV detection was used to analyze supplements with analytes corresponding to the higher concentration range. The second curve (0.156 µM to 5.00 µM) was linear in both the UV (DHB R^2 = 0.9993, bergamottin R^2 = 0.9966) and MS (DHB R^2 = 0.9977, bergamottin R^2 = 0.9968) response; due to the superior resolving power of MS, afforded by the ability to select for specific *m/z*, the MS signals were used to quantify supplements with analyte concentrations in this range. The LODs were 0.073 µM (DHB) and 0.10 (bergamottin) for the PDA curve and 0.054 µM (DHB and bergamottin) for the MS curve. The LOQs were 0.22 µM (DHB) and 1.8 µM (bergamottin) for the PDA curve and 0.16 µM (DHB and bergamottin) for the MS curve. Parameters for the standard curves are summarized in Table 4. When converted to µg/capsule, the LODs were 0.074 µg (DHB) and 0.12 (bergamottin) for the PDA curve and 0.060 µg (DHB and bergamottin) for the MS curve, while the LOQs were 0.22 µg (DHB) and 2.0 µg (bergamottin) for the PDA curve and 0.18 µg (DHB and bergamottin) for the MS curve.

Intraday precision in the PDA curve was below 1.0% for both analytes (Table 5) except at one concentration (10 µM), which had an RSD of 8.0%. Interday precision for the same standard curve ranged from 1.2 to 5.9%. The RE for both analytes, both intra and interday, was below 5.8%. The measurements from the MS curve (Table 6) had

slightly higher RSDs (ranging from 1.2 to 5.4% intraday and 1.4 to 7.0% interday); whether this decrease in precision was inherent to the MS detector or a consequence of the much lower concentrations in the standard curve is unknown. The RE for both analytes was, in general, below 5.4%, with a maximum RE of 8.0% for bergamottin and 6.7% for DHB.

Table 4. Parameters of calibration curves.

	Analyte	Slope (± SD)	r^2	LOD (μM)	LOQ (μM)
PDA Curve	**1**	4.087×10^3 (± 24)	0.9995	0.10	1.8
(5.00 μM to 160.0 μM)	**2**	2.451×10^3 (± 9)	0.9996	0.073	0.22
MS Curve	**1**	2.101×10^6 (± 2.7×10^4)	0.9968	0.054	0.16
(0.313 μM to 5.00 μM)	**2**	2.729×10^6 (± 4.5×10^4)	0.9977	0.054	0.16

Table 5. Intra and interday precision and accuracy of the PDA curve.

Analytes	Concentration of Standard Solution Injected (μM)	Intraday		Interday	
		RSD (%)	RE (%)	RSD (%)	RE (%)
1	160	0.52	5.8	3.0	4.3
	80.0	0.40	3.8	2.3	1.1
	40.0	0.58	0.69	2.3	2.1
	20.0	0.47	1.9	1.9	4.0
	10.0	0.20	3.7	3.8	1.7
	5.00	3.6	1.2	3.7	2.5
2	160	0.47	0.64	0.44	0.81
	80.0	0.37	1.3	1.2	2.1
	40.0	0.32	3.8	5.3	3.1
	20.0	1.9	4.8	4.4	3.7
	10.0	8.0	3.4	5.9	0.65
	5.00	0.45	1.0	1.4	1.9

Table 6. Intra and interday precision and accuracy of MS curve.

Analyte	Concentration of Standard Solution Injected (μM)	Intraday		Interday	
		RSD (%)	RE (%)	RSD (%)	RE (%)
1	5.00	4.4	1.2	4.3	2.8
	2.50	3.0	2.4	3.7	2.2
	1.25	4.6	5.2	4.5	5.4
	0.625	4.9	8.0	7.0	2.7
	0.313	5.4	3.2	5.4	0.35
2	5.00	1.7	1.6	1.4	1.3
	2.50	1.2	4.6	2.1	3.8
	1.25	1.8	6.7	3.4	4.3
	0.625	4.6	1.6	3.8	4.3
	0.313	2.7	2.9	4.9	3.1

Except for Xceler8 DHB, matrix effects (expressed as percent recovery) were all within 15% (Table 7). Because of the substantial matrix effect of Xceler8 DHB, further analysis of this supplement, including quantification and *in vitro* testing, is not reported here. Extraction efficiency was above 84.8% (± 1.1) for all supplements tested, with one exception; AttentionLink demonstrated 77.7% (± 3.7) recovery of bergamottin (Table 8).

Table 7. Matrix effects, expressed as mean recoveries of spiked analyte in supplement extracts.

	% Recovery (± SD)	
	Bergamottin	DHB
SciFit DHB 300	97.1 (± 4.9)	102.2 (± 9.2)
Trisorbagen	100.2 (± 4.9)	99.3 (± 8.1)
Xceler8 DHB	9.2 (± 1.9)	9.54 (± 0.80)
AttentionLink	85.9 (± 6.7)	102.0 (± 3.0)
Finaflex 1-Alpha	100.5 (± 1.9)	104.1 (± 5.3)
Finaflex 1-Andro	88.2 (± 5.9)	87.5 (± 5.4)

Table 8. Extraction efficiency, expressed as mean recoveries of spiked analyte, in supplement extracts.

	% Recovery (± SD)	
	Bergamottin	DHB
SciFit DHB 300*	101. (± 12.)	100.1 (± 7.0)
Trisorbagen	90.4 (± 1.1)	84.8 (± 1.1)
AttentionLink	77.2 (± 3.7)	99.7 (± 4.3)
Finaflex 1-Alpha	93.49 (± 0.80)	98.0 (± 3.2)
Finaflex 1-Andro	98.6 (± 5.1)	86.7 (± 3.1)

*The percent recovery for SciFit DHB 300 was calculated as the amount measured in a spiked capsule minus the average amount of analyte measured in unspiked capsules (12.13 (± 0.23) µg bergamottin and 65.51 (± 0.64) µg DHB).

Quantification of Bergamottin and DHB in Dietary Supplements

Of all the supplements analyzed, only two had detectable amounts of bergamottin and DHB (Appendix, Table S2). The SciFit DHB 300 capsules, the label for which claimed 300 mg pure DHB, contained an average of 12.13 (± 0.23) µg bergamottin and 65.51 (± 0.64) µg DHB per capsule. Bergamottin was detected in Xceler8 DHB, but due to substantial matrix effects (Section 3.1, Table 7) the quantification is not reported here. Complete per-capsule data are available in the Appendix, Table S2.

CYP3A Inhibition Assay

Vehicle control reaction velocities of 416 ± 29 pmol/min/mg protein demonstrated acceptable CYP3A activity in the HIM lot used. The CYP3A inhibitor, ketoconazole, abolished 1'-hydroxymidazolam formation at 1 µM and inhibited activity by ~80% at 0.1 µM (Fig. 5). Bergamottin showed no inhibition at the concentrations

tested (Fig. 5). This lack of effect by bergamottin was expected at these concentrations based on an apparent K_i >10 µM with HIM.[11] DHB at 0.1 and 1 µM inhibited activity by 5 and 42%, respectively. Except for bergamottin, concentration dependency was observed for each treatment ($p<0.05$; 2-way ANOVA with Bonferroni adjustment).

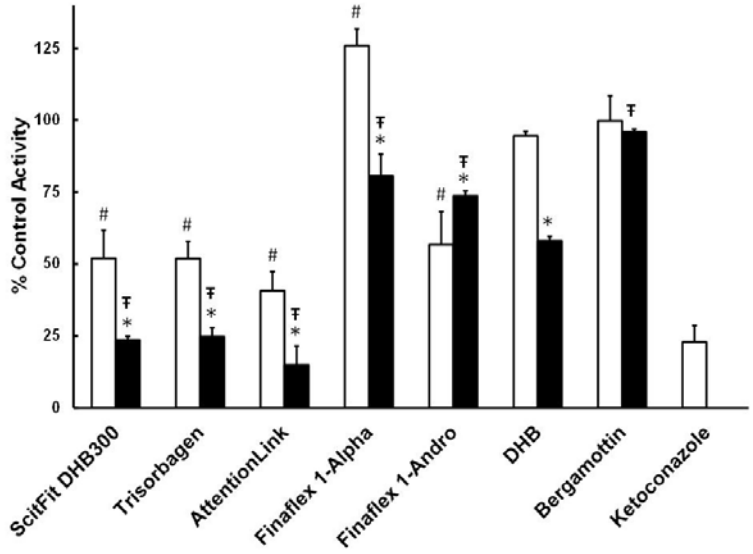

Figure 5. Comparison of the effects of various supplements labeled to contain DHB with known CYP3A inhibitors on CYP3A activity in human intestinal microsomes. DHB, bergamottin, and ketoconazole were tested at 0.1 µM (white) or 1 µM (black). The methanolic extract of SciFit was tested such that the final concentration of DHB was 0.1 or 1 µM. All other methanolic extracts were tested at the same dilutions as SciFit. Bars and error bars denote the means and SDs, respectively, of triplicate incubations. Inhibition by 1 µM ketoconazole was below the limit of quantification. *$p < 0.05$ between supplement extracts; $^{\#}p < 0.05$ versus 1µM DHB standard; $^{\text{Ŧ}}p < 0.05$ versus 0.1 µM DHB standard. Statistical comparisons were made via two-way ANOVA with a Bonferroni adjustment.

Because the extract dilutions were based on the measured DHB content in the SciFit DHB 300 supplement, this supplement was expected to behave most like authentic DHB. However, this supplement was approximately two-fold more potent than DHB (Fig. 5). In addition to SciFit, two supplements (Trisorbagen and AttentionLink)

demonstrated potent inhibition of CYP3A activity despite very low measured amounts of DHB and bergamottin. Finaflex 1-Alpha appeared to stimulate CYP3A activity at the lower concentration, which has been observed with low concentrations of bergamottin (< 2.5 μM) in incubations with HIM and midazolam.[12] Lastly, an inverse relationship between dose and response was observed with Finaflex 1-Andro.

Conclusions

The quantity of DHB measured in one SciFit capsule (0.065 mg) was considerably less than that in a glass of grapefruit juice (2.1 to 3.8 mg) used in clinical studies reporting a significant increase in victim drug systemic exposure when co-administered with the juice.[4, 81-83] A consumer would have to take 32 capsules of SciFit to achieve a dose of DHB equivalent to the lowest effective concentration reported in clinical studies.[82] Despite the expectation that the supplements would lack CYP3A inhibitory activity, several of the extracts were more potent than DHB alone, indicating additional CYP3A inhibitors present in the supplements. Trisorbagen, for example, was labeled to contain a standardized piperine composition, though it did not report actual quantities; piperine has been demonstrated previously to inhibit CYP3A activity in human liver microsomes (K_i ~40 μM) and may be involved in the aforementioned *in vitro* activity.[84] Whether such activity translates to the clinical setting remains to be determined. Further analysis of the supplements would provide additional insight by identifying the constituents responsible for the unexpected inhibitory potency.

Acknowledgments

This research was supported by the National Institutes of Health/National Institute of General Medical Sciences via grant R01 GM077482. Thank you to Brandie M. Ehrmann and Tyler N. Graf for their assistance with the triple quadrupole mass spectrometer and its software.

CHAPTER IV

DRUG DISCOVERY OF MICROBIAL METABOLITES

Natural products as a source of lead compounds for drug discovery

Microorganisms and plants have evolved to produce wide varieties of compounds that cause a biological effect in other organisms[85] – what some researchers have likened to a chemical arms race.[86, 87] Such natural products have been naturally selected to provide array of highly varied and diverse compounds evolved expressly for interactions with biological macromolecules.[88]

Despite the surge in popularity of combinatorial chemistry as a source for high-throughput screening libraries, natural products and their derivatives remain a large majority of both new chemical entities (NCEs) and approved drugs,[89] likely due to the aforementioned inherent diversity and affinity for biological targets.[88, 90] When compared to the libraries of compounds manufactured by combinatorial chemistry, the chemical diversity of natural products has been shown to be significantly greater;[91, 92] key features shared by natural products and current drugs, such as the number of chiral centers, that confer the biological specificity crucial to both secondary metabolites and medications, are often lacking in the products of combinatorial synthesis.[93]

Of all the NCEs discovered in the last 30 years, only 29% were completely synthetic in origin; disregarding the biologics and vaccines, natural product compounds accounted for ~50% of the small-molecule NCEs.[94] Of the antiinfectives approved in

that time span, natural product-derived compounds make up 77% of the total, and 68% of the small molecule antiinfectives.[94] It is noteworthy that the synthetic antiinfective drugs tend to fall into two chemotypes, including the azole-based antifungals, and the quinolone-based antibacterials.[89] Of the currently available small-molecule cancer drugs, 74% are natural product-derived; if the biologically-derived compounds are included, this number rises to 78%. More striking is the fact that natural product-derived compounds make up 79% of *new* small molecule anticancer drugs approved between 1981 and 2010.[94] Indeed, the only *de novo* combinatorial drug approved by the FDA is sorafenib mesylate, which entered the market in 2005 for the treatment of advanced renal cancer.

While combinatorial chemistry is a powerful tool for optimizing known compounds, natural products remain the primary source of new chemical diversity. Several problems associated with natural products screening that originally caused pharmaceutical companies to turn instead to combinatorial libraries (i.e. speed of isolation, identification of active compounds, rediscovery of known compounds, etc.) are being addressed by advances in both technology[91] and techniques.[95] To address the ever-present need for new active compounds, the wealth of secondary metabolites produced by the natural world must be explored.

The role of fungi as source of biologically active secondary metabolites

Historically, fungi have provided the human population with a broad range of medications, ranging from antibiotics such as the penicillins to the cholesterol-lowering drugs based on mevinolin (Lovastatin).[96] More recently, fingolimod, derived from a

fungal secondary metabolite, was approved for the treatment of multiple sclerosis,[97] and trials are ongoing for the use of psilocybin as a treatment for anxiety in cancer patients.[98] Caspofungin, introduced to the market in 2001 as a treatement for refractory invasive aspergilloses, represented the first new class of systemic antifungal agents to be approved in 25 years.[99] Despite the success of these and similar lead compounds, only a fraction of the available fungal diversity has been studied. While estimates of fungal species range from 0.5 million[100] to 9.9 million,[101] the commonly cited conservative estimate is that at least 1.5 million fungal species exist currently, with only 75,000 of these being described in the literature.[102] Accessing new ranges of biological diversity inevitably leads to the discovery of new (and often unique) natural products.[91] The recent foray into endophytic fungi has produced several new groups of compounds;[103, 104] it can only be inferred that exploring further into the huge breadth of the fungal world will provide additional families of molecular scaffolds, with the hopeful outcome of discovering new lead compounds for future drugs.

Mining suppressed genes can lead to new natural products

Fungal secondary metabolites are produced via several key pathways, involving polyketide synthases (PKSs), non-ribosomal peptide synthases (NRPSs), hybrid PKS-NRPS (HPN), as well as pathways coding for terpenes and indole alkaloids.[105] In fungi, these genes are often found in clusters, a fact that has implications on the transcription and regulation of secondary metabolite pathways. With the recent advent of complete fungi genome sequences,[106-109] it has become clear that the number of gene clusters

encoding these pathways greatly outnumbers the known secondary metabolites for these organisms.[110] A study on the sequence of *Aspergillus niger* demonstrated that less than 30% of its PKS-NRPS-, and HPN-encoding gene clusters were transcriptionally active.[111] This transcriptional suppression has led to a variety of studies delving into the mechanisms of transcriptional regulation, as well as techniques designed to "unlock" these suppressed pathways.

Regulation of gene cluster transcription is a complicated, and not fully understood, process, involving many different transcription factors and a variety of epigenetic influences. Transcription factors affecting secondary metabolite production fall into two categories: narrow, or pathway-specific transcription factors, and broad domain transcription factors.[112] The first pathway-specific factor identified was AflR, in 1993, from a strain of *Aspergillus parasiticus*,[113] and has since become a model for understanding such factors and their role in cluster regulation. Like most pathway-specific factors, *aflR* is found embedded within the gene cluster that it regulates;[114] deletion or mutation of the gene suppresses expression of sterigmatocystin and aflatoxin cluster genes,[113] while insertion of additional copies of *aflR* induces increased gene expression.[115] Broad domain transcription factors respond to changes in environmental conditions, such as carbon,[116] nitrogen,[117] and pH.[118] Both negative and positive regulation of gene clusters have been evidenced for each of these conditions and their corresponding transcription factor proteins.[112]

A more recent insight into the regulation of secondary metabolite gene transcription involved the discovery of an *Aspergillus* methyltransferase, LaeA.[119]

Deletion of *laeA* in *A. nudulans*, *A. fumigatus*, and *A. terreus* strains repressed the production of several secondary metabolites through the transcriptional silencing of their encoding genes, while overexpression of *laeA* increased the production of these same compounds.[119] Unlike many other genes that regulate secondary metabolism, the loss of *laeA* did not significantly impact the developmental process of the fungi,[119] indicating the possibility of using other epigenetic modification to access similar metabolite pathways that are normally transcriptionally silent.

Such efforts have begun in the form of small-molecule chemical epigenetic modification. In the normal transcription process, a number of small molecule modifications of the histone proteins in chromatin affect the transcriptional availability of the DNA. Within the chromatin structure, DNA is tightly coiled around core histone proteins, forming nucleosomes; linker histones bind nucleosomes together as chromatin. Methylation, acetylation, phosphorylation, ADP-ribosylation, or ubiquitination of the histone *N*-terminal tail regions affect the binding of the histone proteins to DNA, changing the structure of the chromatin and subsequently the accessibility of transcription factors to DNA regions.[120] By altering these processes, it is possible to affect the transcription of the genes that they regulate.

The most frequently studied and best understood epigenetic process is histone acetylation. Histone acetylation is controlled by the enzymes histone acetyltransferases (HATs) and histone deacetylases (HDACs). HATs direct the addition of acetyl groups to lysine residues in the amino-terminal histone tails, neutralizing that portion of the protein and relaxing the chromatin structure, thereby increasing accessibility of transcription

complexes as well as recruiting transcription cofactors.[120-123] Conversely, HDACs remove acetyl groups from the histone tails, resulting in a more compact and inaccessible form of chromatin, consequently silencing transcription.[120-122]

DNA itself can also be posttranslationally modified; in fungi this process is regulated by DNA methyltransferases (DNMTs). DNMTs add a methyl group to cytosine, resulting in a 5-methylcytosine product, altering gene transcription[124, 125] by affecting the recognition of DNA sequences by transcription factors. DNMT inhibitors tend to be nucleoside analogues that become incorporated into DNA during replication. DNMTs bind irreversibly to the analogue base, thus depleting the enzymes and reducing DNA methylation. This decrease in DNA methylation results in additional gene activation.[126]

Recently, efforts have been made to manipulate the epigenetic regulation of gene transcription by growing fungal strains in the presence of various small-molecule drugs. Such research has focused mainly on HDAC inhibitors[111, 127-129] and DNMT inhibitors,[111, 129-131] in order to make more transcriptionally available the genes that these proteins normally help to suppress. Treatment of *Aspergillus alternata* and *Penicillium expansum* with the HDAC inhibitor trichostatin A (TSA) resulted in increased production of numerous secondary metabolites.[127] A similar study using the HDAC inhibitor suberoylanilide hydroxamic acid (SAHA) to treat *Aspergillus niger* resulted in the isolation of a new metabolite, nygerone A, containing a unique 1-phenylpyridin-4(1*H*)-one core that previously had not been reported from any natural source.[128] Treatment of *Penicillium citreonigrum* with the DNMT inhibitor 5-azacytidine (5-AZA) produced ten

additional secondary metabolites, including two new compounds.[130] New compounds have also been isolated from a SAHA-treated growth of *Cladosporium cladosporioides* and a 5-AZA-treated growth of a *Diatrype* species.[129] The effects of SAHA and 5-AZA on *Apergillus niger* gene expression were further characterized by using real-time quantitative reverse-transcription PCR to analyze the change in expression of PKS, NRPS, and HPN pathways when treated with the epigenetic modifiers.[111] In this study, all but seven of these 55 gene clusters showed increased transcriptional rates.

Aims of this project

The investigations described here utilize two approaches to maximize the genomic potential of fungi. One study investigates the impact of media on the production of fungal secondary metabolites. It has been shown that the manipulation of environment and nutrition can have substantial impacts on the quantity and diversity of secondary metabolite production,[132-139] and optimization of this initial step may have profound effects on the output and success of a natural products screening program.

The second study makes use of the proteasome inhibitor bortezomib (Fig. 6) as an epigenetic modifier to induce the transcription of silent secondary metabolite genes. Initial research on the epigenetic modification of fungi has focused on agents that directly target the transcription of genes. HDAC inhibitors cause chromatin to become more open and transcriptionally active; DNMTs alter gene transcription by posttranslationally modifying DNA. Bortezomib affects the transcriptional process by inhibiting proteasomes, which are large protein complexes responsible for the degradation of

proteins by proteolysis. Among the many proteins degraded by the proteasome pathway, several transcriptional regulators have been identified,[140, 141] implicating proteasomes as a crucial player in the complicated functions of gene transcription.

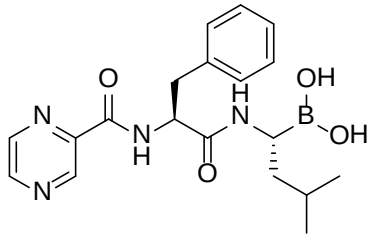

Figure 6. The proteasome inhibitor, bortezomib.

There are no references in the current literature describing the use of bortezomib, or any proteasome inhibitor, as an epigenetic modifier to induce the production of new secondary metabolites in fungus.

CHAPTER V

EVALUATION OF CULTURE MEDIA FOR THE PRODUCTION OF SECONDARY METABOLITES IN A NATURAL PRODUCTS SCREENING PROGRAM

This chapter has been published in *AMB Express* and is presented in that style. VanderMolen, K.M., Raja, H.A., El-Elimat, T., Oberlies, N.H. Evaluation of Culture Media for the Production of Secondary Metabolites in a Natural Products Screening Program. *AMB Express.* **2013**. 3:71.

Introduction

Fungi provide a plentiful and diverse source of unique and often bioactive metabolites, and they have produced a number of medicinally important compounds, including penicillin, mevinolin (Lovastatin),[96] fingolimod,[97] and caspofungin.[99] The search for new and active compounds from microbial sources is a pursuit for many natural products laboratories. Typically, these efforts will employ a standard culture procedure that most or all microbial strains pass through as a preliminary step to the natural products discovery process. The manipulation of environment and nutrition has been shown to have substantial impacts on the quantity and diversity of secondary metabolite production,[132-139] and optimization of this initial step, the microbial culture, may have profound effects on the output and success of a natural products screening program.

Methodical modification of culture growing conditions is often referred to as the OSMAC (one strain, many compounds) approach.[132, 142] This concept is ideal for fully

exploiting the metabolomic diversity of a single or handful of organisms, but it becomes cumbersome when applied to a large-scale screening program. Applying a suite of culture conditions for even one factor, whether it is media, salinity, pH, temperature, etc., to every screened organism quickly becomes so labor and material intensive as to be impractical. The aim of this study, therefore, was to determine an ideal culture medium that could be applied to a drug discovery screening program as a standard preliminary medium.

This ideal medium would have to fit several criteria. In a medium-throughput but academic setting, large volumes of media will be used, so only inexpensive, readily available, and easily prepared media were evaluated. In addition, some media that have shown promise as metabolite inducers in other studies, such as vermiculite,[143] were excluded due to the high start-up cost necessary for such cultures. Our aim was to evaluate different media that could be integrated into the screening process with minimal changes to the existing equipment available. Six liquid broths and five solid-state media were chosen for evaluation. Three fungal strains were grown on each medium, and the resulting metabolite profiles were assessed.

In addition to a qualitative examination of the metabolite profile, the production of several marker compounds was tracked. Each fungus chosen for this study was previously studied and characterized by our laboratory, and each produced a known compound sharing many structural features with compounds that our research group isolates. Two [*Glomerella acutata* (G2) and a *Hypocreales* sp. (G24)] were isolated as endophytes from pawpaw (*Asimina triloba* L., *Annonaceae*) leaves collected in North

America. The third strain, a *Nectriacaea* sp. (G142), was isolated from freshwater submerged wood collected in North America. All strains used belonged to *Hypocreales*, of the phylum *Ascomycota.*[144] G2 and G142 both produced aurofusarin, while G24 produced PC3. The goal was to identify two distinct fungi, one an endophyte and one from freshwater, that produced identical secondary metabolites, and two from the same source, endophytes from pawpaw, that biosynthesized distinct metabolites. The production of these metabolites was tracked to provide a more in-depth assessment of the fungal extracts.

Materials and methods

Isolation of fungi

Study site, collection and isolation of fungal endophyte strains. Healthy living twigs and leaves of pawpaw (*Asimina triloba* L., *Annonaceae*) were randomly collected from a mature tree located at a private property in Indianapolis, Indiana, USA in July 2011 (9012 Colgate St.). Extra moisture was removed from the samples, and they were transported back to the laboratory in paper bags, where they were processed within 24–48 hours.[145] In the lab, the twigs and leaves were cut into small pieces (approximately 2-5 mm in length) and washed in distilled water (H_2O). Subsequently, the segments were surface-sterilized by sequential immersion in 95% ethyl alcohol (EtOH; 10 s), sodium hypochlorite (10-15% available chlorine; 2 min), and 70% EtOH (2 min).[145] After the sterilization procedure, the plant segments were washed in distilled H_2O and allowed to dry. The surface sterilized segments were then transferred using sterile conditions onto

2% malt extract agar [MEA; Difco, 20 g MEA, 1 L sterile distilled H_2O amended with streptomycin sulfate (250 mg/L) and penicillin G (250 mg/L)]. To test the efficiency of the surface-sterilization procedure, and to confirm that emergent fungal colonies were indeed endophytic and not of epiphytic origin, individual surface-sterilized leaf and stem segments were spread on separate 2% MEA plates with antibiotics; the absence of fungal growth on the nutrient media confirmed the effectiveness of the sterilization procedure.[146] Plates were sealed with parafilm and incubated at room temperate in 12 h dark/light cycles until the emergence of fungal colonies was observed. Axenic cultures of emergent fungal endophytes are maintained at the University of North Carolina at Greensboro, Department of Chemistry and Biochemistry Fungal collection.

Isolation of fungi from submerged wood in fresh water. Submerged, dead woody debris was collected randomly in a freshwater lake in North Carolina, USA in October 2011 (Lake Brandt, 36°10'1"N, 19°50' 18"W). Efforts were made to identify and collect substrates that had been submerged for a considerable time. This was estimated by observation of the degree of softening by fungal soft rot and colonization by other aquatic organisms. Samples were further processed in the laboratory to obtain axenic fungal cultures using established procedures.[147, 148] Axenic cultures of freshwater fungi are maintained at the University of North Carolina at Greensboro, Department of Chemistry and Biochemistry Fungal collection.

Molecular identification of fungal strains by DNA extraction, PCR and sequencing. Methods employed to identify fungi isolated in this study using the nuclear ribosomal internal transcribed spacer region 1, 2, along with the short structural gene (5.8S) have been outlined in the supporting information of earlier studies.[149-151] The ITS region was chosen to identify fungal species, as it has been recently identified as a barcode marker for fungi.[152] Sequence data were deposited in GenBank; the accession numbers for G2, G24, and G142 were AB858344, AB858345, and AB858346, respectively. Cultures were deposited with the Leibniz Institute DSMZ-German Collection of Microorganisms and Cell Cultures; the accession numbers for G2, G24, and G142 were DSM 27861, DSM 27862, and DSM 27863, respectively.

Liquid media cultivation

Each fungal strain was first cultivated on 2% malt extract agar. Plugs from these cultures were used to inoculate 50 mL of six different culture broths in 250 mL Erlenmeyer flasks. These broths included Czapek Dox (CD)(Sigma Aldrich), 2% Malt Extract (ME)(Difco), Potato Dextrose (PD)(Difco), YPSS (4 g yeast extract, 14 g soluble starch, 1 g dibasic K_2HPO_4, 0.5 g $MgSO_4 \cdot 7H_2O$, 1 L H_2O), YESD (20 g soy peptone, 20 g dextrose, 5 g yeast extract, 1 L H_2O), and PYG (1.25 g soy peptone, 1.25 g yeast extract, 5 g D-glucose, 1 L H_2O). Liquid cultures were grown for 14 days on an orbital shaker (100 rpm) at room temperature before extraction. Each culture was grown in triplicate.

Solid media cultivation

Five forms of solid media, including rice, grits, oatmeal, wheat germ, and a 3:1:1:1 mixture of the same were used. To prepare the solid media, 10 g of medium were mixed with 25 mL of deionized H_2O in a 250 mL Erlenmeyer flask, sealed with a foam plug and tinfoil, and autoclaved. Plugs (from the 2% malt extract agar cultures listed above) of each fungus were used to inoculate 15 mL of YESD. These seed cultures were grown for three days on an orbital shaker (100 rpm) at room temperature, and these were used to inoculate the solid media, which was allowed to grow (stationary) for an additional 11 days at room temperature. Each culture was grown in triplicate.

Extraction of fungal cultures

To each culture, 60 mL of 1:1 chloroform:methanol ($CHCl_3$:MeOH) were added. Solid media cultures were chopped with a spatula to ensure proper mixing. The cultures were shaken overnight (100 rpm) at room temperature and subsequently filtered by vacuum. The filtrate was stirred for 1 h with 90 mL of $CHCl_3$ and 100 mL deionized H_2O. This mixture was then transferred to a separatory funnel, and the bottom organic layer was evaporated to dryness *in vacuo*. The dried organic extract was reconstituted with 100 mL 1:1 acetonitrile (CH_3CN):MeOH and 100 mL hexanes. This biphasic solution was stirred for 1 h and transferred to a separatory funnel. The bottom, defatted organic extract was evaporated to dryness *in vacuo.*

Analysis of fungal metabolite profiles by ultra performance liquid chromatography-mass spectrometry (UPLC-MS)

The defatted organic extract of each fungal culture was examined by UPLC-MS. The method used was developed as part of a dereplication procedure.[153] In brief, analyses were performed using a Waters Acquity UPLC system utilizing a BEH C18 column (Waters; 50 mm × 2.1 mm i.d., 1.8 µm). The mobile phase consisted of CH_3CN and 0.1% formic acid-H_2O, increasing linearly from 15% CH_3CN at the time of injection to 100% CH_3CN at 10 min. The flow rate was 0.3 mL/min and column temperature was 40 °C. The UPLC system was coupled to a Thermo Scientific LTQ Orbitrap XL equipped with electrospray ionization (ESI) source. The production of several known metabolites (Fig. 7) was tracked using high-resolution mass spectrometry (HRMS). Crude extracts were dissolved in 1:1 MeOH:dioxane at a concentration of 2.0 mg/mL; 6.0 µL were injected, and the peak areas of each metabolite measured. Additionally, extracts were also examined using the same UPLC system equipped with an evaporative light scattering detector (ELSD; Waters); all other conditions were the same.

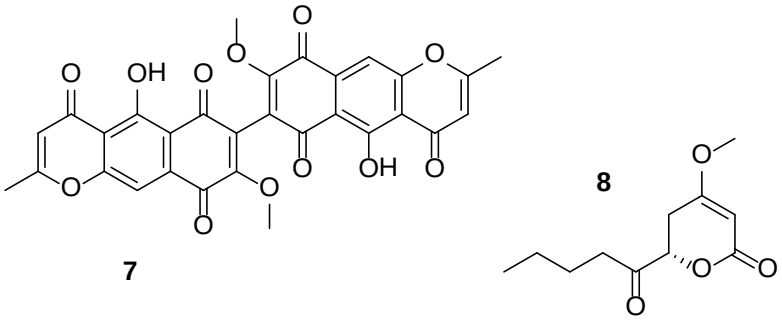

Figure 7. Marker compounds used to track the production potential of various media; (**7**) aurofusarin, (**8**) PC3.

Results

Effects of media on fungal growths

The visual differences in fungal growth were the most immediately apparent result of varying the culture medium and were a primary instigator of this study; striking differences in color occurred as various secondary metabolites were stimulated by a new medium (Fig. 8). These color changes were most notable in liquid media, but the amount of sporulation (orange) and exudate (black) produced varied between solid media, too. As an example, after the 11 days of growth on solid media, the rice cultures of G2 exhibited almost no sporulation or exudate (Fig. 8), while the grits culture showed a small amount of black exudate, the oatmeal culture exhibited heavy sporulation (orange), and the wheat germ culture had a large amount of both.

Effects of media on the profile of secondary metabolites

The various media tested exhibited marked differences in the mass of extract (Figs. 9a and b). On the whole, the cultures grown on solid media produced extracts with masses one to two orders of magnitude larger than the same fungus grown in any of the liquid media. In both solid and liquid cultures, G2 consistently produced the lowest mass of extract, though this difference was more notable in the liquid media. The variation of the amount of extract produced was greater in liquid media than solid. The greatest variation between liquid media was shown by G24; in Czapek Dox broth, the culture produced less than two mg of total defatted extract, while it produced more than 20 mg when grown in potato dextrose broth and YESD broth (Fig. 9a).

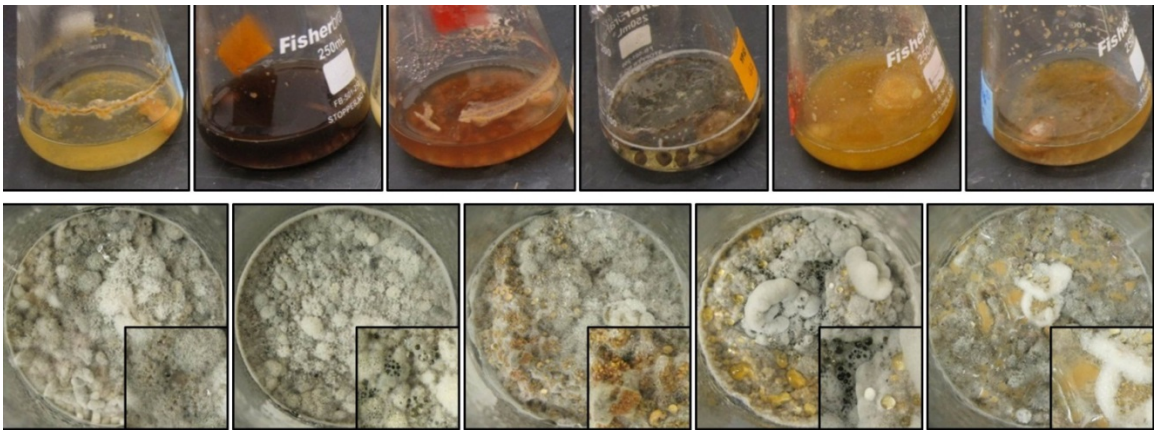

Figure 8. Photos of G2 in liquid media (top); from left to right: Czapek dox, 2% malt extract, potato dextrose, YPSS, YESD, and PYG broths. Photos of G2 on solid media (bottom); from left to right: rice, grits, oatmeal, wheat germ, and 3:1:1:1, respectively, of the same. Enlargements of the photos (2.5x) are provided in the lower right hand corner to help visualize the production of spores (orange) and/or exudates (black).

The mass of the defatted extract was also compared to the mass of the extract prior to the defatting step of the extraction procedure (Fig. 9c and d). Defatting is an important step in the extraction process for two reasons. The hexane wash eliminates some common but unwanted metabolites, such as fatty acids, that are not of interest to most natural product screening programs. It also cleans the extract of the very nonpolar constituents that are detrimental to reverse phase columns. Analyzing the percentage of extract lost in this defatting step can help to characterize the composition of the fungal extract.

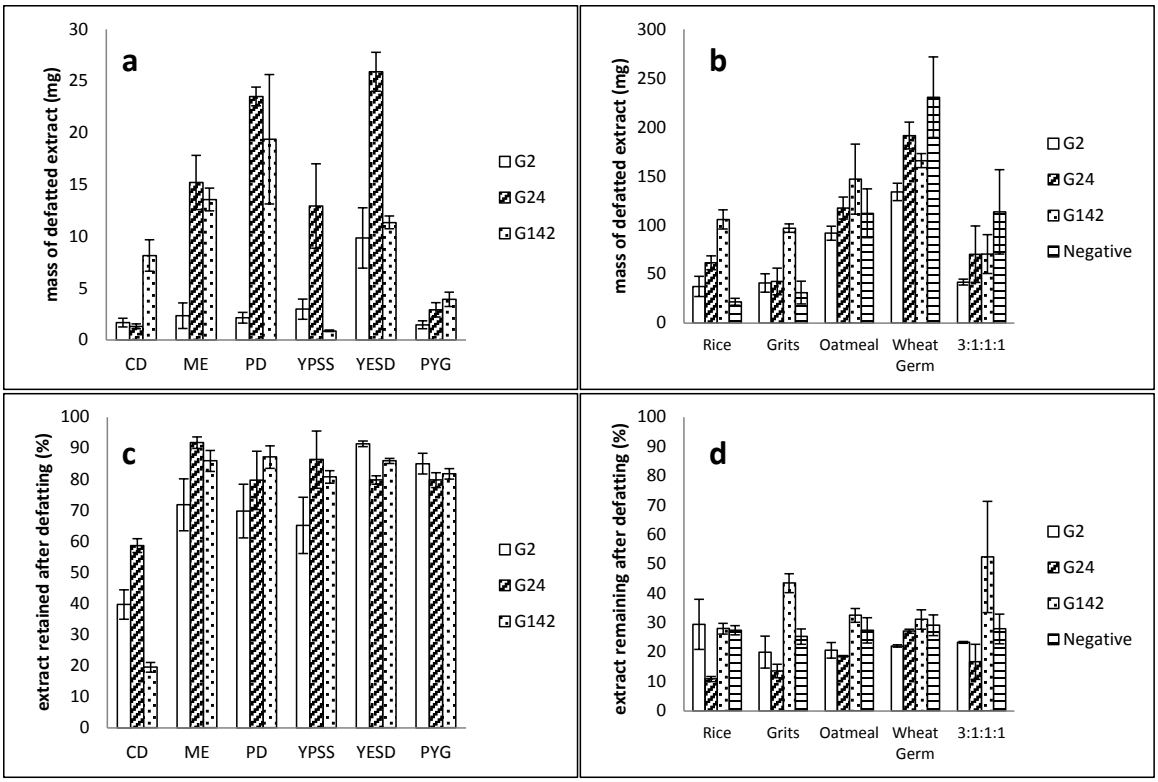

Figure 9. A comparison of the (a) mass of defatted extract of fungal growths in liquid media, (b) mass of defatted extract of fungal growths on solid media, (c) percentage of organic extract retained after the defatting step (liquid media), and (d) the percentage of organic extract retained after the defatting step (solid media). Data plotted are means±SD of three replicate growths per culture medium. The "Negative" series in solid media (b and d) refers to the mass of extracted solid media alone, with no fungal growth. The same data for liquid cultures were negligible and therefore not shown. Abbreviations of media are defined in the Methods section.

Extracts from solid media cultures retained a much smaller percentage of the original mass, typically between 10 and 30%, though G142 retained higher percentages of 42 and 52% on grits and the 3:1:1:1 mixture, respectively. Growths on liquid media, on the other hand, retained between 70 and 90% of their mass after the defatting wash, though all three fungi grown on Czapek Dox lost significant portions of their extract in this step.

Effects of media on composition of extract

The UPLC profiles of the fungal extracts showed wide variation between media (Fig. S3, Appendix). Particularly in the liquid cultures, metabolites with vastly different retention times were produced. Grown in 2% malt extract broth (ME), G142 produced nine major peaks that eluted between 4 and 6.5 min on a 10-min CH_3CN gradient. The same fungus grown in YPSS produced only five major peaks that all eluted after 7.5 min (Fig. S3, Appendix).

The production of marker compounds (Fig. 7) was compared between media by measuring the peak areas of each metabolite via UPLC-MS and multiplying by total mass of the defatted extract, in order to more accurately compare the total production of each metabolite instead of the percentage of extract the metabolite comprised. This value was expressed as relative percentage of metabolite production, normalized to the largest value of each metabolite's set. Aurofusarin was the metabolite of interest in both G2 and G142, while the metabolite of interest produced by G24 was PC3. Aurofusarin is a mycotoxin and red pigment common in *Fusarium* species.[154-156] PC3 is an analog of pestalotin, which was first described as a product of an unidentified fungus in 1973;[157] pestalotins synergistically augment the plant hormone gibberellin.[158-160] While the structural diversity of compounds from fungi can be vast,[161] these were chosen as representative compounds for a drug screening program, since they contain heteroatoms, conjugated rings, carbonyl groups, hydroxy, methoxy, and methyl moieties, and polyketide derived chains.

For all fungi, rice and grits consistently produced greater quantities of the marker compounds, while wheat germ consistently produced little or no marker compound. Few of the liquid cultures produced meaningful quantities of the marker compounds (Fig. 10), though they were detectable in most (Table 9). G2 produced modest amounts of aurofusarin when grown on oatmeal, when compared to the production when grown on rice; however, G142 consistently produced much greater quantities of aurofusarin on rice, grits, and oatmeal. While G2 produced little or no aurofusarin in the liquid cultures, G142 produced quantities in ME and PD comparable to the production by G2 on several solid cultures (Fig. 10). PC3 production was highest when G24 was grown on rice and the 3:1:1:1 mixture, though its production in CD, ME, and PD were similar to the production on solid media.

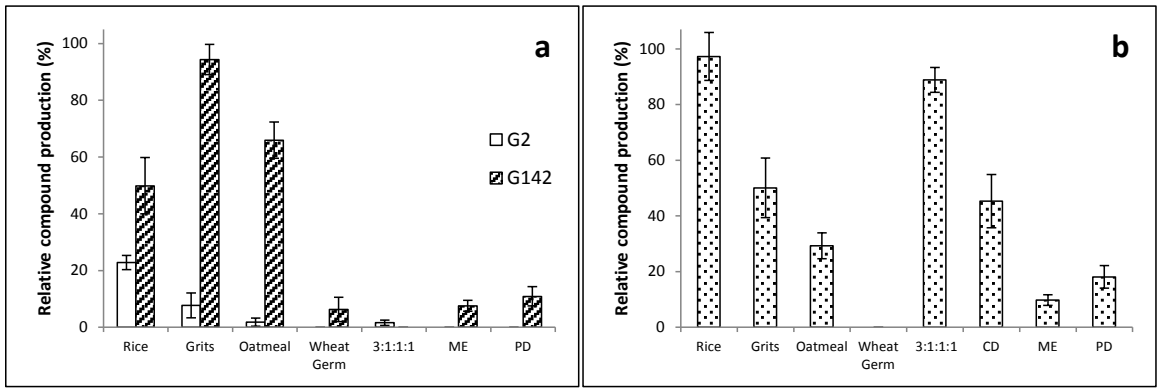

Figure 10. Relative production of marker compounds aurofusarin in G2 and G142 (a), and PC3 in G24 (b). Data plotted are means±SD of three replicate growths per culture medium.

Table 9. Summary of the production of marker compounds in solid and liquid media

	Rice	Grits	Oatmeal	Wheat Germ	3:1:1:1	CD	ME	PD	YPSS	YESD	PYG
Aurofusarin (G2)	m	m	m	d	m	u	d	d	d	u	u
PC3 (G24)	m	m	m	d	m	m	m	m	d	u	u
Aurofusarin (G142)	m	m	m	m	d	d	m	m	d	d	m

Detection of marker compounds in solid and liquid media extracts; m = measured, as shown in bar graphs (Fig. 4), d = detected at low levels, u = undetected. Limit of detection 0.22 mg/g extract.

Discussion

It has been shown that media conditions have varying effects on the production of fungal secondary metabolites.[132, 137] Often, the variation of culture conditions is used to optimize the yields of a specific compound, such as the active metabolite in a medicinal fungus[134] or drug-producing microbe.[162] In other cases, the OSMAC approach can be used to fully exploit the biodiversity of a small number of microbes, usually fewer than five.[135, 163, 164] These techniques can be very valuable for manipulating the metabolomes of several fungi at a time, but they also increase the manpower necessary to process a single culture by several fold for each growth condition being manipulated. Our laboratory processes approximately 400 new fungal cultures every year; applying the OSMAC approach to each and every culture would be impractical without the implementation of specialized equipment and procedures for the parallel cultivation of screened fungi.[133]

This study was designed to evaluate media with the intention of optimizing a drug-discovery screening program, which is a different goal than finding the ideal

medium for a specific microbial strain producing one or two key metabolites. What may be the best medium for one fungus could often prove unproductive for other strains. For example, G2 produced very little aurofusarin when grown on oatmeal, while G142 produced quantities equivalent to its production on rice. In potato dextrose broth, G24 and G142 produced large extracts, but the extract of G2 was less than 2 mg. Similarly, media that facilitate increased fungal growth and large amounts of extract may not produce compounds of interest. G24, when grown in PD or YESD liquid broths, produced extracts of similar masses to both each other and to its extracts when grown on rice, yet the metabolite of interest (PC3), was produced in significantly smaller quantities in PD and undetected in YESD. Thus, media in this study were evaluated with respect to both the amount of extract produced and the composition of that extract, including the production of the chosen marker compounds (Fig. 7). Because the media were being assessed for use in a screening program, consistency of production across all three fungal strains was a more important criterion than excellent production in just one of the strains.

The variation in extract composition and marker compound production was more pronounced than expected when this study was designed. The most surprising outcome was that the marker compounds were undetected by UPLC-MS in several of the liquid culture extracts (Table 9). This was surprising, given that the limit of detection for the method was approximately 0.22 mg/g extract.[153] Indeed, the amount of extract produced was often so drastically smaller than those produced by solid media cultures, that for a drug-discovery screening program, it would be impractical to use liquid cultures as a standard culture procedure; isolating sufficient quantities of compounds of interest would

be challenging. While it was enticing that the liquid cultures produced a lower percentage of fats than the solid media cultures, since fats complicate the purification process (Figs. 9c and d), the overall paucity of metabolites negated this benefit.

The production of marker compounds varied widely between all cultures. On oatmeal, G142 (isolated from freshwater) produced amounts of aurofusarin similar to cultures grown on rice; G2 (an endophyte) had very poor production on oatmeal. The use of only G142 in such a media survey would indicate that oatmeal may be an ideal candidate as a standard solid medium, while the added information provided by using the second fungus producing the same compound refuted this conclusion. A further example was the production of PC3 by G24 when grown on the 3:1:1:1 mixture. Again, while PC3 was produced in quantities similar to that of the rice or grits media, G2 and G142 showed poor aurofusarin production on this same medium. In general, rice appeared to more consistently produce high quantities of the metabolites of interest, while wheat germ consistently did not.

For the purposes of a fungal metabolite screening program, it seems clear that rice would serve well as a standard culture medium. The data supporting the use of rice as an ideal medium may not be surprising to researchers who routinely culture fungi; this study validates the empirical knowledge of many mycologists and natural products researchers who use rice as a go-to culture substrate. While liquid media did not perform well in this study, they should not be discounted as a viable culture condition in other circumstances. Different microbes, such as those found in marine environments, may be far more suited to a liquid growing environment than those cultured here. However, new metabolites

have been reported when marine fungi have been grown on rice,[135] which supports the use of complex solid media as a standard culture condition.

Acknowledgements

The authors thank the City of Greensboro for permission to collect samples.

CHAPTER VI

EPIGENETIC MANIPULATION OF A FILAMENTOUS FUNGUS BY THE PROTEASOME-INHIBITOR BORTEZOMIB INDUCES THE PRODUCTION OF AN ADDITIONAL SECONDARY METABOLITE

This chapter is intended for publication in the journal *RSC Advances* and is presented in that style. Coauthors include Blaise A. Darveaux, Wei-LunChen, Steven M. Swanson, Cedric J. Pearce, Nicholas H. Oberlies.

Introduction

Fungal secondary metabolites are produced via several key pathways, including those involving polyketide synthases (PKSs), non-ribosomal peptide synthases (NRPSs), hybrid PKS-NRPS (HPN), as well as pathways coding for terpenes and indole alkaloids.[105] In fungi, these genes are often found in clusters, a fact that has implications on the transcription and regulation of secondary metabolite pathways. With the recent completion of fungal genome sequences,[106-109] it has become clear that the number of gene clusters encoding these pathways greatly outnumbers the known secondary metabolites for these organisms.[110] A study on the sequence of *Aspergillus niger* demonstrated that less than 30% of its PKS-NRPS- and HPN-encoding gene clusters were transcriptionally active.[111] This transcriptional suppression has led to a variety of studies delving into the mechanisms of transcriptional regulation, as well as developing techniques to induce these suppressed pathways.

Efforts have been made to manipulate the epigenetic regulation of gene transcription by growing fungi in the presence of various small-molecule modifiers. Such research has focused mainly on HDAC (histone deacetylase) inhibitors[127-129, 165-168] and DNA methyltransferase (DNMT) inhibitors,[129-131, 166-169] in order to make more transcriptionally available the genes that these proteins normally help to suppress. Treatment of *A. alternata* and *Penicillium expansum* with the HDAC inhibitor trichostatin A resulted in increased production of numerous secondary metabolites.[127] A similar study using the HDAC inhibitor suberoylanilidehydroxamic acid (SAHA) to treat *A. niger* resulted in the isolation of a new metabolite, nygerone A, containing a unique 1-phenylpyridin-4(1*H*)-one core that previously had not been reported from any natural source.[128] Treatment of *P. citreonigrum* with the DNMT inhibitor 5-azacytidine (5-AZA) produced ten additional secondary metabolites, including two new compounds.[130] New compounds have also been isolated from a SAHA-treated culture of *Cladosporium cladosporioides* and a 5-AZA-treated culture of a *Diatrype* species.[129] The effects of SAHA and 5-AZA on *A. nigerone* expression were further characterized by using real-time quantitative reverse-transcription PCR to analyze the change in expression of PKS, NRPS, and HPN pathways when treated with the epigenetic modifiers;[166] all but seven of these 55 gene clusters showed increased transcriptional rates.

This study examined the capability of bortezomib, a proteasome inhibitor, to induce the production of secondary metabolites in a fungus (MSX 63935, order Pleosporales) that had been shown previously to biosynthesize a series of resorcylic acid lactones of polyketide origin.[170] Proteasomes are protein complexes responsible for the

degradation of proteins by proteolysis. Among the many proteins degraded by the proteasome pathway, several transcriptional regulators have been identified,[140, 141] implicating proteasomes as a crucial player in gene transcription. Growing MSX 63935 in the presence of bortezomib induced the production of an additional secondary metabolite. An analogue was also isolated after degradation of the original metabolite in solution, yielding a new compound.

Results and Discussion

Preliminary experiments tested the effects of an HDAC inhibitor (SAHA), a DNMT inhibitor (5-AZA), and a proteasome inhibitor (bortezomib), on the secondary metabolite production of MSX 63935 in several growth media. Initial experiments with solid media (rice) showed poor results, regardless of very high doses of the epigenetic modifiers (as much as 100 mg per flask). Tests with liquid media, including CzapekDox broth and potato dextrose broth (PDB), were more promising. Increased production to the expected metabolites as well as a number of additional chromatographic peaks was observed in cultures dosed with epigenetic modifiers (Fig. 11). Secondary metabolite production was greater in PDB than CzapekDox (Fig. S4, Appendix), so subsequent experiments used PDB as the culture medium. Bortezomib was chosen for further experiments because the number of additional metabolites in preliminary experiments was greater when the fungus was grown with bortezomib than with SAHA (Fig. 11); while production by bortezomib-dosed cultures was similar to 5-AZA-dosed cultures, bortezomib had not been previously studied for this application.

Triplicate growths of the fungus in PDB containing 0, 25, 50, 75, 100, and 125 µg/mL bortezomib were extracted and their organic extracts compared via gradient UPLC-ELSD. Relative levels of the resorcylic acid lactones[170] and several fatty acids varied between replicate growths. In addition to those expected compounds, a new peak was evident in the chromatograms of the bortezomib-dosed growths (arrow, Fig. 12). Growths containing this peak were combined; the compound was isolated via preparative high pressure liquid chromatography (HPLC), and the structure analyzed.

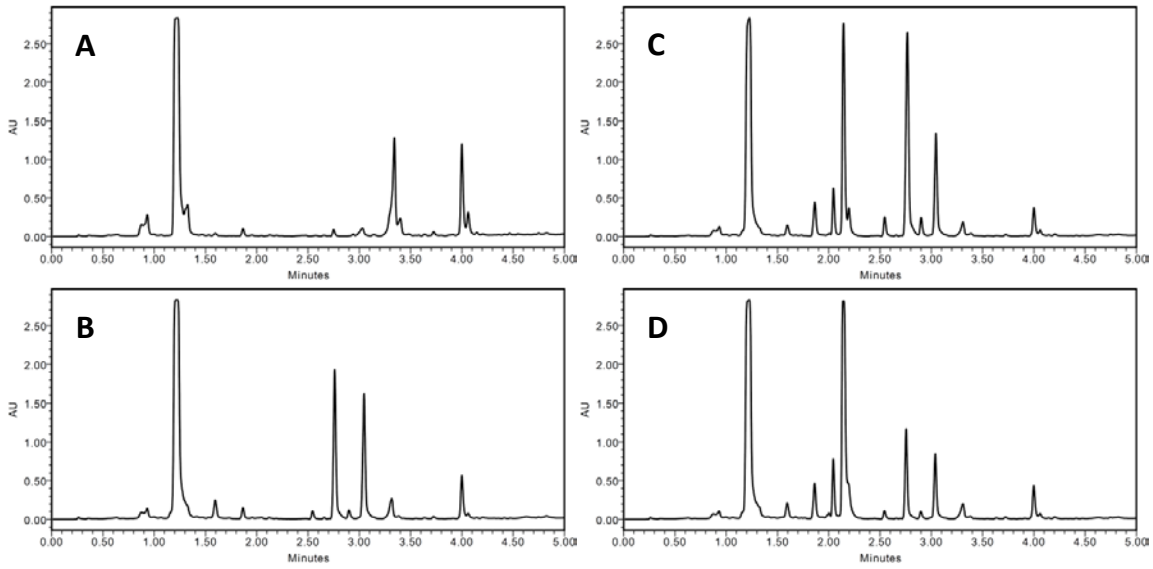

Figure 11. Comparison of control (A) and dosed (B-D) growths of MSX 63935 grown in potato dextrose broth. The culture shown in (B) was grown with 50 µg/mL SAHA, (C) with 100 µg/mL 5-AZA, and (D) with 50 µg/mL bortezomib. The separation was performed via UPLC-PDA (235 nm), using a C_{18} column and a gradient increasing linearly from 10% CH_3CN (H_2O) at 0.0 min to 100% at 4.5 min, held at 100% for an additional 0.5 min. All extracts were solubilized at 0.2 mg/mL and injected at a volume of 6 µL.

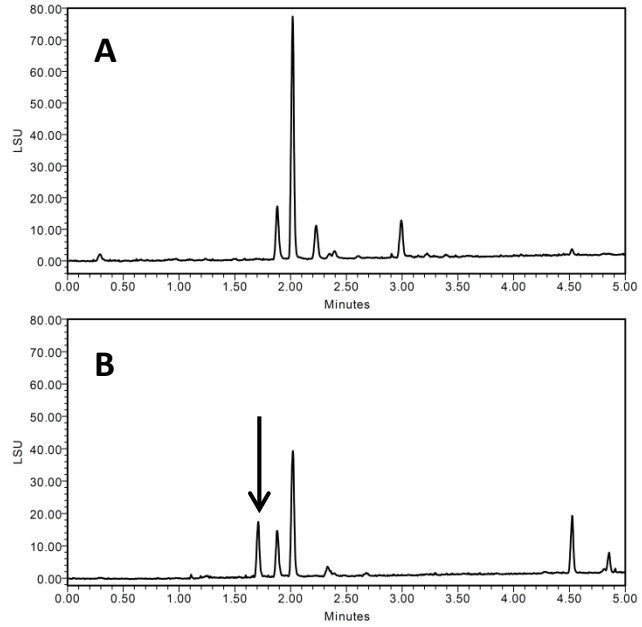

Figure 12. Comparison of control (A) and dosed (B) growths of MSX 63935, grown in potato dextrose broth with 75 µg/mL bortezomib. The arrow indicates a peak that does not appear in extracts of control growths. The peaks in (B) after 4.5 minutes were attributed to fatty acids. The separation was performed via UPLC-ELSD, using a C_{18} column and a gradient increasing linearly from 10% CH_3CN (H_2O) at 0.0 min to 100% at 4.5 min, held at 100% for an additional 0.5 min.

Compound **9** (Fig. 13, Table 10) was obtained as a white powder. Using HRESIMS, a molecular ion was measured at 307.1165 $[M+H]^+$ (calcd for $C_{16}H_{19}O_6$, 307.1176), indicating a molecular formula of $C_{16}H_{18}O_6$ with eight degrees of unsaturation. The ^1H NMR spectrum displayed two aromatic *m*-coupled protons at δ_H 7.20 (H-6) and δ_H 7.22 (H-8), a singlet at δ_H 6.28 (H-3), a methoxy signal at δ_H 3.96, and signals for six protons corresponding to the hydroxylated aliphatic side chain at δ_H 4.06 (H-2′), 2.88 and 2.70 (H-1′a/b), 1.56 (H-3′), 1.56 and 1.45 (H-4′), and 0.98 (H-5′). The structure of this side chain was assigned based on examination of COSY data (Fig. 14). HMBC correlations (Fig. 14) between H-3 and carbons C-2 (δ 167.0) and C-1′ (δ_C 43.3),

as well as between the diastereotopic H-1′ protons and the C-2 and C-3 (δ_C 112.0) carbons, determined the C-2/C-1′ bond. Further analysis of the HMBC and HSQC data and a search of the literature suggested the chromone skeleton, which accounted for seven degrees of unsaturation.[171-173] An HMBC correlation between the methoxy singlet and the C-7 carbon (δ_C 165.4) established its connectivity to the aromatic ring. The mass indicated a carboxylic acid moiety as the remaining substituent, accounting for the last degree of unsaturation; this was corroborated by a correlation between the H-6 proton and the carboxylic acid carbon (δ_C 171.9). A four-bond correlation between the H-3 proton and C-5 (δ_C 136.8), established the position of the carboxylic acid moiety. The absolute configuration was assigned using a modified Mosher's ester analysis (Fig. 15).[174]

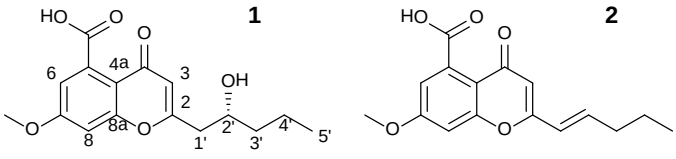

Figure 13. Compound **9** was isolated from bortezomib-dosed growths of MSX 63935, and **10** was isolated from a degraded solution of **9**.

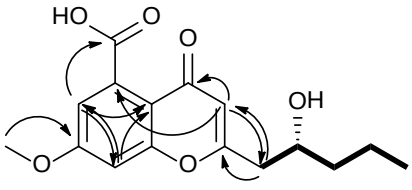

Figure 14. Key HMBC (⟶) and COSY (▬) correlations of compound **9**.

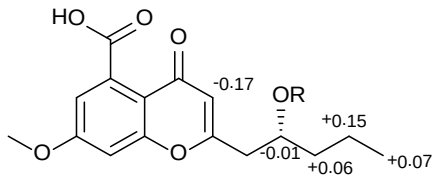

9a: R = (*R*)-MTPA
9b: R = (*S*)-MTPA

Figure 15. $\Delta\delta_H$ values [$\Delta\delta$(in ppm) = $\delta_S - \delta_R$] obtained for (*R*)- and (*S*)-MTPA esters (**9a** and **9b,** respectively) in pyridine-d_5.

A compound with the same planar structure as **9** was isolated from the plant *Stratiotes aloides* in 2009.[172] Those authors did not assign the absolute configuration, possibly due to paucity of material (less than 200 μg).[172] Due to signal overlap of the DMSO-d_6 solvent, the data reported here were obtained in MeOH-d_4, though ^{1}H and ^{13}C NMR spectra were also acquired in DMSO-d_6. Key differences between NMR signals in DMSO-d_6 were noted at positions H-3, H-6, H-8, and C-5 (Table S3, Appendix). However, both the NMR data and the UV maxima[175] at 233 and 291 supporedt the chromone skeleton, and the structure of the alkyl side chain was firmly assigned by 2D NMR. Coupling of the H-6 and H-8 protons (J = 2.3) established the *meta* positions of the aromatic protons, and the strong four-bond H-3 to C-5 correlation confirmed the position of the carboxylic acid.

Table 10. NMR Data (400 MHz, MeOH-d_4) of compounds **9** and **10**.

	9			**10**		
position	δ_H, mult. (*J* in Hz)	δ_C, type	HMBC[a]	δ_H, mult. (*J* in Hz)	δ_C, type	HMBC[a]
2		167.0, C			161.8, C	
3	6.28, s	112.0, CH	2, 4, 4a, 5, 1'	6.21, s	107.3, CH	2, 4, 4a, 5, 1'
4		179.4, C			177.6, C[c]	
4a		114.9, C			112.9, C	
5		136.8, C			138.5, C[c]	
6	7.20, d (2.3)	103.3, CH	4a, 8, 5-*C*OOH	7.13, d (2.3)	100.8, CH	4a, 8, 5-*C*OOH
7		165.4, C			163.4, C	
8	7.22, d (2.3)	116.8, CH	4a, 6, 7, 8a	7.20, d (2.3)	114.0, CH	4a, 7, 8a
8a		160.6, C			157.9, C	
1a'	2.88, dd (4.1, 14.7)	43.3, CH_2	2, 3, 2', 3'	6.33, dd (1.4, 15.6)	121.5, CH	2, 3'
1b'	2.70, dd (9.2, 14.7)		2, 3, 2', 3'			
2'	4.06, m	70.0, CH		6.98, dt (7.3, 15.6)	141.8, CH	2, 3', 4'
3'	1.56, m[b]	40.8, CH_2	1', 2', 4', 5'	2.31, ddt (1.4, 7.3,	34.0, CH_2	1', 2', 4', 5'
4'	1.56, m[b] / 1.45, m	20.1, CH_2	2', 3', 5'	1.58, sextet (7.3)	20.9, CH_2	2', 3', 5'
5'	0.98, t (6.9)	14.5, CH_3	3', 4'	1.00, t (7.3)	12.1, CH_3	3', 4'
7-OCH_3	3.96, s	57.1, CH_3	7	3.95, s	54.9, CH_3	7
5-COOH		171.9, C			171.5, C[c]	

[a]HMBC correlations are from the proton(s) listed to the indicated carbons.
[b]Overlapping signals
[c]The quaternary ^{13}C signals for C-4, C-5, and 5-COOH werevery weak, and their δ_C values were corroborated by HMBC data.

During an unsuccessful attempt to crystalize **9**, the molecule degraded in solution, yielding several analogues, one in quantities sufficient to assign a structure. Compound **10** (Fig. 13), which was new, represented the dehydro analogue of **9**, which was supported by an 18 amu difference in the HRMS data and an increase by one in the index of hydrogen deficiency. COSY data, especially a correlation between H-2′ (δ_H 6.98) and H-3′ (δ_H 2.31), helped assign the alkene side chain. The large vicinal coupling constant between H-2′ and H-3′ (J = 15.1) established the trans configuration.

Both **9** and **10** were tested for cytotoxicity against human melanoma and colon cancer cells and were found to be inactive (*i.e.*, IC_{50} values > 20 μM).

To our knowledge, this is the first use of a proteasome inhibitor in epigenetic modification studies to induce additional secondary metabolites from microorganisms, and may inspire new methods for the up-regulation of silent metabolite genes.

Experimental Section

Culture Methods

Mycosynthetix fungal strain 63935 was isolated in 1992 by Dr. Barry Katz of MYCOsearch from leaf litter. The culture was stored on a malt extract slant and was transferred periodically. A fresh culture was grown on malt extract agar in a 10 cm diameter Petri plate at 22 °C for 20 d, until the cultures were approximately 2.5 cm in diameter. The cultures were cut into small squares, which were used to inoculate 250-mL Erlenmeyer flasks containing 50 mL of potato dextrose broth (PDB). At the time of inoculation, 0.5 mL aliquots of DMSO-dissolved bortezomib was added in triplicate to 15

flasks, resulting in final concentrations in the liquid media of 25, 50, 75, 100, and 125 µg/mL bortezomib. Three flasks were treated with 0.5 mL DMSO (vehicle control), and three flasks were untreated (negative control). The cultures were grown with shaking (100 rpm) at 22 °C for 14 d.

Extraction and Isolation

The cultures were shaken overnight with 60 mL of 1:1 $CHCl_3$:MeOH and filtered the next day. To the filtrate was added 90 mL of $CHCl_3$ and 100 mL of deionized H_2O to produce a 4:1:5 mixture of $CHCl_3$:MeOH:H_2O (including the 50 mL of H_2O from the liquid media). This mixture was stirred for 1 h, then transferred to a separatory funnel. The organic portions were dried *in vacuo*, then shaken with a 1:1:2 mixture of CH_3CN:MeOH:hexanes. The CH_3CN:MeOH layers were separated, and all extracts were dried *in vacuo*, transferred to scintillation vials, then dried completely under air. The extracts of the cultures exhibiting the presence of the new metabolite (Fig. 2) were combined (90.85 mg) and subjected to preparative C_{18} HPLC using an isocratic 40:60 CH_3CN:H_2O method over 25 min, followed by a 100% CH_3CN column wash (10 min). Compound **1** eluted at ~14 min (6.32 mg).

Instrumentation

Optical rotation was measured with a Rudolph Autopol III polarimeter; UV spectra were obtained using a Varian Cary 3 UV-vis spectrophotometer. NMR experiments were performed on a JEOL ECS 400 MHz NMR equipped with a high

sensitivity JEOL Royal probe and an autosampler. Selected samples were measured using a Bruker Avance-III 600 MHz NMR. HRESIMS data were acquired using a Thermo LTQ Orbitrap XL mass spectrometer equipped with an electrospray ionization source. UPLC was performed using a Waters Aquity system, equipped with a photodiode array detector (PDA) and evaporative light scattering detector (ELSD) with data collected and analyzed using Empower software. A Waters BEH C_{18} column (1.7 µm; 50 × 2.1 mm) was used with a 0.6 mL/min flow rate. Preparative HPLC was performed using a Varian Prostar HPLC system equipped with ProStar 210 pumps and a Prostar 335 PDA, with data collected and analyzed using Galaxie Chromatography Workstation software (version 1.9.3.2). A YMC ODS-A C_{18} column (5 µm; 250 × 20 mm) was used with a 9.45 mL/min flow rate.

(*R*)-2-(2-hydroxypentyl)-5-carboxy-7-methoxychromone (9)

White powder; $[\alpha]^{20}_{D}$ −26 (*c* 0.179, MeOH); UV(MeOH) λ_{max} (log ε) 233 (3.01), 291 (2.85); ^{1}H NMR (400 MHz, MeOD-d_4) see Table 10; ^{13}C NMR (400 MHz, MeOD) see Table 10; HRESIMS *m/z* 307.1165 (calcd for $C_{16}H_{19}O_6$, 307.1176) $[M+H]^+$.

(*E*)-2-(pent-1-en-1-yl)-5-carboxy-7-methoxychromone (10)

White powder; UV(MeOH) λ_{max} (log ε) 256 (3.28), 317 (3.31); ^{1}H NMR (400 MHz, MeOD-d_4) see Table 10; ^{13}C NMR (400 MHz, MeOD) see Table 10; HRESIMS *m/z* 289.1069 (calcd for $C_{16}H_{17}O_5$, 289.1071) $[M+H]^+$.

Preparation of (*R*)- and (*S*)-MTPA ester derivatives of (9)

To 1.00 mg of compound **9**, 1000 µL of pyridine-d_5 were added; from this, 500 µL were transferred to two separate NMR tubes. To initiate the reaction, 10 µL of *S*-(+)-α-methoxy-α-(trifluoromethyl)phenylacetyl (MTPA) chloride were added to one NMR tube and shaken. The reaction was monitored immediately by ^{1}H NMR at the following time points: 0, 15, and 30 min. At 30 min, an additional 10 µL of *S*-MTPA chloride were added and the tube shaken. The reaction was monitored further at 40, 45, and 55 min, at which point it was determined to be complete, yielding the mono (R)-MTPA ester derivative (**9a**) of **9**. To the second NMR tube was added 20 µL of the (R)-MTPA chloride; the reaction was shaken, then monitored immediately by ^{1}H NMR at the following time points: 0, 15, 30, and 40 min. The reaction was found to be complete within 40 min, yielding the mono (*S*)-MTPA ester derivative (**9b**) of **9**. ^{1}H NMR (500 MHz, pyridine-d_5) of **9a**: δ_H 0.80 (3H, t, H-5′), 1.28 (2H, m, H-4′), 1.71 (2H, m, H-3′), 3.14 (2H, m, H-1′), 5.78 (1H, m, H-2′), 6.62 (1H, s, H-3). The signals from H-6, H-8, and the methoxy group were obscured by solvent and reagent peaks. ^{1}H NMR (500 MHz, pyridine-d_5) of **9b**: δ_H 0.87 (3H, t, H-5′), 1.43 (2H, m, H-4′), 1.77 (2H, m, H-3′), 5.77 (1H, m, H-2′), 6.45 (1H, s, H-3). The signals from H-1′, H-6, H-8, and the methoxy group were obscured by solvent and reagent peaks.

Cytotoxicity Assays

Human melanoma cancer cells designated MDA-MB-435 and human colon cancers designated HT-29 were purchased from the American Type Culture Collection

(Manassas, VA). The cell lines were propagated at 37°C in 5% CO_2 in RPMI 1640 medium supplemented with fetal bovine serum (10%), penicillin (100 units/mL), and streptomycin (100 µg/mL). Cells in log phase growth were harvested by trypsinization followed by two washing to remove all traces of enzyme. A total of 5,000 cells were seeded per well of a 96-well clear, flat-bottom plate and incubated overnight (37°C in 5% CO_2). Samples dissolved in DMSO were then diluted and added to the appropriate wells (concentrations: 20, 4, 0.8, 0.16, and 0.032 µM; total volume: 100 µL; DMSO: 0.5%). The cells were incubated in the presence of test substance for 72 h at 37°C and evaluated for viability with a commercial absorbance assay (CellTiter 96® AQ_{ueous} One Solution Cell Proliferation Assay, Promega Corp, Madison, WI) that measured viable cells. IC_{50} values were expressed by µM relative to the solvent (DMSO) control. The positive control was vinblastine tested at 1 nM in MDA-MB-435 cells, yielding 16% viable cells or 10 nM in HT-29 cells, which yielded 39% viable cells.

Acknowledgement

This research was supported by program project Grant P01 CA125066 from the National Cancer Institute/National Institutes of Health, Bethesda, MD, USA. Selected NMR data were obtained by Dr. Kevin Knagge at the David H. Murdock Research Institute Kannapolis.

CHAPTER VII

ROMIDEPSIN (ISTODAX®, NSC 630176, FR901228, FK228, DEPSIPEPTIDE): A NATURAL PRODUCT RECENTLY APPROVED FOR CUTANEOUS T-CELL LYMPHOMA

This chapter has been published in the *Journal of Antibiotics* and is presented in that style. VanderMolen, K.M., McCulloch, W., Pearce, C.J. and Oberlies, N.H. *J. Antibiot.* **2011**. 64, 525-531.

Romidepsin, a histone deacetylase inhibitor with a unique chemical structure, was approved for the treatment of cutaneous T-cell lymphoma in November 2009 by the US FDA. It was discovered from cultures of *Chromobacterium violaceum*, a bacterium isolated from a Japanese soil sample. This bicyclic compound acts as a prodrug, its disulfide bridge being reduced by glutathione upon uptake into the cell, allowing the sulfhydryls to interact with Zn ions in the active site of class I and II histone deacetylase enzymes. Due to the synthetic complexity of the compound, as well as the low yield from the producing organism, analogs are sought to create synthetically accessible alternatives. As a T-cell lymphoma drug, romidepsin offers a valuable new treatment for diseases with few effective therapies.

Introduction to HDAC Inhibitors

Alteration of gene expression due to epigenetic modification of the chromatin structure has been implicated as an important factor in tumorigenesis.[122, 176] In chromatin,

DNA is tightly coiled around core histone proteins, forming nucleosomes; linker histones bind nucleosomes together as chromatin. Methylation, acetylation, phosphorylation, ADP-ribosylation, or ubiquitination of the histone tail regions affect the binding of the histone proteins to DNA, changing the structure of the chromatin and subsequently the accessibility of transcription factors to DNA regions.[120] Such epigenetic processes alter levels of gene expression without changing the nucleotide sequence.[177] Of these modifications, histone acetylation is the most widely studied due to its role in the development and progression of tumors.[122]

Histone acetylation is controlled by the enzymes histone acetyltransferases (HATs) and histone deacetylases (HDACs). HATs direct the addition of acetyl groups to lysine residues in the amino-terminal histone tails, neutralizing that portion of the protein and relaxing the chromatin structure, thereby increasing accessibility of transcription complexes as well as recruiting transcription cofactors.[120-123] Conversely, HDACs remove acetyl groups from the histone tails, resulting in a more compact and inaccessible form of chromatin, consequently silencing transcription.[120-122] These effects are highly localized, and only 2-5% of encoding genes are transcriptionally regulated by the histone acetylation state.[122] Importantly, this selection includes genes that control the cell cycle and apoptosis, and HDACs have been associated with several well characterized oncogenes and tumor suppressor genes.[178, 179] Certain tumors have overexpressed HDACs and downregulated or mutated HATs.[180] It has been suggested that an imbalance of HDAC relative to HAT activity can lead to a diminished expression of such regulatory genes and ensuing tumorigenesis.[180]

HDAC inhibitors have been found to have therapeutic properties in many different tumor cell lines, including human cancer cell lines derived from the bladder, breast, prostate, lung, ovary, colon, among others,[181] indicating that the inhibition of HDAC activity may be a viable strategy for the treatment of cancers.[182-184] It is also likely that HDAC inhibitors affect a number of subcellular pathways, and time will tell what impact these other mechanisms have on treatment of cancer and/or other diseases. HDAC inhibitors can be divided into four classes, namely hydroximates, cyclic peptides, aliphatic acids, and benzamides.[185] A new HDAC inhibitor, romidepsin, which has been referred to by several different names in the literature, including FK228, FR 901228, NSC 630176, depsipeptide, and Istodax®, is a pentapeptide isolated from cultures of *Chromobacterium violaceum*.[186] The structure (Fig. 16, **11**) is composed of four amino acids (D-valine, D-cysteine, Z-dehydrobutyrine, L-valine) and (3*S*,4*E*)-3-hydroxy-7-mercapto-4-heptenoic acid, arranged as a bicyclic depsipeptide. The numbering of **11** is based on Xiao et al.[187, 188]Romidepsin was approved by the U.S. FDA in 2009 for use in patients with cutaneous T-cell lymphoma (CTCL).

Background on Cutaneous T-Cell Lymphoma

The incidence of CTCL in the general population is estimated to be 1-4/100 000,[189, 190] with approximately 1500 new cases and 500 deaths per year in the United States (US).[191] CTCL is twice as prevalent in males as in females, and the median age of presentation is 57 years. In the US, the disease is also more common among African-Americans than in other race categories.[190] Approximately 16 000 to 20 000 individuals

in the US are affected by CTCL.[191] One study from 1973 to 1984[192] found a 3.2-fold increase in the incidence of CTCL over that time period; a similar study from 1973 to 2002[193] reported a 3.4-fold increase in incidence over the course of the study.

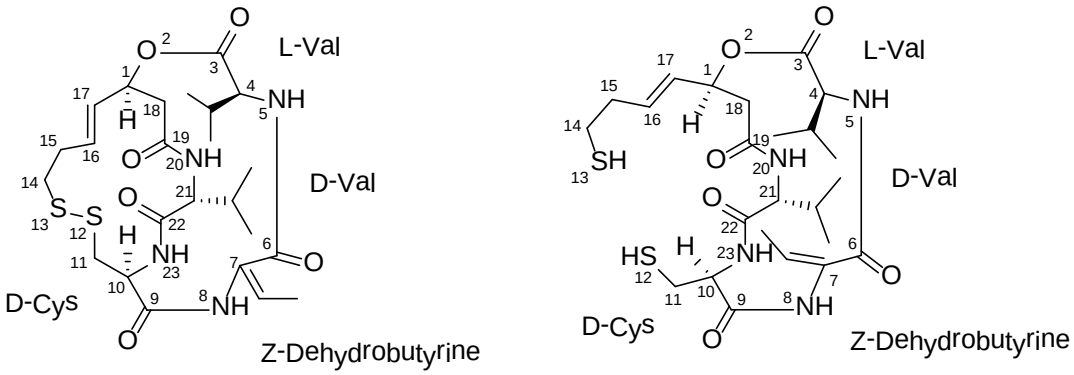

11 **12**

Figure 16. Structures of romidepsin (**11**) and the reduced counterpart (**12**).[188]

The most common types of CTCL are mycosis fungoides (MF), so called because early physicians believed it to be a fungal infection although it is not, and the Sézary syndrome. Sézary syndrome, the leukemic variant, is characterized by pruritus, generalized exfoliative erythroderma, and abnormal lymphoid cells in the blood. The blood is usually not affected in MF, especially in the early stages. Skin lesions are characterized as patches, plaques, or tumors that have a "bathing trunk" distribution. The lymphoma may extend to cover a large surface area, lymph nodes, and, in later stages, viscera.

MF is the most common type of CTCL, and is characterized by pink or erythematous scaly patches and plaques, with varying degrees of scaling and pruritus.[194]

At the time of diagnosis, the majority of patients with MF have limited plaques on ≤10% of their total body surface. However, approximately one-third (30%) have extensive plaques. Relatively small proportions of patients present with cutaneous tumors (16%) or generalized erythroderma (12%). Non-skin lesions are more likely to be seen in later stage disease, with 8% seen in stage T2, 30% in stage T3, and 42% in stage T4. The primary non-skin and non-lymph node sites are lung, gastrointestinal (GI), liver, and central nervous system (CNS). Bone marrow (BM) involvement is rare in early stage disease.

CTCL is uniformly fatal. The ultimate cause of death for patients with CTCL is commonly infection, particularly sepsis, from *Pseudomonas aeruginosa* or *Staphylococcus aureus*, caused by chronic skin infection and subsequent systemic infections.[195] Prognosis is dependent on age as well as disease stage at diagnosis,[196] with earlier stage disease associated with higher 5-year overall survival and disease-free survival rates than later stage disease. The overall 5-year survival rate for patients with mycosis fungoides (MF) is 91%, while it is only 40% for those with Sézary syndrome (SS).[197] Typically, those presenting with early stages of CTCL have a favorable prognosis, with around 95% 5-year survival;[196, 198, 199] more advanced stages have lower survival rates ranging from 30% to 84%,[196, 198, 199] again depending on form and stage of the cancer. According to one study, the 10-year survival rate drops from around 100% for those with stage T1 CTCL to 67% for T2; by stage T3, this number drops to 40%.[200] While most patients present with the early-stage disease, approximately 10-20% of these will progress to a later and often fatal disease.[196, 198, 201] Patients that undergo

transformation to large-cell lymphoma have a mean survival ranging from 2 to 19 months.[201]

Discovery and Early Development of Romidepsin

Romidepsin was discovered in 1993 through a program that was evaluating fermentation products for antimicrobial and antitumor activities. The producing organism, *Chromobacterium violaceum*, is a Gram-negative, rod-shaped bacterium with a single polar flagellum. The strain was isolated from a soil sample collected in the Yamagata-prefecture in Japan.[186] Presently, the commercial supply of romidepsin is generated via fermentation, although the yield and exact conditions are proprietary.

C. violaceum was cultured in nutrient broth with additional glucose and incubated at 30°C aerobically and with agitation. The organism reached stationary phase after 72 h, providing a maximal yield of romidepsin at this time of 19 μg/mL, which was present in the aqueous part of the culture. The fermentation was filtered, and the filtrate extracted twice with EtOAc. The extract was evaporated *in vacuo* to give an oily residue, which was then purified via normal phase chromatography to yield a yellow powder.

This powder was dissolved in CH_2Cl_2:CH_3OH:CH_3CN (10:1:20), and romidepsin crystallized as colorless prisms. It displayed weak antifungal but no antibacterial activity, but it showed potent cytotoxicity against several human lung carcinoma cell lines, as well as human stomach, breast, and colon adenocarcinoma cell lines.[186] The structure of **11**, which is a cage-shaped bicyclic depsipeptide, was determined using a combination of spectroscopic techniques, primarily NMR and x-ray crystallography.[202]

Romidepsin demonstrated the ability to reverse the effects of the *ras* oncogene *in vitro*, which has been shown to play a role in tumor development; expression of the Ha-*ras* oncogene appears to be directly correlated with tumorigenic potential.[203] Because of romidepsin's ability to reverse the *ras*-transformed phenotype to normal, as well as its cytotoxic effects, it was developed initially by the US National Cancer Institute as an anti-*ras* compound,[204, 205] but recently it has been shown to be an HDAC inhibitor.[206, 207] A program screening a number of known microbial metabolites for transcriptional activation of the SV40 promoter identified romidepsin as an antitumor compound.[206] Comparison of its activity to that of TSA revealed that romidepsin was a new HDAC inhibitor.[206]

Mechanisms of Action

Romidepsin is converted in cells to its active form by the reduction of the disulfide bond by glutathione, resulting in a monocyclic dithiol (**12**),[187, 208] and thus romidepsin serves as a prodrug that is activated only after uptake into cells. This reduced form (**2**) is inactivated rapidly in serum, perhaps due to sequestration by serum proteins.[208] A cysteine in the active site pocket (Cys-151 in HDAC1) was thought to covalently bind with the reduced sulfur atom at position 13, but a mutant HDAC1 in which this cysteine was replaced by a serine was still sensitive to romidepsin, though a higher concentration (~8×) of the drug was necessary for inhibition.[208] This fact, combined with the reversibility of the inhibition, suggests that while the cysteine may play a role in the affinity of the drug, it most likely does not bind covalently to the sulfur

atom.[208] Crystallographic and computer modeling studies using a HDAC-trichostatin A complex suggested that one of the sulfhydryl groups of the reduced depsipeptide interacts with zinc ions in the active site pocket of certain enzymes, preventing access of the substrate.[209] A computer modeling study by Furumai *et al.*[208] concluded that when interacting with HDAC1 the sulfur atom of the reduced romidepsin was located at a position that allowed interaction with the zinc ion via a water molecule. They also suggested that, based on a similar mechanism in protease inhibitors, the sulfur may tetrahedrally coordinate with the zinc, displacing the water molecule.[208] The interaction between the sulfhydryl group and the active site of the enzyme prevents other substrates from binding.

The reduced form more strongly inhibits HDAC1 and HDAC2 enzymes (class I) than HDAC4 and HDAC6 enzymes (class II).[208] By inhibiting HDAC Class I enzymes, romidepsin inhibits the removal of acetyl groups from the lysine residues of *N*-terminal histone tails, maintaining a more open and transcriptionally active chromatin state.[121]

Romidepsin also results in altered acetylation of other nuclear and cytoplasmic proteins, though the precise pathways by which it affects the cell cycle, apoptosis, and angiogenesis have not been defined completely.[210]

Cell Cycle Arrest

The induction of growth arrest and/or apoptosis by romidepsin depends on the cell line tested and the concentration of drug applied.[210] Growth arrest, as opposed to apoptosis, is the predominant response in cell lines in which the application of

romidepsin induces the expression of the p21 tumor-suppressor gene.[211] Cell lines with reduced p21 expression preferentially undergo apoptosis.[212] Tumor cells are more susceptible to romidepsin than normal cells,[186] a fact that leads to a viable therapeutic index in the clinic.

Direct acetylation of non-histone proteins may also trigger growth arrest or apoptosis, and several pathways have been studied, though the complete role of HDAC inhibitors is not fully understood. Exposure of whole cells to romidepsin results in a decrease of cyclin D1 and c-myc, accompanied by an increase in p53-independent p21 WAF1/Cip 1 induction. The p21 induction leads to inhibition of cyclin-dependent kinase (CDK) and dephosphorylation of the retinoblastoma protein (Rb), which results in early G1 phase cell cycle arrest.[213, 214] A different mechanism involves altered expression of cyclin A and D, and p27/Kip1, again resulting in reduced CDK activity and cell cycle arrest.[214]

Apoptosis

There are two mechanisms leading to apoptosis: the death receptor pathway and the intrinsic pathway.[215] While exposure to romidepsin and other HDAC inhibitors can lead to hyper-acetylation of death receptor promoters, including TRAIL (tumor-necrosis factor-related apoptosis-inducing ligand), death receptor 5, Fas ligand and Fas,[216] the significance of this mechanism does not seem to be universally acknowledged. Some leukemia cells do not show induction of the TRAIL or Fas pathways, or undergo apoptosis after exposure to HDAC inhibitors.[217] The intrinsic pathway involves the

perturbation of mictochondrial membranes resulting in the generation of reactive oxygen species (ROS). In normal cells exposed to HDAC inhibitors, ROS do not accumulate due to breakdown by thioredoxin; some tumor cells that do not express the thioredoxin gene accumulate ROS and undergo apoptosis. [215]

Romidepsin has also been shown to increase acetylation of the HSP 90 chaperone protein, causing proteasomal degradation and inducing apoptosis.[218] The proteasome inhibitor bortezomib appears to work synergistically with HDAC inhibitors,[219] but it is interesting that the HSP 90 inhibitor, geldanamycin, antagonizes HDAC inhibitor activity.[220]

Angiogenesis Inhibition

Romidepsin inhibits hypoxia-induced angiogenesis of endothelieal cells *in vitro*, but does not cause cytotoxicity. It decreased angiogenesis in a chick embryo model, with no signs of thrombosis or hemorrhage, and inhibited angiogenesis strongly in mouse model tumors.[221] Romidepsin appears to reduce angiogenic-stimulating factors such as VEGFs, VEGF receptor, FLT1 and FLK1, and increases induction of angiogenic inhibitory factors VHL and neurofibromin2,[221] however, the correlation between anti-VEGF activity and *in vivo* efficacy has not been established.

Pharmacology

Pharmacokinetics

A two-compartment model with linear kinetics can be used in the pharmacokinetic analysis of romidepsin.[222, 223] Two dosing schedules were studied in

separate Phase I trials. One schedule involved a 4-h infusion on days 1 and 5 of a 21-day cycle, where the MTD (maximum tolerated dose) was determined as 17.8 mg/m^2,[223] while the second involved a 4-h infusion on days 1, 8, and 15 of a 28-day cycle, where the MTD was determined as 13.3 mg/m^2.[224] With both schedules, romidepsin exhibited linear pharmacokinetics up to the MTD.[223, 224] Total clearance volumes in adults have been reported as 4.8 L/h/m^2 at a 13 mg/m^2 dose,[225] and 10.5 L/h/m^2 at a 17.8 mg/m^2 dose.[223] A Phase I study in pediatric patients (2-21 years, median age 13) with refractory solid tumors who received romidepsin in 4-h infusions of 17 mg/m^2 reported a clearance volume of 6.8 L/h/m^2.[226] The elimination half-life has been reported as 3.5 h[222] and 3.67 h[225] at 13 mg/m^2, and 8.1 h[223] at 17.8 mg/m^2.

Pharmacodynamics

A typical assay for pharmacodynamic studies is to monitor histone acetylation of peripheral blood mononuclear cells (PBMCs).[223, 226, 227] Increased acetylation is observed in patients' PBMCs after treatment with romidepsin, with maximal accumulation of acetyl H3 histones in PBMCs occurring at 4 h after the end of an infusion.[226]A study in patients with acute myelogenous leukemia and chronic lymphocytic leukemia (CLL) using a 4 h 13mg/m^2 infusion on days 1, 8, and 15 of a 28-day cycle reported 100% histone acetylation of H3 and H4 histones for all CLL patients after 4 h, and for 6 out of 7 CLL patients after 24 h.[225] This study also reported an increase in p21 protein expression concurrent with H4 acetylation of the p21 promoter gene.[225]

A Phase II study of T-cell lymphoma patients monitored several biomarkers: PBMC histone acetylation, *ABCB1* gene expression in PBMCs, *ABCB1* gene expression in biopsy samples, and blood fetal hemoglobin (HbF) levels.[228] A global increase in PBMC histone acetylation was reported in 73% of patients within 4 h of treatment, and in 40% of patients after 24 to 48 h.[228] The number of patients having a twofold or higher than baseline *ABCB1* expression in PBMCs was 56% at 4 h, and 30% at 48 h.[228] A fourfold or greater increase in circulating HbF was reported in 60% of the patients. The histone H3 acetylation in PBMCs at the 24-h time point appeared to correlate with response; there was no correlation between the levels of *ABCB1* induction and pharmacokinetic parameters, or between *ABCB1* induction in biopsy samples and clinical disease reponse.[228] These data suggested that peak drug concentration (C_{max}) and overall exposure were important in determining response.[228, 229]

T-Cell Lymphoma Clinical Trials

In preclinical studies, greater antitumor activity was observed with intermittent administration than with daily administration.[223] Short infusions (>30 s to 4 min) and prolonged infusions (>24 h) caused greater toxicity than infusions of 1-4 h.[223] Therefore, in Phase I trials, romidepsin was tested using a 4-h intravenous infusion. Patients who consent to be treated in Phase I trials have cancers for which no known standard therapy exists, or such therapy has already failed, so that patients are not denied any curative or definitely life-extending options. One Phase I study[223] administered a 4-h infusion on days 1 and 5 of a 21-day cycle; the MTD was defined at 17.8 mg/m^2 with dose-limiting

toxicity (DLT) manifest as grade-3 fatigue, grade-3 nausea and vomiting, grade-4 thrombocytopenia (low platelet levels), and grade-4 cardiac arrhythmia. Another Phase I study[224] administered romidepsin in a 4-h infusion on days 1, 8, and 15 of a 28-day cycle; the MTD in this trial was defined at 13.3 mg/m^2 with DLT manifesting as grade 3 thrombocytopenia and fatigue. A partial response was seen in a patient with renal cell carcinoma.[223] Several patients with T-cell lymphoma (cutaneous or peripheral) exhibited significant reductions in skin lesions and tumor size after treatment with romidepsin.[224, 230]

A Phase II trial to define the response rate and toxicity profile in patients with T-cell lymphoma was initiated due to the dramatic responses seen in Phase I trials.[40] Romidepsin was administered via a 4-h infusion on days 1, 8, and 15 of a 28-day cycle. Complete responses were observed in 4 patients (6%), and partial responses were observed in 20 patients (28%).[231] The toxicities observed were consistent with those reported previously, including extreme fatigue, nausea and vomiting.[223] Granulocytopenia (failure of bone marrow to make white blood cells) and thrombocytopenia (low platelet counts) were observed as well, with values returning to baseline by the next cycle of treatment.[231]

Defining a clear path for the development of romidepsin was somewhat complicated due to the many different parties involved. Fujisawa Corporation (now Astellas Inc.) discovered the compound in the early 1990s via a search for molecules that would revert the *ras*-driven oncogenic phenotype, and then, under a Cooperative Research and Development Agreement (CRADA), further oncology investigations were

initiated by the NCI in 1998. When the NCI confirmed that romidepsin was a powerful anticancer agent, Fujisawa Corporation initiated their own, separate clinical trials program in 2002. Romidepsin was licensed to Gloucester Pharmaceuticals in 2004; the company was later acquired by Celgene Corporation in 2010. Gloucester approached the U.S. FDA (beginning in 2004), obtained both Orphan Drug Status and Fast Track Status, and were able to come to an agreement, through the U.S. FDA Special Protocol Assessment (SPA) process, on a path to approval which was a pivotal single arm (Phase II) design, although data from the NCI's ongoing study was also to be part of the New Drug Application (NDA) filing. Essentially, the activity of romidepsin, coupled with the unmet medical need in cutaneous T-cell lymphoma, were persuasive enough arguments to move the drug forward.

Clinical Trials of Romidepsin

Table 11 highlights the published clinical trial data on romidepsin; all of the Phase I trials were on patients who had non-responsive cancers. The favorable results of the NCI-sponsored multi-institutional Phase II trial,[222, 228, 231, 232] followed by consistent results by the pivotal Phase II trial conducted by Gloucester Pharmaceuticals[233] led to the approval by the U.S. FDA in November of 2009.

Toxicity and Side Effects

Cardiac toxicities were a primary concern in the early clinical trials due to preclinical results, leading to electrocardiograms (ECGs) and other measures related to

cardiac function being taken before and after every treatment.[223] Many of the early toxicities were abnormalities of the ECG waveform, which represent repolarisation abnormalities in the electric functioning of the heart; grade 1 T-wave flattening or grade 2 ST segment depression was observed in more than half of the ECGs, but although these abnormalities can also be indicative of cardiac ischemia, in the case of romidepsin this was not so, since they were not associated with elevation of cardiac troponin or with altered left ventricular function.[232] Further follow up over 3 years with a larger body of clinical data confirms that the ECG abnormalities are not clinically significant or indicative of any real cardiac toxicity.[210] Therefore, this observation is no longer a clinical concern, except that patients are screened with an ECG to check for pre-existing cardiac rhythm abnormalities, including the very rare congenital long QT syndrome, which is a condition where the interval between the Q-wave and the T-wave on the ECG is prolonged, and this can lead to further, even fatal, problems if the electrical circuitry of the heart is further affected in these patients.

The majority of patients receiving romidepsin experience nausea, vomiting, and anorexia,[223, 225, 229, 231, 234] and Grant *et al.*[229] note that the antiemetic routine followed at the National Cancer Institute (NCI) was to administer 1 mg granisetron intravenously prior to romidepsin, followed by 1 mg orally every 12 h for 3 days.[229] Progressive fatigue and occasional fever were also noted with romidepsin.[223-225, 231, 234]

Table 11. Clinical trials of romidepsin

Phase	Target Disease	Number of Patients	Dose and Schedule	Outcome	References
I	Advanced or refractory neoplasms	37	17.8 mg/m^2 Day 1 and 5 of a 21-day cycle	Dramatic response in two patients with T-cell lymphoma.	223, 230
II	Cutaneous and Peripheral T-cell lymphoma	98	14mg/m^2 Day 1, 8, and 15 of a 28-day cycle	34% response rate, complete response in 4 patients. Cardiac pharmacokinetic, and pharmacodynamic data acquired.	222, 228, 231, 232
II	Refractory cutaneous T-cell lymphoma	96	14mg/m^2 Day 1, 8, and 15 of a 28-day cycle	34% response rate, 6 patients with complete response.	233
I	Advanced cancers	33	13.3 mg/m^2 Day 1, 8, and 15 of a 28-day cycle	No demonstrated activity.	224
I	Chronic lymphocytic leukemia and acute myeloid leukemia	10 (CLL) 10 (AML)	13 mg/m^2 Day 1, 8, and 15 of a 28-day cycle	Some clinical activity; more evident anti-leukemic activity in CLL patients.	225
I	Children with refractory or recurrent neoplasms	18	13 mg/m^2 Day 1, 8, and 15 of a 28-day cycle	No objective responses.	226
I-II	Acute myelogenous leukemia and advanced myelodysplastic syndromes	9 (AML) 3 (MDS)	18 mg/m^2 Day 1 and 5 of a 21-day cycle	Limited clinical activity, though results indicated genetics may play a role in patient response to the drug.	227
II	Acute myeloid leukemia	20	13 mg/m^2 Day 1, 8, and 15 of a 28-day cycle	Limited antileukemic activity, possibility for combination therapy.	236
II	Colorectal cancer	25	13 mg/m^2 Day 1, 8, and 15 of a 28-day cycle	No objective responses.	237
II	Lung cancer	19	17.8 mg/m^2 Day 1 and 7 of a 21-day cycle	Limited clinical activity, possibility for combination therapy.	238
II	Refractory metastatic renal cell cancer	26	13 mg/m^2 Day 1, 8, and 15 of a 28-day cycle	Limited clinical activity.	234
II	Metastatic castration-resistant prostate cancer	35	13 mg/m^2 Day 1, 8, and 15 of a 28-day cycle	Limited antitumor activity, possibility for combination therapy.	239

Also of concern are the hematological side effects; regular blood tests are administered to patients on romidepsin to monitor these symptoms.[235] Leukopenia, granulocytopenia, and thrombocytopenia were all observed; in each case the effect is quickly reversed after cessation of the treatment.[229, 231]

Synthetic Studies

The main challenges in romidepsin's synthesis include the asymmetric construction of the hydroxy mercapto heptenoic acid, the 16-membered cyclic depsipeptide ring itself (i.e. four amino acids and hydroxy mercapto heptenoic acid), and the intramolecular oxidative coupling of the thiols to produce the stable prodrug form of the molecule. The total synthesis was first completed in 1996 in 14 steps with an 18% overall yield.[240] An improved synthesis utilizing 9 steps with a 13% overall yield was published in 2007,[241] using, as in the first scheme, an asymmetric acetate aldol reaction and a lactonization step for macrolization. In 2008, Wen *et al.*[242] utilized a lactamization as an alternative route to cyclization, reporting increased cyclization efficiency. However, due both to the chemical complexity of synthesis and the low yield of the producing organism, development was hindered mainly by shortages of the product.[243] Therefore, attempts have been made to develop active analogs.

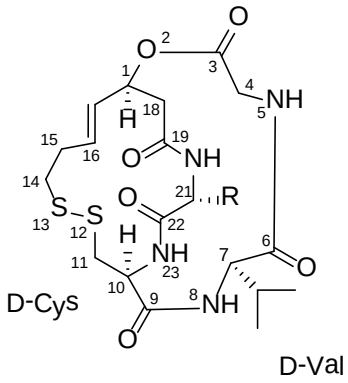

13, R = Me
14, R = i-Pr

Figure 17. Structures of two romidepsin analogs (compounds **13** and **14**), where the Z-dehydrobutyrine (Z-Dhb) residue, which may be susceptible to a Michael addition, has been replaced with a valine moiety.[244]

Using a series of synthetic analogs, Yurek-George *et al.*[244] were able to examine the importance of several features of the romidepsin structure. They concluded that while the sulfur at position 13 does indeed function as a Zn-binding group within the HDAC active site, the cysteine residue is non-essential, provided that the Zn-binding thiol remains protected as in the oxidized pro-drug form.[244] This assertion is supported by work done with linear compounds in which the thiol was masked as a thioester, undergoing enzymatic hydrolysis in the cell to produce the free thiol.[245, 246] Yurek-George *et al.* also found that the unsaturated dehydrobutyrane residue could be replaced by less reactive side chains with no loss in *in vitro* potency, but that the macrocyclic scaffold itself was an essential component of HDAC inhibition.[244] However, several small methyl ester structures without the macrocyclic backbone have proved to induce hyperacetylation in *Drosophila* S2 cells.[247] These structures retain the disulfide link of romidepsin, thus preserving its prodrug quality. The analogs studied consisted of several

small cyclic disulfides; the number of methylene units in the ring was varied to provide a range of lengths for the linker from the ester to the reduced sulfhydryl group.[247] Studies with HDAC inhibitors TSA and SAHA showed important interactions between the drugs and several phenylalanine residues surrounding the enzyme active site pocket,[209] so the methyl ester was used to attach various lipophilic caps, in an effort to improve enzyme interaction.[247] Despite these interesting medicinal chemistry studies, to the best of our knowledge, no analogs of romidepsin are in advanced stages of development.

Conclusions

As a potent HDAC inhibitor, romidepsin offers a promising new treatment for a disease with few existing therapies. It was approved by the U.S. FDA on November 5, 2009 for use in patients with cutaneous T-cell lymphoma (CTLC), under the trade name Istodax®, marketed by Celgene Corporation (Summit, NJ). The dosing schedule was approved as 14 mg/m^2 on days 1, 8 and 15 of a 28-day cycle.[235] After a year of approval as an antineoplastic agent, preliminary information suggests that romidepsin is finding a real place in the treatment of CTCL, and the activity and manageable toxicity are helpful for both patients receiving treatment and doctors prescribing it (personal communication by several medical doctors to W.M.). At the time of preparation of this review, a supplemental new drug application (NDA) was being prepared for peripheral T-cell lymphoma (PTCL),[248] and only time will tell if romidepsin's use expands to the treatment of other cancers.

Acknowledgement

This review was prepared in support of grant P01-CA125066 from the National Cancer Institute/National Institutes of Health, Bethesda, MD. Some details were added (by WM) with permission from Celgene Corporation.

REFERENCES

(1) Bailey, D. G., et al.; *Clinical and Investigative Medicine.* **1989,** 12, 357-362.
(2) Bailey, D. G., et al.; *Lancet.* **1991,** 337, 268-269.
(3) Bailey, D. G., et al.; *Br. J. Clin. Pharmacol.* **1998,** 46, 101-110.
(4) Paine, M. F., et al.; *Am. J. Clin. Nutr.* **2006,** 83, 1097-1105.
(5) Seden, K., et al.; *Drugs.* **2010,** 70, 2373-2407.
(6) Hanley, M. J., et al.; *Expert Opin. Drug Metab. Toxicol.* **2011,** 7, 267-286.
(7) Won, C. S.; Oberlies, N. H.; Paine, M. F.; *Pharmacol. Ther.* **2012,** 136, 186-201.
(8) Wilkinson, G. R.; *N. Engl. J. Med.* **2005,** 352, 2211-2221.
(9) Ohnishi, A., et al.; *Br. J. Pharmacol.* **2000,** 130, 1369-1377.
(10) Tassaneeyakul, W., et al.; *Arch. Biochem. Biophys.* **2000,** 378, 356-363.
(11) Paine, M. F.; Criss, A. B.; Watkins, P. B.; *Drug Metab. Dispos.* **2004,** 32, 1146-1153.
(12) Paine, M. F.; Criss, A. B.; Watkins, P. B.; *J. Pharmacol. Exp. Ther.* **2005,** 312, 1151-1160.
(13) Bailey, D. G.; Dresser, G. K.; Bend, J. R.; *Clin. Pharmacol. Ther. (St. Louis, MO, U. S.).* **2003,** 73, 529-537.
(14) Schwarz, U. I., et al.; *Br. J. Clin. Pharmacol.* **2006,** 62, 485-491.
(15) Goosen, T. C., et al.; *Clin. Pharmacol. Ther. (St. Louis, MO, U. S.).* **2004,** 76, 607-617.
(16) Lown, K. S., et al.; *J. Clin. Invest.* **1997,** 99, 2545-2553.
(17) Lilja, J. J.; Kivisto, K. T.; Neuvonen, P. J.; *Clin. Pharmacol. Ther. (St. Louis).* **2000,** 68, 384-390.
(18) Greenblatt, D. J., et al.; *Clin. Pharmacol. Ther. (St. Louis, MO, U. S.).* **2003,** 74, 121-129.
(19) Wacher, V. J.; Wu, C. Y.; Benet, L. Z.; *Mol. Carcinog.* **1995,** 13, 129-134.
(20) Dahan, A.; Amidon, G. L.; *Pharm. Res.* **2009,** 26, 883-892.
(21) Paine, M. F.; Oberlies, N. H.; *Expert Opin. Drug Metab. Toxicol.* **2007,** 3, 67-80.
(22) Becquemont, L., et al.; *Clin. Pharmacol. Ther. (St. Louis, MO, U. S.).* **2001,** 70, 311-316.
(23) Parker, R. B., et al.; *Pharmacotherapy.* **2003,** 23, 979-987.
(24) Dresser, G. K., et al.; *Clin. Pharmacol. Ther.* **2002,** 71, 11-20.
(25) Wang, X.; Wolkoff, A. W.; Morris, M. E.; *Drug Metab. Dispos.* **2005,** 33, 1666-1672.
(26) Satoh, H., et al.; *Drug Metab. Dispos.* **2005,** 33, 518-523.
(27) Lilja, J. J.; Juntti-Patinen, L.; Neuvonen, P. J.; *Clin. Pharmacol. Ther. (St. Louis, MO, U. S.).* **2004,** 75, 184-190.
(28) Glaeser, H., et al.; *Clin. Pharmacol. Ther.* **2007,** 81, 362-370.
(29) Greenblatt, D. J.; *J. Clin. Pharmacol.* **2009,** 49, 1403-1407.
(30) Dahan, A.; Amidon, G. L.; *Pharm. Res.* **2009,** 26, 883-892.
(31) Ohnishi, A., et al.; *Br. J. Pharmacol.* **2000,** 130, 1369-1377.
(32) Lown, K. S., et al.; *Clin. Pharmacol. Ther.* **1997,** 62, 248-260.
(33) Edwards, D. J., et al.; *Clin. Pharmacol. Ther.* **1999,** 65, 237-244.
(34) De Castro, W. V., et al.; *J. Pharm. Sci.* **2007,** 96, 2808-2817.

(35) Paine, M. F., et al.; *Am. J. Clin. Nutr.* **2008,** 87, 863-871.
(36) Dresser, G. K.; Bailey, D. G.; *Eur. J. Clin. Invest.* **2003,** 33, 10-16.(37) Dresser, G. K.; Kim, R. B.; Bailey, D. G.; *Clin. Pharmacol. Ther.* **2005,** 77, 170-177.
(38) Avula, B.; Upparapalli, S. K.; Khan, I. A.; *J. AOAC Int.* **2007,** 90, 633-640.
(39) Vanamala, J., et al.; *J. Food Compos. Anal.* **2005,** 19, 157-166.
(40) Bailey, D. G., et al.; *Clin. Pharmacol. Ther.* **2007,** 81, 495-502.
(41) Ross, S. A., et al.; *Fitoterapia.* **2000,** 71, 154-161.
(42) Fukuda, K., et al.; *J. Chromatogr. B.* **2000,** 741, 195-203.
(43) De Castro, W. V., et al.; *J. Agr. Food Chem.* **2006,** 54, 249-255.
(44) Manthey, J. A.; Buslig, B. S.; *J. Agr. Food Chem.* **2005,** 53, 5158-5163.
(45) Widmer, W.; Huan, C.; *J. Food Sci.* **2005,** 70, C307-C312.
(46) Lin, Y. K., et al.; *J. Chromatogr. Sci.* **2009,** 47, 211-215.
(47) Fujita, T., et al.; *Biol. Pharm. Bull.* **2008,** 31, 925-930.
(48) Medina-Remon, A., et al.; *J. Agr. Food Chem.* **2011,** 59, 6353-6359.
(49) Huang, W., et al.; *Pharmazie.* **2012,** 67, 586-589.
(50) Cao, J., et al.; *Anal. Methods.* **2012,** 4, 4121-4128.
(51) Baranowska, I.; Magiera, S.; *J. AOAC Int.* **2011,** 94, 786-794.
(52) De Paepe, D., et al.; *Food Chem.* **2013,** 136, 368-375.
(53) MacNair, J. E.; Lewis, K. C.; Jorgenson, J. W.; *Anal. Chem.* **1997,** 69, 983-989.
(54) MacNair, J. E.; Patel, K. D.; Jorgenson, J. W.; *Anal. Chem.* **1999,** 71, 700-708.
(55) Wu, N.; Lippert, J. A.; Lee, M. L.; *J. Chromatogr. A.* **2001,** 911, 1-12.
(56) Swartz, M. E.; *J. Liq. Chromatogr. R. T.* **2005,** 28, 1253-1263.
(57) Gerber, F., et al.; *J. Chromatogr. A.* **2004,** 1036, 127-133.
(58) Kumar, A., et al.; *Acta Pol. Pharm.* **2012,** 69, 371-380.
(59) Won, C. S., et al.; *AAPS J.* **2010,** 12, S2 (available at www.aapsj.org).
(60) Wolf, K. K., et al.; *Clin. Pharmacol. Ther.* **2011,** 89, S61-S62.
(61) Harris, D. C., *Quantitative Chemical Analysis*. 7 ed.; W. H. Freeman and Co.: New York, 2007.
(62) Wilson, E. G., et al.; *Acta Farm. Bonaerense.* **2000,** 19, 277-279.
(63) Wanwimolruk, S.; Marquez, P. V.; *Drug Metab. Drug Interact.* **2006,** 21, 233-243.
(64) *NBJ's Supplement Business Report*; Nutrition Business Journal: 2012; p 23.
(65) Paibir, S.; Rahavendran, S. V. In *ADME of herbal dietary supplements*, 2012; John Wiley & Sons, Inc.: 2012; pp 793-840.
(66) *Sports Nutrition & Weight Loss Report*; Nutrition Business Journal 2012; p 13.
(67) VanderMolen, K. M., et al.; *Phytochem. Anal.* **2013,** 24, 654-660.
(68) Durr, D., et al.; *Clin. Pharmacol. Ther.* **2000,** 68, 598-604.
(69) Dell'Aica, I., et al.; *Clin Chim Acta.* **2007,** 381, 69-77.
(70) Madabushi, R., et al.; *Eur J Clin Pharmacol.* **2006,** 62, 225-233.
(71) Schwarz, U. I., et al.; *Clin. Pharmacol. Ther.* **2007,** 81, 669-678.
(72) Mai, I., et al.; *Clin. Pharmacol. Ther.* **2004,** 76, 330-340.
(73) De Smet, P. A. G. M.; *N. Engl. J. Med.* **2005,** 352, 1176-1178.
(74) Woo, J. J. Y.; *Am. J. Clin. Nutr.* **2007,** 85, 323S-324S.
(75) Herbert, V.; *Mayo Clin Proc.* **1999,** 74, 531-532.
(76) Hensrud, D. D.; Engle, D. D.; Scheitel, S. M.; *Mayo Clin Proc.* **1999,** 74, 443-447.

(77) Klepser, T. B., et al.; *Pharmacotherapy.* **2000,** 20, 83-87.
(78) Peroutka, R., et al.; *J Sci Food Agr.* **2007,** 87, 2152-2163.
(79) ICH; *US FDA Federal Register.* **1997,** 62, 27463-27467.
(80) Rogatsky, E.; Stein, D.; *J. Am. Soc. Mass Spectrom.* **2005,** 16, 1757-1759.
(81) Malhotra, S., et al.; *Clin. Pharmacol. Ther. (St. Louis, MO, U. S.).* **2001,** 69, 14-23.
(82) Strauch, K., et al.; *Food and Chemical Toxicology.* **2009,** 47, 1928-1935.
(83) Kakar, S. M., et al.; *Clin. Pharmacol. Ther. (St. Louis, MO, U. S.).* **2004,** 75, 569-579.
(84) Volak, L. P., et al.; *Drug Metab. Dispos.* **2008,** 36, 1594-1605.
(85) Firn, R. D.; Jones, C. G.; *Nat Prod Rep.* **2003,** 20, 382-391.
(86) Ehrlich, P. R.; Raven, P. H.; *Evolution.* **1964,** 18, 586-608.
(87) Fraenkel, G. S.; *Science.* **1959,** 129, 1466-1470.
(88) Hong, J.; *Curr. Opin. Chem. Biol.* **2011,** 15, 350-354.
(89) Newman, D. J.; Cragg, G. M.; *J. Nat. Prod.* **2007,** 70, 461-477.
(90) Verdine, G. L.; *Nature.* **1996,** 384, 11-13.
(91) Clardy, J.; Walsh, C.; *Nature.* **2004,** 432, 829-837.
(92) Rosen, J., et al.; *J. Med. Chem.* **2009,** 52, 1953-1962.
(93) Feher, M.; Schmidt, J. M.; *J. Chem. Inf. Comp. Sci.* **2003,** 43, 218-227.
(94) Newman, D. J.; Cragg, G. M.; *J. Nat. Prod.* **2012**.
(95) Sy-Cordero, A. A., et al.; *J. Antibiot.* **2010,** 63, 539-544.
(96) Gloer, J. B., Applications of fungal ecology in the search for new bioactive natural products. In *The Mycota*, Vol. IV; Wicklow, D. T.; Soderstrom, B. E., Eds. Springer-Verlag: New York, 2007; pp 257-283.
(97) Strader, C. R.; Pearce, C. J.; Oberlies, N. H.; *J. Nat. Prod.* **2011,** 74, 900-907.
(98) Grob, C. S., et al.; *Arch. Gen. Psychiat.* **2011,** 68, 71-78.
(99) Keating, G.; Figgitt, D.; *Drugs.* **2003,** 63, 2235-2263.
(100) May, R. M., The dimensions of Life on Earth. In *Nature and Human Society: the quest for a sustainable world*; Raven, P. H.; Williams, T., Eds. National Academy Press: Washington, DC, 2000; pp 30-45.
(101) Cannon, P. F.; *Biodivers. Conserv.* **1997,** 6, 669-680.
(102) Hawksworth, D. L.; *Mycol. Res.* **2001,** 105, 1422-1432.
(103) Ondeyka, J. G., et al.; *J. Nat. Prod.* **2003,** 66, 121-124.
(104) Brady, S. F.; Bondi, S. M.; Clardy, J.; *J. Am. Chem. Soc.* **2001,** 123, 9900-9901.
(105) Keller, N. P.; Turner, G.; Bennett, J. W.; *Nat. Rev. Microbiol.* **2005,** 3, 937-947.
(106) Galagan, J. E., et al.; *Nature.* **2003,** 422, 859-868.
(107) Nierman, W. C., et al.; *Nature.* **2005,** 438, 1151-1156.
(108) Bentley, S. D., et al.; *Nature.* **2002,** 417, 141-147.
(109) Galagan, J. E., et al.; *Nature.* **2005,** 438, 1105-1115.
(110) Scherlach, K.; Hertweck, C.; *Org. Biomol. Chem.* **2009,** 7, 1753-1760.
(111) Fisch, K. M., et al.; *J. Ind. Microbiol. Biot.* **2009,** 36, 1199-1213.
(112) Hoffmeister, D.; Keller, N. P.; *Natural Product Reports.* **2007,** 24, 393-416.
(113) Chang, P. K., et al.; *Appl. Environ. Microbiol.* **1993,** 59, 3273-3279.
(114) Brown, D. W., et al.; *Proc. Natl. Acad. Sci. U. S. A.* **1996,** 93, 1418-1422.
(115) Chang, P.-K., et al.; *Appl. Environ. Microbiol.* **1995,** 61, 2372-2377.
(116) Dowzer, C. E.; Kelly, J. M.; *Curr Genet.* **1989,** 15, 457-459.

(117) Hynes, M. J.; *Aust. J. Biol. Sci.* **1975,** 28, 301-313.
(118) Tilburn, J., et al.; *EMBO J.* **1995,** 14, 779-790.
(119) Bok, J. W.; Keller, N. P.; *Eukaryot. Cell.* **2004,** 3, 527-535.
(120) Glaser, K. B.; *Biochem. Pharmacol.* **2007,** 74, 659-671.
(121) Kuo, M. H.; Allis, C. D.; *Bioessays.* **1998,** 20, 615-626.
(122) Emanuele, S.; Lauricella, M.; Tesoriere, G.; *Int. J. Oncol.* **2008,** 33, 637-646.
(123) Fukuda, H., et al.; *Brief. Funct. Genomic. Proteomic.* **2006,** 5, 190-208.
(124) Bird, A.; *Gene. Dev.* **2002,** 16, 6-21.
(125) Suzuki, M. M.; Bird, A.; *Nat. Rev. Genet.* **2008,** 9, 465-476.
(126) Egger, G., et al.; *Nature.* **2004,** 429, 457-463.
(127) Shwab, E. K., et al.; *Eukaryot. Cell.* **2007,** 6, 1656-1664.
(128) Henrikson, J. C., et al.; *Org. Biomol. Chem.* **2009,** 7, 435-438.
(129) Williams, R. B., et al.; *Org. Biomol. Chem.* **2008,** 6, 1895-1897.
(130) Wang, X. R., et al.; *J. Nat. Prod.* **2010,** 73, 942-948.
(131) Kritsky, M. S., et al.; *Appl. Biochem. Microbiol.* **2001,** 37, 243-247.
(132) Bode, H. B., et al.; *ChemBioChem.* **2002,** 3, 619-627.
(133) Bills, G. F., et al.; *J. Appl. Microbiol.* **2008,** 104, 1644-1658.
(134) Xu, P., et al.; *Enzyme Microb. Technol.* **2008,** 42, 325-331.
(135) Shang, Z., et al.; *Chem. Biodivers.* **2012,** 9, 1338-1348.
(136) Mohanty, S. S.; Prakash, S.; *Acta Tropica.* **2009,** 109, 50-54.
(137) Miao, L.; Kwong, T. F. N.; Qian, P.-Y.; *Appl. Microbiol. Biotechnol.* **2006,** 72, 1063-1073.
(138) Kossuga, M. H., et al.; *Rev. Bras. Farmacogn.* **2012,** 22, 257-267.
(139) Fiedurek, J.; Gromada, A.; Jamroz, J.; *J. Basic Microb.* **1996,** 36, 27-32.
(140) Zimmermann, J., et al.; *Oncogene.* **2000,** 19, 2913-2920.
(141) Szutorisz, H., et al.; *Cell.* **2006,** 127, 1375-1388.
(142) Scherlach, K.; Hertweck, C.; *Org. Biomol. Chem.* **2006,** 4, 3517-3520.
(143) Bills, G. F.; Dombrowski, A. W.; Goetz, M. A., The "FERMEX" method for metabolite-enriched fungal extracts. In *Fungal Secondary Metabolism*, Vol. 944; Keller, N. P.; Turner, G., Eds. Humana Press: New York, 2012; pp 79-96.
(144) Author; In 10th ed.; CABI Publishing: Wallingford, 2011.
(145) Stone, J. K.; Polishook, J. D.; White Jr., J. F., Endophytic Fungi. In *Biodiversity of Fungi: Inventory and Monitoring Methods*; Foster, M.; Bills, G., Eds. Academic Press: Burlington, 2004; pp 241-270.
(146) Schulz, B., et al.; *Mycol. Res.* **1993,** 97, 1447-1450.
(147) Shearer, C. A.; Langsam, D. M.; Longcore, J. E., Fungi in freshwater habitats. In *Measuring and monitoring biological diversity: standard methods for Fungi*; Mueller, G. M.; Bills, G. F.; Foster, M. S., Eds. Smithsonian Institution Press: Washington DC, 2004; pp 513–531.
(148) Raja, H. A.; Schmit, J. P.; Shearer, C. A.; *Biodivers. Conserv.* **2009,** 18, 419-455.
(149) Figueroa, M., et al.; *J. Nat. Prod.* **2013,** 76, 1007-1015.
(150) El-Elimat, T., et al.; *J. Nat. Prod.* **2013,** 76, 382-387.
(151) El-Elimat, T., et al.; *Tetrahedron Lett.* **2013,** 54, 4300-4302.
(152) Schoch, C. L., et al.; *Proc. Natl. Acad. Sci. USA.* **2012,** 109, 6241-6246.
(153) El-Elimat, T., et al.; *J. Nat. Prod.* **2013,** 76, 1709-1716.

(154) Soerensen, J. L.; Nielsen, K. F.; Sondergaard, T. E.; *Fungal Genet. Biol.* **2012,** 49, 613-618.
(155) Mikusova, P., et al.; *Mycotoxin Res.* **2013,** 29, 97-102.
(156) Ezekiel, C. N., et al.; *Eur. Food Res. Technol.* **2012,** 235, 285-293.
(157) Strunz, G. M., et al.; *Can. J. Chem.* **1974,** 52, 825-826.
(158) Kirihata, M., et al.; *Biosci. Biotechnol. Biochem.* **1996,** 60, 677-679.
(159) Kimura, Y., et al.; *Plant Cell Physiol.* **1977,** 18, 1177-1179.
(160) Kimura, Y., et al.; *Agr. Biol. Chem.* **1971,** 35, 1313-1314.
(161) El-Elimat, T., et al.; *ACS Med. Chem. Lett.* **2012,** 3, 645-649.
(162) Pu, X., et al.; *Appl. Microbiol. Biotechnol.* **2013,** 97, 9365-9375.
(163) Hestbjerg, H., et al.; *J. Agr. Food Chem.* **2002,** 50, 7593-7599.
(164) Paranagama, P. A.; Wijeratne, E. M. K.; Gunatilaka, A. A. L.; *J. Nat. Prod.* **2007,** 70, 1939-1945.
(165) Vervoort, H. C.; Draskovic, M.; Crews, P.; *Org. Lett.* **2011,** 13, 410-413.
(166) Fisch, K. M., et al.; *J. Ind. Microbiol. Biotechnol.* **2009,** 36, 1199-1213.
(167) Yakasai, A. A., et al.; *J. Am. Chem. Soc.* **2011,** 133, 10990-10998.
(168) Beau, J., et al.; *Mar. Drugs.* **2012,** 10, 762-774.
(169) Chung, Y.-M., et al.; *Bioorg. Med. Chem.* **2013,** 21, 3866-3872.
(170) Ayers, S., et al.; *J. Nat. Prod.* **2011,** 74, 1126-1131.
(171) Cagide, F., et al.; *J. Mol. Struct.* **2013,** 1049, 125-131.
(172) Conrad, J., et al.; *J. Nat. Prod.* **2009,** 72, 835-840.
(173) Sun, R.-R., et al.; *Magn. Reson. Chem.* **2013,** 51, 65-68.
(174) Hoye, T. R.; Jeffrey, C. S.; Shao, F.; *Nat. Protoc.* **2007,** 2, 2451-2458.
(175) Wiley, P. F.; *J. Am. Chem. Soc.* **1952,** 74, 4326-4328.
(176) Kurdistani, S. K.; *Br. J. Cancer.* **2007,** 97, 1-5.
(177) Zheng, Y. G., et al.; *Med. Res. Rev.* **2008,** 28, 645-687.
(178) Mitsiades, C. S., et al.; *Proc. Natl. Acad. Sci. USA.* **2004,** 101, 540-545.
(179) Melnick, A.; Licht, J. D.; *Curr. Opin. Hematol.* **2002,** 9, 322-332.
(180) Mahlknecht, U.; Hoelzer, D.; *Mol. Med.* **2000,** 6, 623-644.
(181) Marks, P. A., et al.; *Curr. Opin. Oncol.* **2001,** 13, 477-483.
(182) Klisovic, M. I., et al.; *Leukemia.* **2003,** 17, 350.
(183) Bieliauskas, A. V.; Pflum, M. K.; *Chem. Soc. Rev.* **2008,** 37, 1402-1413.
(184) Papeleu, P., et al.; *Crit. Rev. Toxicol.* **2005,** 35, 363-378.
(185) Dokmanovic, M.; Marks, P. A.; *J. Cell. Biochem.* **2005,** 96, 293-304.
(186) Ueda, H., et al.; *J. Antibiot.* **1994,** 47, 301-310.
(187) Xiao, J. J., et al.; *Rapid Commun. Mass Sp.* **2003,** 17, 757-766.
(188) Anonymous, In.
(189) Willemze, R., et al.; *Blood.* **2005,** 105, 3768-3785.
(190) Whittaker, S. J., et al.; *Br. J. Dermatol.* **2003,** 149, 1095-1107.
(191) Litvinov, I. V., et al.; *Clin. Cancer Res.* **2010,** 16, 2106-2114.
(192) Weinstock, M. A.; Horm, J. W.; *JAMA.* **1988,** 260, 42-46.
(193) Criscione, V. D.; Weinstock, M. A.; *Arch. Dermatol.* **2007,** 143, 854-859.
(194) Kim, E. J., et al.; *J. Clin. Invest.* **2005,** 115, 798-812.
(195) Lorincz, A. L.; *Lancet.* **1996,** 347, 871-876.

(196) Kim, Y. H., et al.; *Arch. Dermatol.* **2003,** 139, 857-866.
(197) Bradford, P. T., et al.; *Blood.* **2009,** 113, 5064-5073.
(198) Kim, Y. H., et al.; *Arch. Dermatol.* **1999,** 135, 26-32.
(199) Duvic, M., et al.; *J. Am. Acad. Dermatol.* **2003,** 49, 35-49.
(200) Zackheim, H. S., et al.; *J. Am. Acad. Dermatol.* **1999,** 40, 418-425.
(201) Siegel, R. S., et al.; *J. Clin. Oncol.* **2000,** 18, 2908-2925.
(202) Shigematsu, N., et al.; *J. Antibiot.* **1994,** 47, 311-314.
(203) Manoharan, T. H., et al.; *Carcinogenesis.* **1985,** 6, 1295-1301.
(204) Wang, R., et al.; *Oncogene.* **1998,** 17, 1503-1508.
(205) Rajgolikar, G.; Chan, K. K.; Wang, H. C.; *Breast Cancer Res. Treat.* **1998,** 51, 29-38.
(206) Nakajima, H., et al.; *Exp. Cell. Res.* **1998,** 241, 126-133.
(207) Yoshida, M., et al.; *Cancer Chemother. Pharmacol.* **2001,** 48, S20-S26.
(208) Furumai, R., et al.; *Cancer Res.* **2002,** 62, 4916-4921.
(209) Finnin, M. S., et al.; *Nature.* **1999,** 401, 188-193.
(210) Piekarz, R.; Bates, S.; *Curr. Pharm. Des.* **2004,** 10, 2289-2298.
(211) Archer, S. Y., et al.; *Proc. Natl. Acad. Sci. USA.* **1998,** 95, 6791-6796.
(212) Burgess, A. J., et al.; *Mol. Pharmacol.* **2001,** 60, 828-837.
(213) Rosato, R. R.; Almenara, J. A.; Grant, S.; *Cancer Res.* **2003,** 63, 3637-3645.
(214) Sandor, V., et al.; *Br. J. Cancer.* **2000,** 83, 817-825.
(215) Peart, M. J., et al.; *Cancer Res.* **2003,** 63, 4460-4471.
(216) Insinga, A., et al.; *Nat. Med.* **2005,** 11, 71-76.
(217) Nebbioso, A., et al.; *Nat. Med.* **2005,** 11, 77-84.
(218) Yu, X., et al.; *J. Natl. Cancer Inst.* **2002,** 94, 504-513.
(219) Yu, C., et al.; *Blood.* **2003,** 102, 3765-3774.
(220) Huang, H. C., et al.; *Life Sci.* **2002,** 70, 1763-1775.
(221) Kwon, H. J., et al.; *Int. J. Cancer.* **2002,** 97, 290-296.
(222) Woo, S., et al.; *Clin. Cancer Res.* **2009,** 15, 1496-1503.
(223) Sandor, V., et al.; *Clin. Cancer Res.* **2002,** 8, 718-728.
(224) Marshall, J. L., et al.; *J. Exp. Ther. Oncol.* **2002,** 2, 325-332.
(225) Byrd, J. C., et al.; *Blood.* **2005,** 105, 959-967.
(226) Fouladi, M., et al.; *J. Clin. Oncol.* **2006,** 24, 3678-3685.
(227) Klimek, V. M., et al.; *Clin. Cancer Res.* **2008,** 14, 826-832.
(228) Bates, S. E., et al.; *British Journal of Haematology.* **2009,** 148, 256-267.
(229) Grant, C., et al.; *Expert Rev. Anticanc.* **2010,** 10, 997-1008.
(230) Piekarz, R. L., et al.; *Blood.* **2001,** 98, 2865-2868.
(231) Piekarz, R. L., et al.; *J. Clin. Oncol.* **2009,** 27, 5410-5417.
(232) Piekarz, R. L., et al.; *Clin. Cancer Res.* **2006,** 12, 3762-3773.
(233) Whittaker, S. J., et al.; *J. Clin. Oncol.* **2010,** 28, 4485-4491.
(234) Stadler, W. M., et al.; *Clin. Genitourin. Canc.* **2006,** 5, 57-60.
(235) Anonymous, In 2010.
(236) Odenike, O. M., et al.; *Clin. Cancer Res.* **2008,** 14, 7095-7101.
(237) Whitehead, R. P., et al.; *Invest. New Drugs.* **2009,** 27, 469-475.
(238) Schrump, D. S., et al.; *Clin. Cancer Res.* **2008,** 14, 188-198.
(239) Molife, L. R., et al.; *Ann. Oncol.* **2010,** 21, 109-113.

(240) Li, K. W., et al.; *J. Am. Chem. Soc.* **1996,** 118, 7237-7238.
(241) Greshock, T. J., et al.; *Org. Lett.* **2008,** 10, 613-616.
(242) Wen, S.; Packham, G.; Ganesan, A.; *J. Org. Chem.* **2008,** 73, 9353-9361.
(243) Jones, P.; Steinkuhler, C.; *Curr. Pharm. Des.* **2008,** 14, 545-561.
(244) Yurek-George, A., et al.; *J. Med. Chem.* **2007,** 50, 5720-5726.
(245) Suzuki, T., et al.; *J. Med. Chem.* **2005,** 48, 1019-1032.
(246) Suzuki, T., et al.; *Bioorg. Med. Chem. Lett.* **2007,** 17, 1558-1561.
(247) Mays, J. R., et al.; *Tetrahedron Lett.* **2007,** 48, 4579-4583.
(248) Pro, B., et al.; *52nd American Society of Hematology Annual Meeting and Exposition.* **2010,** Abstract 114.

APPENDIX A

SUPPLEMENTARY FIGURES AND TABLES

Figure S1. UV spectra of compounds **1**-**6** as standards and in Juice D (two pages).

Figure S2. Co-injections of analytes **3**-**6** and Juice D (two pages).

Table S1. The mass of each capsule's contents. AttentionLink was weighed in its entirety.

Table S2. Calculated content of bergamottin and DHB in supplements. These analytes were not detected in any of the other supplements tested.
DHB = 6',7'-dihydroxybergamottin.

Figure S3. UPLC-ELSD chromatograms of G142 in liquid media. The column was a BEH-C18, and the gradient increased linearly from 15:85 CH_3CN:H_2O to 100:0 over 10 min. Abbreviations of media are defined in the Methods section.

Table S3. NMR data (400 MHz, DMSO-d_6) of compound **1**. The experimental values were measured directly, as were the ^{1}H NMR literature values (500 MHz, DMSO-d_6). The ^{13}C NMR values reported in the literature were derived through HMBC and HSQC experiments.

Figure S4. Comparison of control (A) and dosed (B-D) growths of MSX 63935 grown in potato dextrose broth (left) and Czapek Dox broth (right). Cultures shown in (B) were grown with 50 µg/mL SAHA, (C) with 100 µg/mL 5-AZA, and (D) with 50 µg/mL bortezomib. The separation was performed via UPLC-PDA (235 nm), using a C_{18} column and a gradient increasing linearly from 10% CH_3CN (H_2O) at 0.0 min to 100% at 4.5 min, held at 100% for an additional 0.5 min.

Figure S5. ^{1}H NMR spectrum **9** [400 MHz, MeOH-d_4].

Figure S6. ^{13}C NMR spectrum of **9** [400 MHz, MeOH-d_4].

Figure S7. ^{1}H NMR spectrum of **10** [400 MHz, MeOH-d_4].

Figure S8. ^{13}C NMR spectrum of **10** [600 MHz, MeOH-d_4].

Figure S9. UPLC-PDA (235 nm detection) chromatograms of compounds **1** (top) and **2** (bottom) demonstrating purity. The purity of compound **1** is >99%, and the purity of compound **2** is >91%. The separation was performed using a C_{18} column and a gradient increasing linearly from 10% CH_3CN (H_2O) at 0.0 min to 100% at 4.5 min, held at 100% for an additional 0.5 min.

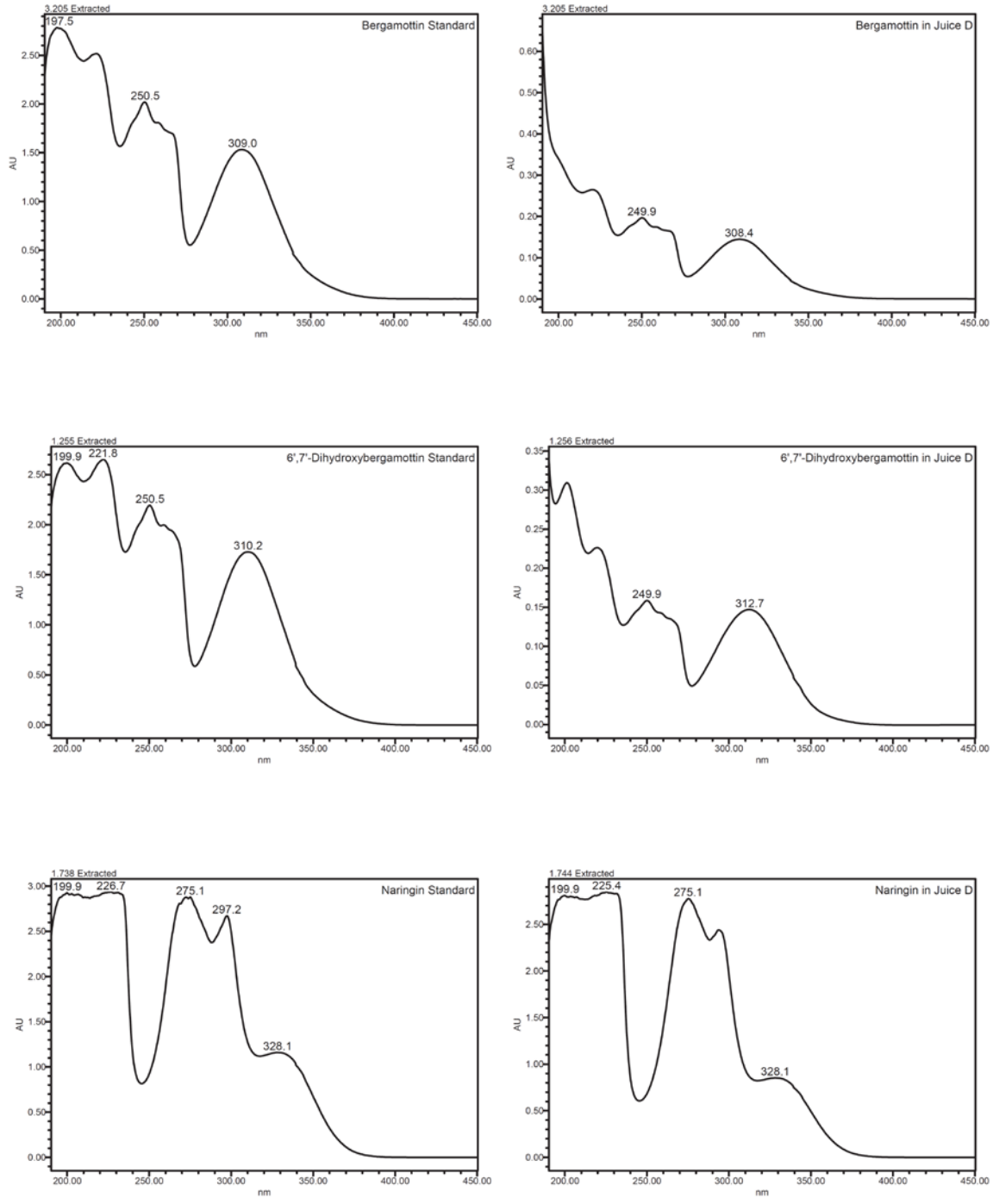

Figure S1. UV spectra of compounds **1**-**6** as standards and in Juice D. Continued on next page.

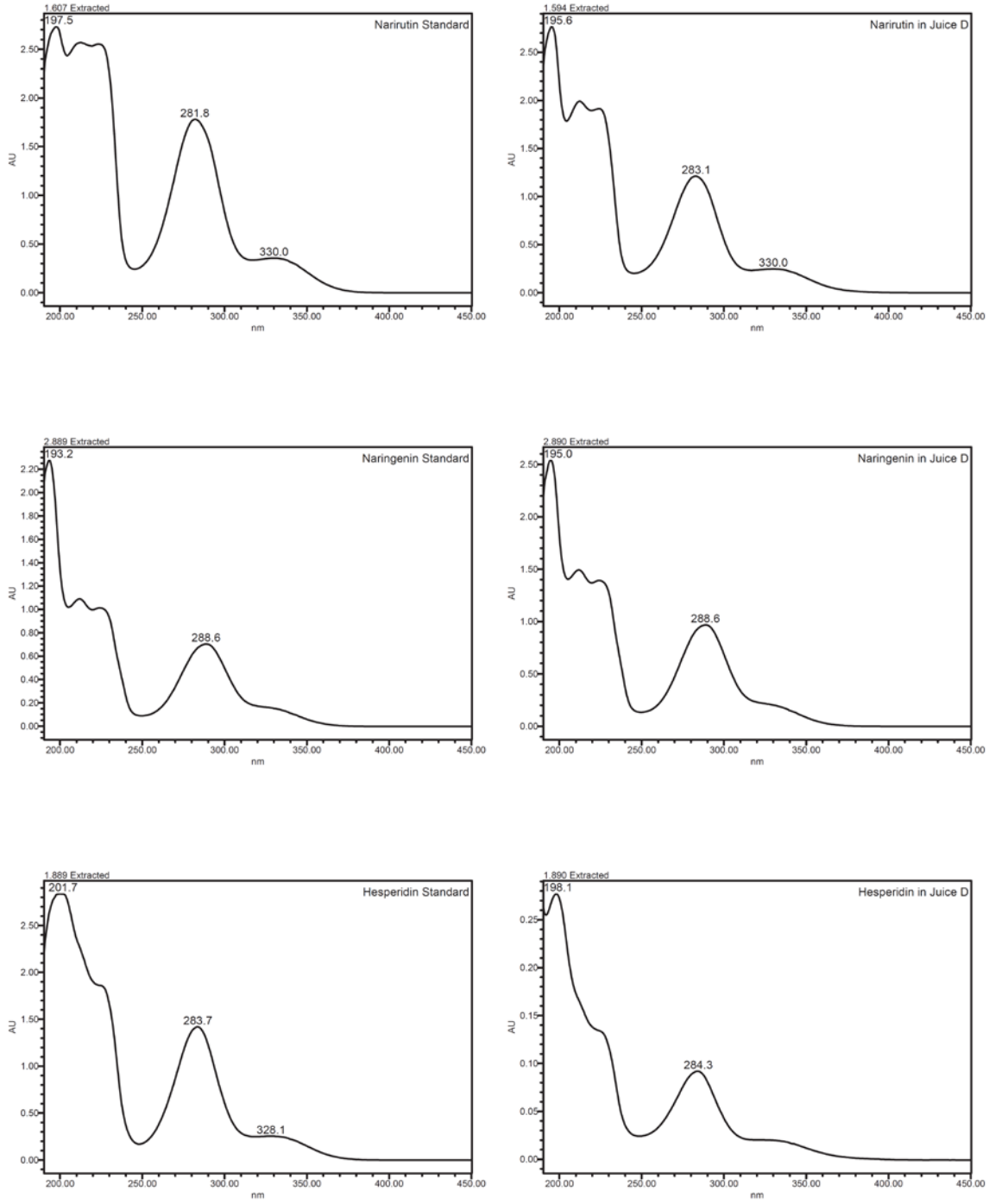

Figure S1 (continued). UV spectra of compounds **1**-**6** as standards and in Juice D.

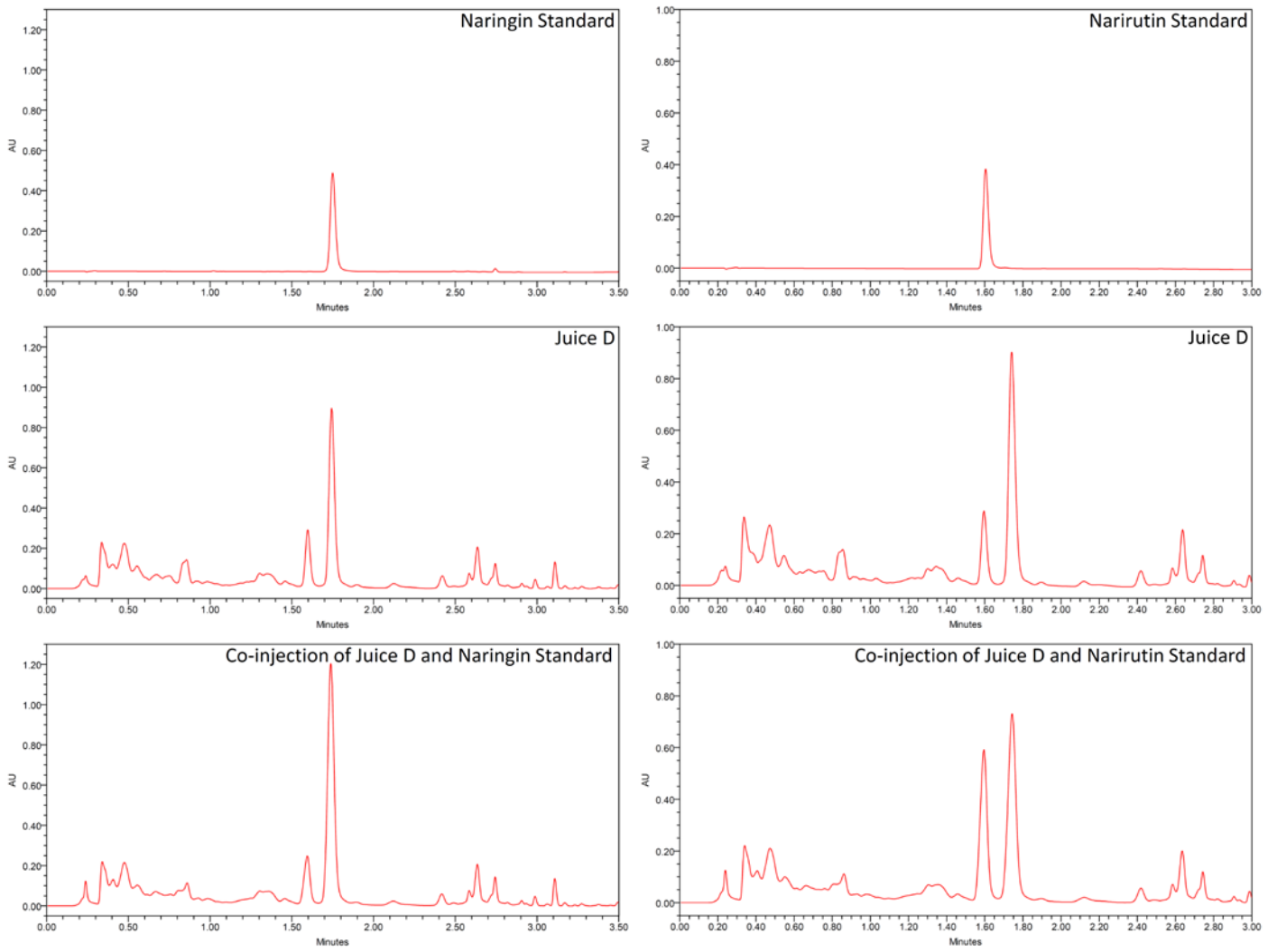

Figure S2. Co-injections of analytes **3-6** and Juice D. Continued on next page.

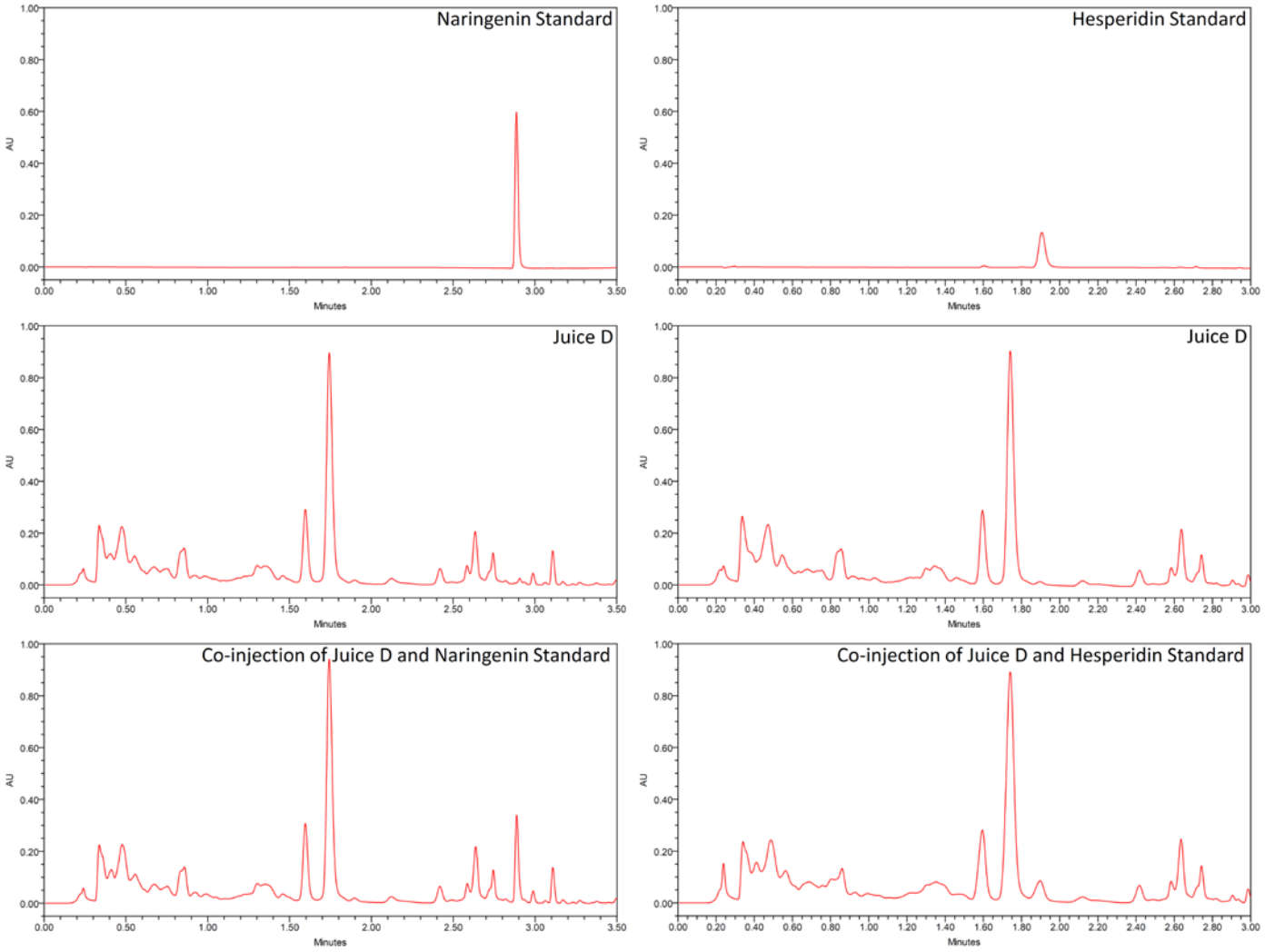

Figure S2 (continued). Co-injections of analytes **3**-**6** and Juice D.

Table S1. The mass of each capsule's contents. (AttentionLink was weighed in its entirety.)

	1	2	3	4	5	AVE	RSD
SciFit DHB 300	383.77	366.58	350.90	384.20	402.60	377.6	5.20
Trisorbagen	350.69	345.86	353.62	313.65	358.61	344.5	5.18
Xceler8 DHB	242.50	203.86	191.22	205.59	216.94	212.0	9.11
AttentionLink	990.58	943.97	973.68	942.45	1011.71	972.5	3.08
Finaflex Alpha	621.29	636.33	664.30	632.12	617.64	634.3	2.90
Finaflex Andro	703.27	677.01	682.31	677.53	671.31	682.3	1.81

Table S2. Calculated content of bergamottin and DHB in supplements. These analytes were not detected in any of the other supplements tested.
DHB = 6',7'-dihydroxybergamottin.

	µg/capsule	SD	% weight of capsule	SD
DHB in SciFit (PDA)				
LOQ	0.22			
LOD	0.074			
Capsule 1 (383.77 mg)	66.68	0.64	0.01738	0.00017
Capsule 2 (366.58 mg)	57.83	0.64	0.01577	0.00017
Capsule 3 (350.9 mg)	64.06	0.64	0.01826	0.00018
Capsule 4 (384.2 mg)	68.29	0.64	0.01778	0.00017
Capsule 5 (402.6 mg)	70.69	0.64	0.01756	0.00016
Bergamottin in SciFit (PDA)				
LOQ	2.0			
LOD	0.12			
Capsule 1 (383.77 mg)	11.70	0.23	0.003050	0.000061
Capsule 2 (366.58 mg)	11.56	0.23	0.003152	0.000064
Capsule 3 (350.9 mg)	11.86	0.23	0.003380	0.000066
Capsule 4 (384.2 mg)	12.29	0.23	0.003200	0.000061
Capsule 5 (402.6 mg)	13.24	0.23	0.003289	0.000058
Bergamottin in Xceler8 (MS)				
LOQ	0.18			
LOD	0.060			
Capsule 1 (242.5 mg)	2.977	0.069	0.001227	0.000029
Capsule 2 (203.86 mg)	2.644	0.069	0.001382	0.000036
Capsule 3 (191.22 mg)	2.582	0.069	0.001267	0.000034
Capsule 4 (205.59 mg)	2.509	0.069	0.001220	0.000034
Capsule 5 (216.94 mg)	2.816	0.069	0.001298	0.000032

Table S3. NMR data (400 MHz, DMSO-d_6) of compound **1**. The experimental values were measured directly, as were the ^{1}H NMR literature values (500 MHz, DMSO-d_6). The ^{13}C NMR values reported in the literature were derived through HMBC and HSQC experiments.

	Experimental Values		**Literature Values**[a]	
position	δ_C	δ_H, mult. (*J* in Hz)	δ_C	δ_H, mult. (*J* in Hz)
5'	13.9	0.86, t (7.1)	14.7	0.86, t (6.9)
4'	18.2	1.41, 1.32, m	18.9	1.41, 1.32, m
3'	obscured (DMSO)	1.41, m	39.8	1.41, m
1'	41.7	2.55, dd (8.7, 14.2) 2.70, dd (4.6, 14.2)	42.1	2.55, dd (8.1, 14.5) 2.66, dd (4.6, 14.3)
O-Me	56.1	3.87, s	56.2	3.82, s
2'	67.4	3.88, m	68.0	3.87, m
6	100.6	6.84, d (2.3)	98.2	6.50, d (2.4)
3	110.7	6.09, s	110.3	5.98, s
4a	111.8		111.5	
8	113.1	7.07, d (2.3)	113.4	6.78, d (2.4)
5	not observed		147.1	
8a	157.8		158.8	
7	162.7		163.5	
2	166.7		166.4	
COOH	169.2		172.6	
4	175.4		177.2	

[a]Conrad, J., et al.; *J. Nat. Prod.* **2009,** 72, 835-840.

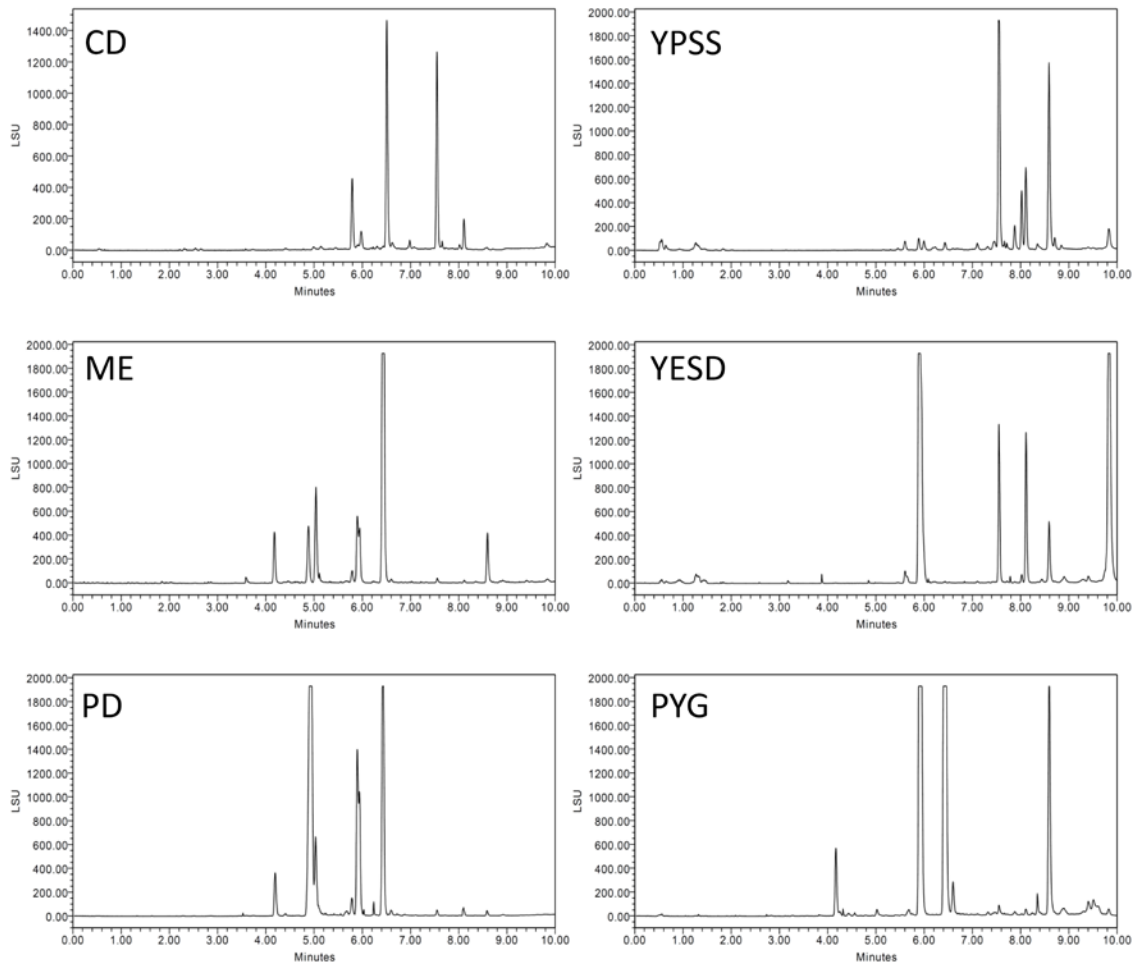

Figure S3. UPLC-ELSD chromatograms of G142 in liquid media. The column was a BEH-C18, and the gradient increased linearly from 15:85 CH_3CN:H_2O to 100:0 over 10 min. Abbreviations of media are defined in the Methods section.

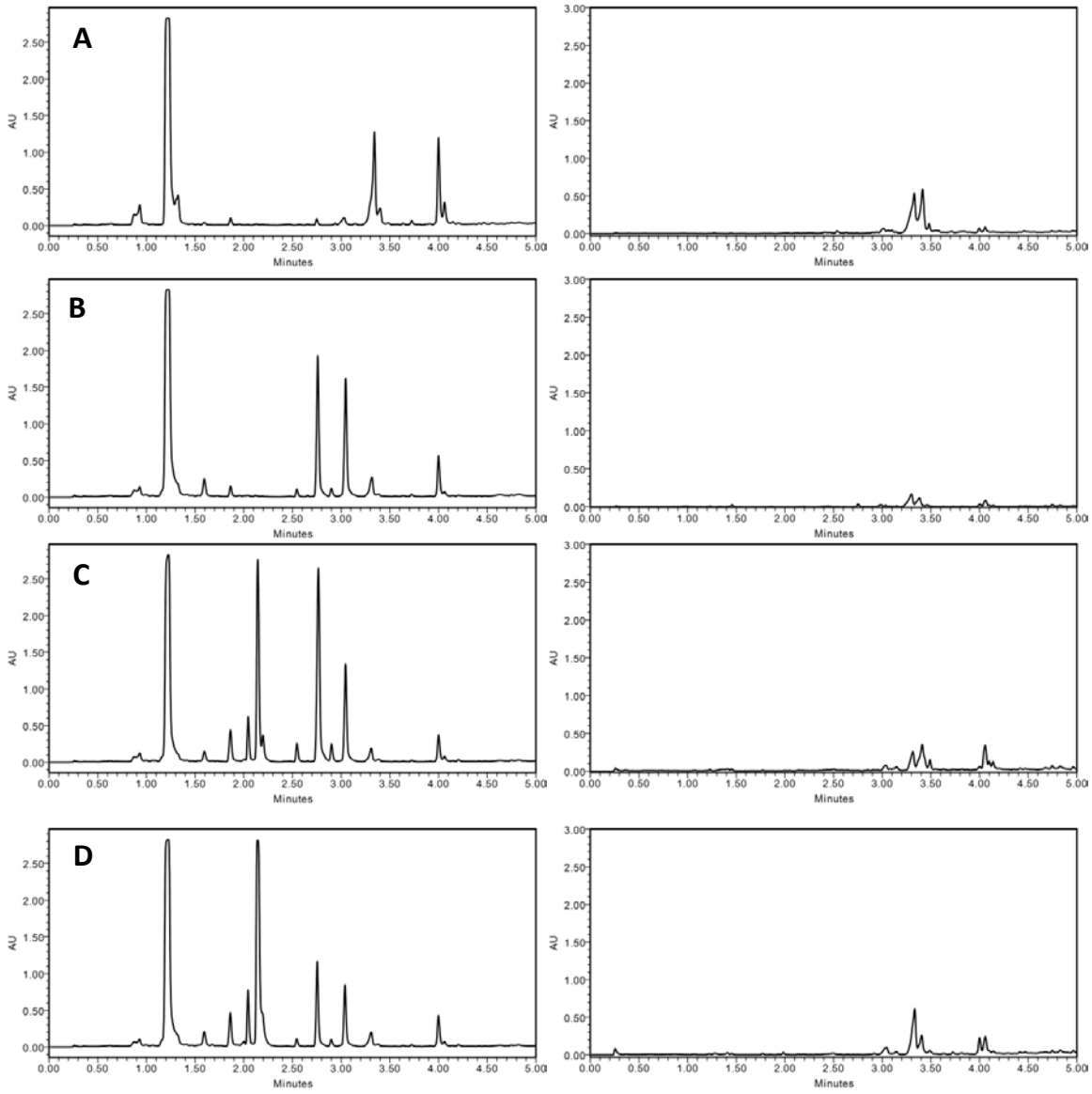

Figure S4. Comparison of control (A) and dosed (B-D) growths of MSX 63935 grown in potato dextrose broth (left) and Czapek Dox broth (right). Cultures shown in (B) were grown with 50 µg/mL SAHA, (C) with 100 µg/mL 5-AZA, and (D) with 50 µg/mL bortezomib. The separation was performed via UPLC-PDA (235 nm), using a C_{18} column and a gradient increasing linearly from 10% CH_3CN (H_2O) at 0.0 min to 100% at 4.5 min, held at 100% for an additional 0.5 min.

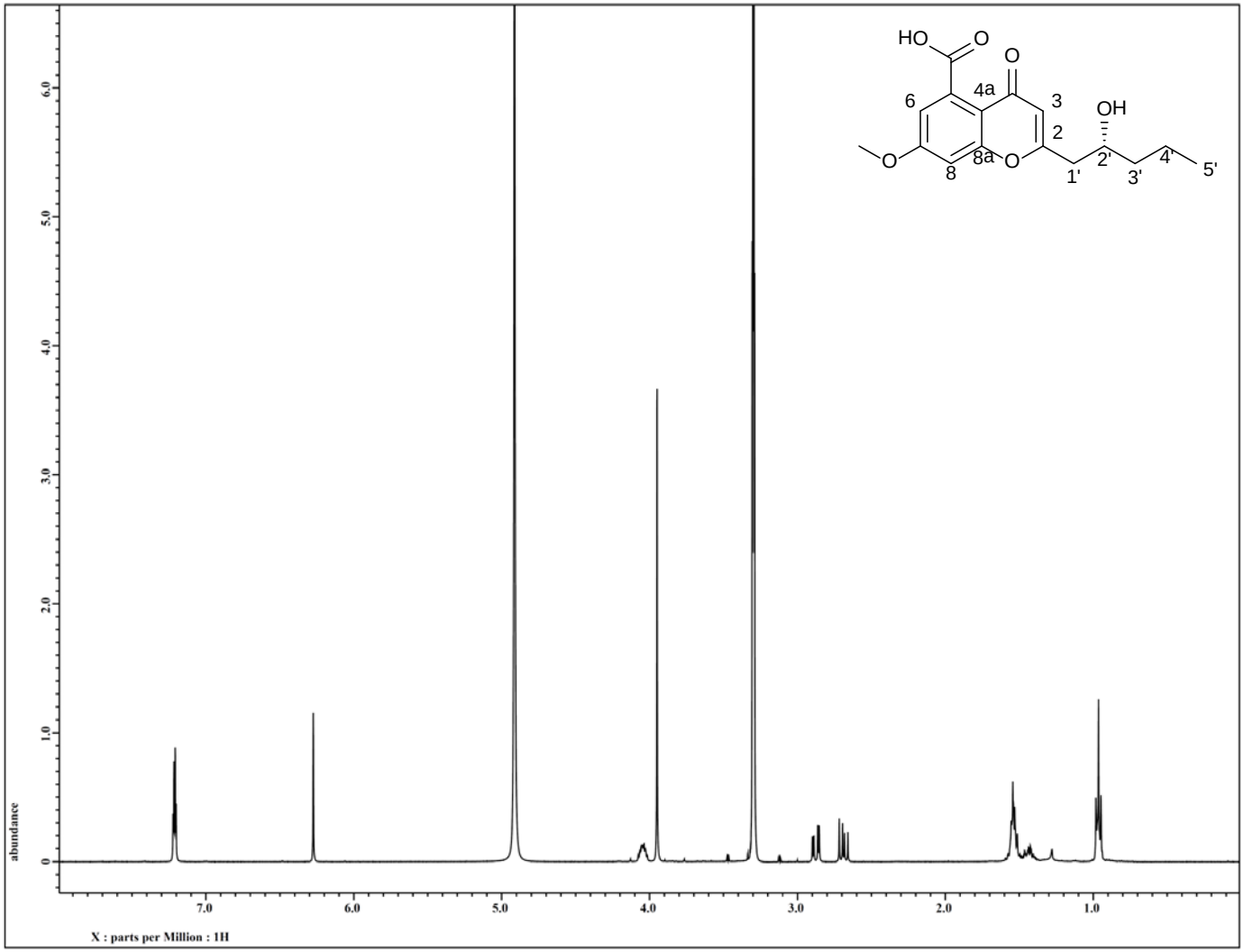

Figure S5. ^{1}H NMR spectrum **9** [400 MHz, MeOH-d_4].

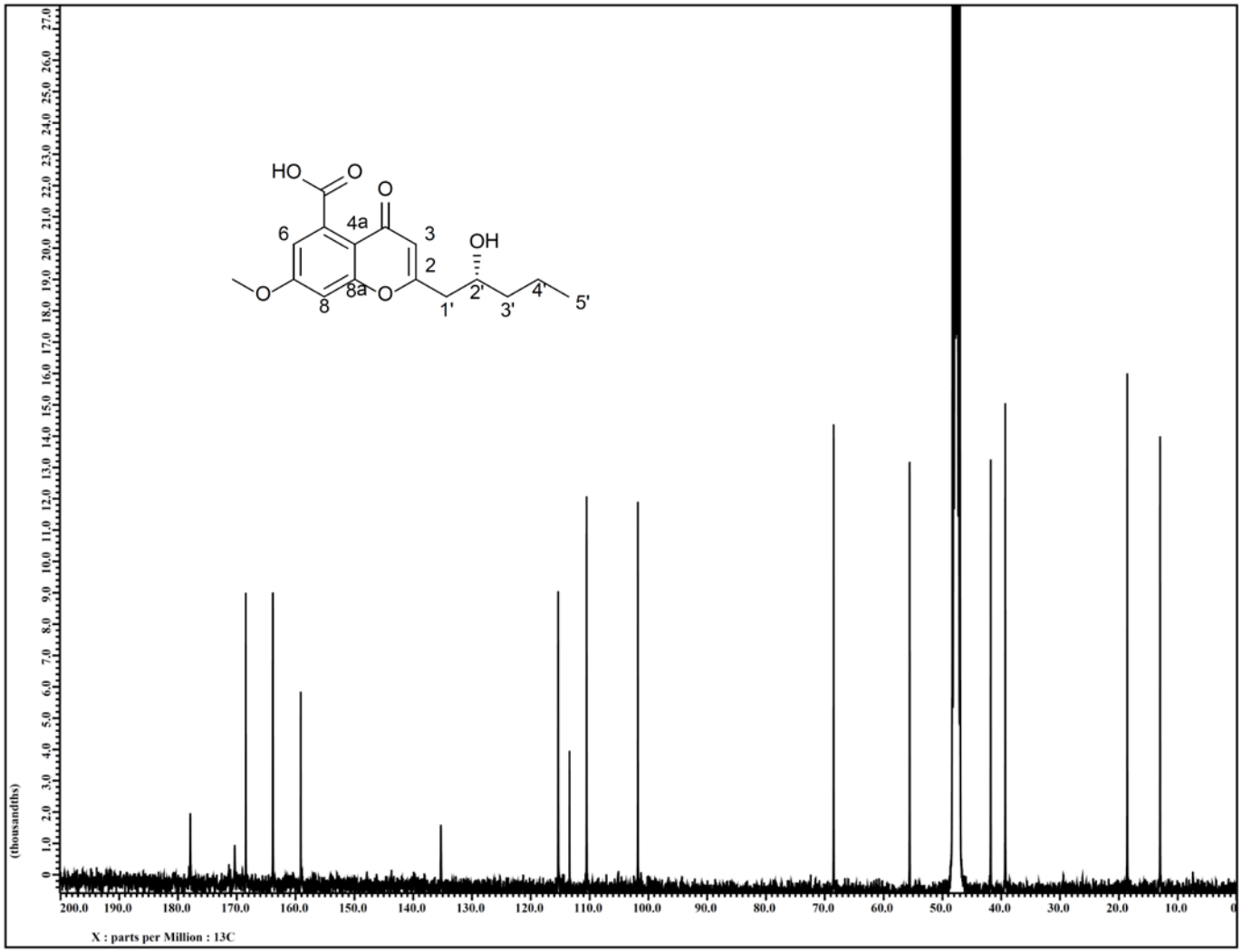

Figure S6. ^{13}C NMR spectrum of **9** [400 MHz, MeOH-d_4].

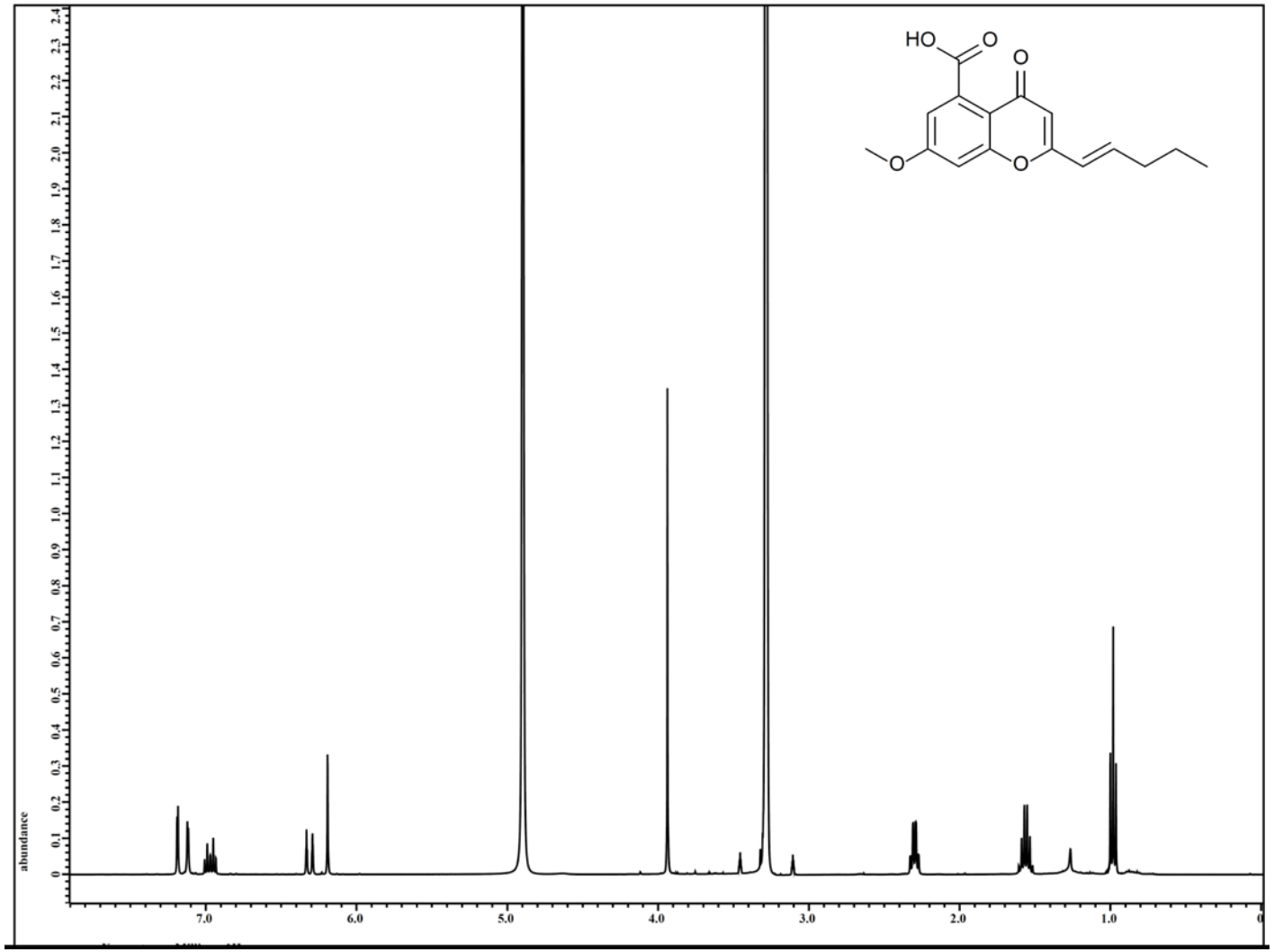

Figure S7. ^{1}H NMR spectrum of **10** [400 MHz, MeOH-d_4].

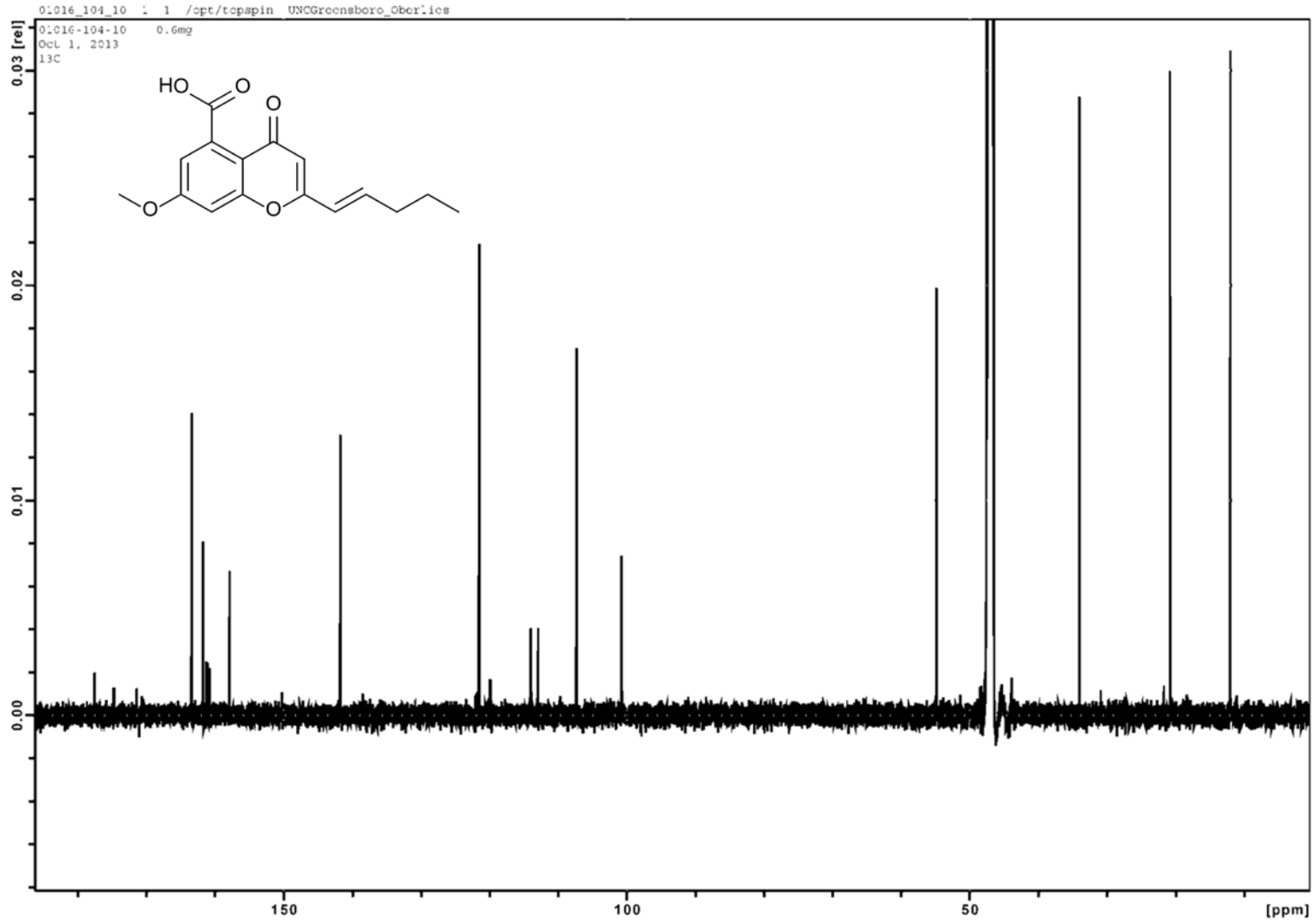

Figure S8. ^{13}C NMR spectrum of **10** [600 MHz, MeOH-d_4].

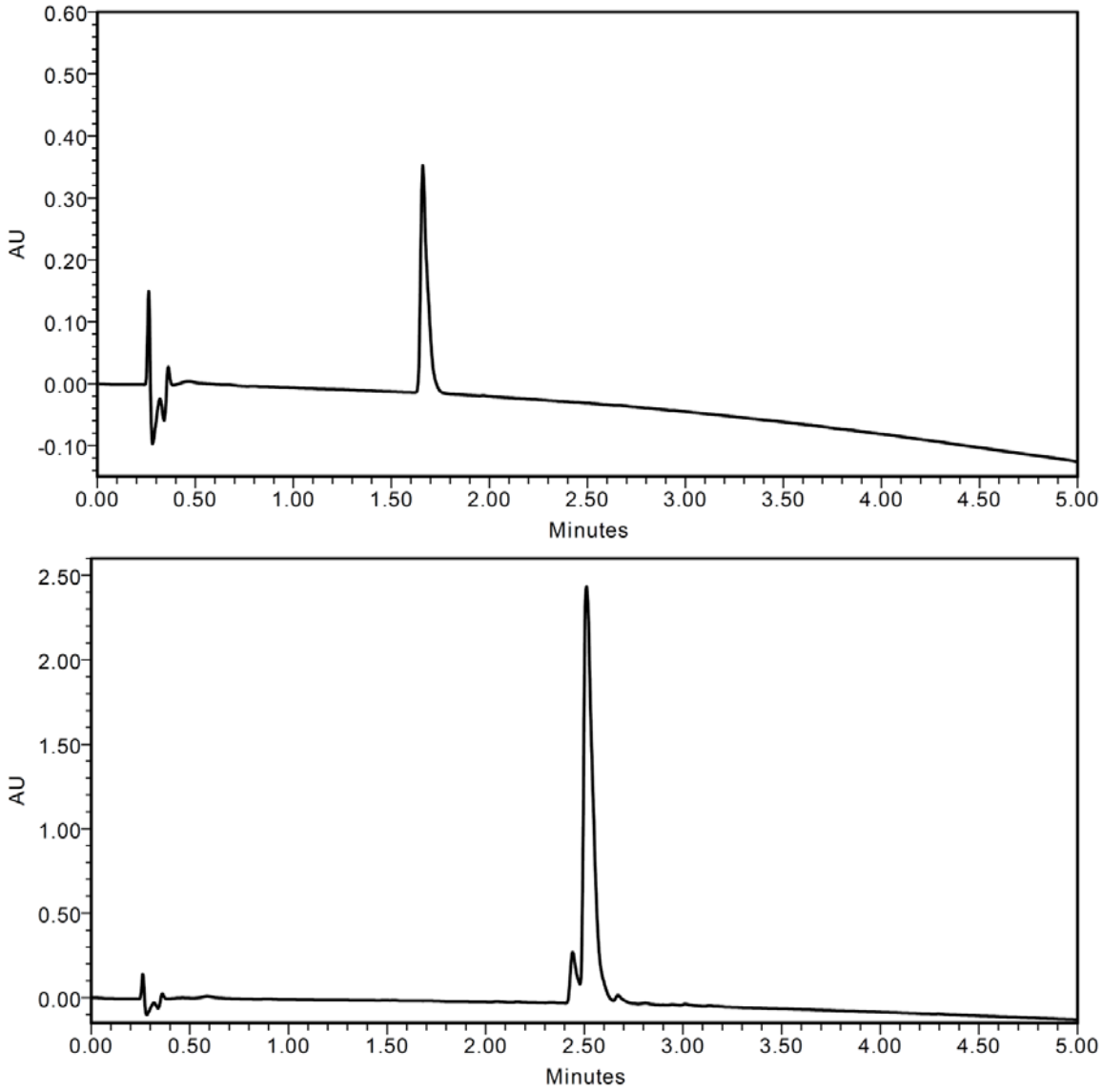

Figure S9. UPLC-PDA (235 nm detection) chromatograms of compounds **1** (top) and **2** (bottom) demonstrating purity. The purity of compound **1** is >99%, and the purity of compound **2** is >91%. The separation was performed using a C_{18} column and a gradient increasing linearly from 10% CH_3CN (H_2O) at 0.0 min to 100% at 4.5 min, held at 100% for an additional 0.5 min.